

1971

Optimum expansion of sand filters during backwash

Appiah Amirtharajah
Iowa State University

Follow this and additional works at: <https://lib.dr.iastate.edu/rtd>

 Part of the [Civil and Environmental Engineering Commons](#)

Recommended Citation

Amirtharajah, Appiah, "Optimum expansion of sand filters during backwash " (1971). *Retrospective Theses and Dissertations*. 4523.
<https://lib.dr.iastate.edu/rtd/4523>

This Dissertation is brought to you for free and open access by the Iowa State University Capstones, Theses and Dissertations at Iowa State University Digital Repository. It has been accepted for inclusion in Retrospective Theses and Dissertations by an authorized administrator of Iowa State University Digital Repository. For more information, please contact digirep@iastate.edu.

72-12,534

AMIRTHARAJAH, Appiah, 1940-
OPTIMUM EXPANSION OF SAND FILTERS DURING
BACKWASH.

Iowa State University, Ph.D., 1971
Engineering, sanitary and municipal

University Microfilms, A XEROX Company, Ann Arbor, Michigan

THIS DISSERTATION HAS BEEN MICROFILMED EXACTLY AS RECEIVED.

Optimum expansion of sand filters
during backwash

by

Appiah Amirtharajah

A Dissertation Submitted to the
Graduate Faculty in Partial Fulfillment of
The Requirements for the Degree of
DOCTOR OF PHILOSOPHY
Major Subject: Sanitary Engineering

Approved:

Signature was redacted for privacy.

In Charge of Major Work

Signature was redacted for privacy.

For the Major Department

Signature was redacted for privacy.

For the Graduate College

Iowa State University
Ames, Iowa

1971

PLEASE NOTE:

**Some pages have indistinct
print. Filmed as received.**

UNIVERSITY MICROFILMS.

TABLE OF CONTENTS

	Page
NOTATION	v
ABBREVIATIONS	ix
I. INTRODUCTION	1
II. OBJECTIVES AND SCOPE OF STUDY	4
A. Theoretical	4
B. Experimental	5
III. A REVIEW OF THE THEORIES OF TURBULENCE- PHENOMENOLOGICAL AND STATISTICAL	7
A. A Capsular Summary	7
B. The Basic Equations of Turbulence	10
1. General	10
2. Introduction to turbulence	11
3. The Continuity and Navier-Stokes equations	13
4. The Reynolds equations for turbulent motion	16
C. The Phenomenological Theories	19
D. The Statistical Theory of Turbulence	22
1. Some basic concepts and definitions	23
2. Turbulent dispersion or diffusion	29
IV. LITERATURE REVIEW	38
A. The Sanitary Engineering Literature	38
1. Filter backwashing	38
2. A critique of Salim Ulug's work on back- washing	48
B. The Fluidization Literature	57
1. Predominance of hydrodynamic forces in cleaning mechanism	57
2. Particulate fluidization and optimum turbulence	62
C. A Summary	73
V. THEORY OF OPTIMUM BACKWASHING	75
A. The Formulation of the Physical Model	75
1. An introduction to filtration	75
2. The backwashed filter	76

	Page
B. A New Mathematical Theory for Optimum Backwashing	79
VI. EXPERIMENTAL INVESTIGATION	94
A. Experimental Apparatus	94
1. General layout	94
2. Details of filters and appurtenances	98
B. Laboratory Analytical Procedures	104
1. Preparation and nature of influent suspension	104
2. Measurement of influent and effluent iron	108
3. Measurement of backwash water quality	114
4. Sand analysis using a magnetic stirrer wash	114
C. Experimental Observations	119
1. Chronology and general description of runs	119
2. The check list procedure for backwashing	124
3. Observations made during a run	127
4. Sieve analysis of expanded layers of fluidized bed	129
D. Data Analysis	130
VII. RESULTS AND ANALYSIS	134
A. Results	134
1. Cumulative effluent quality and porosity	134
2. Initial effluent quality and porosity	149
3. Head loss increases and porosity	153
4. Backwash water quality and porosity	157
5. Physical sandwash and porosity	165
B. Analysis	174
1. An analytical summary of the results	174
2. The evidence in the literature	176
3. Rationalization of parameters and results	178
4. A concluding summary	183
VIII. DESIGNING FOR OPTIMUM BACKWASH	185
A. The Effective Size as Controlling Parameter	185
B. An Illustrative Design Calculation	185

	Page
IX. SUMMARY AND CONCLUSIONS	192
X. LITERATURE CITED	199
XI. ACKNOWLEDGMENTS	205

NOTATION

1.	a, b	= fluctuations in A and B	-
2.	A, B	= arbitrary quantities	-
3.	$\overline{A}, \overline{B}$	= means of A and B	-
4.	C	= volume	L^3
5.	d	= particle size or length characteristic of bed	L
6.	D_t	= diameter of tube or bed	L
7.	$\frac{D}{Dt}$	= $\frac{\partial}{\partial t} + U_x \frac{\partial}{\partial x} + U_y \frac{\partial}{\partial y} + U_z \frac{\partial}{\partial z}$ = substantial derivative	-
8.	e	= eddy diffusivity for mass	$L^2 T^{-1}$
9.	E	= $L_L \sqrt{(u^2)}$ = eddy diffusivity	$L^2 T^{-1}$
10.	F_D	= total drag force on system	MLT^{-2}
11.	F_s	= external force per unit mass acting on species s	LT^{-2}
12.	$F(n')$	= fraction of total energy of turbulence in energy spectrum	-
13.	g	= acceleration due to gravity	LT^{-2}
14.	G	= $\frac{dV'}{dz}$ = mean velocity or shear gradient in pores	T^{-1}
15.	h	= head loss	L
16.	i	= $\frac{dh}{dz}$ = hydraulic gradient	-
17.	J	= mass flux	$ML^{-2} T^{-1}$
18.	K	= $f(V_s, \psi, d/D_t)$ = constant for a particular fluidized system	LT^{-1}

19.	l	= Prandtl's mixing length	L
20.	l_o	= depth of fixed bed	L
21.	l'	= depth of expanded bed	L
22.	L_E	= Eulerian scale of turbulence	L
23.	L_L	= Lagrangian length scale of turbulence	L
24.	m	= exponent	-
25.	mf	= subscript denoting condition at minimum fluidization	-
26.	n	= expansion coefficient in Richardson and Zaki's equation	-
27.	n'	= frequency of sine wave	T^{-1}
28.	N	= total number of particles in bed	-
29.	p	= pressure intensity	$ML^{-1}T^{-2}$
30.	P	= power dissipated	ML^2T^{-3}
31.	r	= distance between two points	L
32.	Re_o	= $\frac{\rho_f V_s d}{\mu}$ = Reynolds Number based on unhindered settling velocity of particle	-
33.	Re'	= modified Reynolds Number	-
34.	$R_E(r)$	= Eulerian correlation function	-
35.	$R_L(t)$	= Lagrangian correlation function	-
36.	s	= species s	-
37.	S	= mean shear stress	$ML^{-1}T^{-2}$
38.	t	= time	T
39.	T	= time sufficiently large to obtain average values of the fluctuations	T
40.	T_L	= Lagrangian time scale of turbulence	T

41.	u	= fluctuating velocity	LT^{-1}
42.	u'	= root mean square velocity fluctuation	LT^{-1}
43.	U	= $iU_x + jU_y + kU_z$ = velocity vector	LT^{-1}
44.	\bar{U}	= mean velocity	LT^{-1}
45.	U^*	= $\sqrt{\frac{\tau_w}{\rho_f}}$ = friction velocity	LT^{-1}
46.	$U_{\Delta c}$	= velocity of propagation of small porosity fluctuation	LT^{-1}
47.	V	= superficial fluid velocity or velocity based on open tube	LT^{-1}
48.	V_s	= unhindered settling velocity of particle	LT^{-1}
49.	V'	= $\frac{V}{\epsilon}$ = average fluid velocity within pores of filter	LT^{-1}
50.	x, y, z	= Cartesian co-ordinates	L
51.	x_c	= iron concentration in mg/l	ML^{-3}
52.	X	= displacement of fluid particle in time t	L
53.	y_T	= percent transmittance	-
54.	z	= vertical height above some datum	L

Greek Symbols

55.	α	= $\sqrt{[\mu g K (\rho_s - \rho_f)]}$ = constant for a particular fluidized system in optimum backwashing theory	$ML^{-1}T^{-2}$
56.	γ_f	= specific weight of fluid	$ML^{-2}T^{-2}$
57.	γ_s	= specific weight of solid	$ML^{-2}T^{-2}$

58.	δ	= $\frac{x}{d}$ = dimensionless spacing of particles in fluidized state	
59.	Δ	= prefix signifying increment	-
60.	ϵ	= porosity	-
61.	λ'	= modified friction factor	-
62.	μ	= viscosity	$ML^{-1}T^{-1}$
63.	ν	= $\frac{\mu}{\rho}$ = kinematic viscosity	L^2T^{-1}
64.	ρ	= density	ML^{-3}
65.	ρ_f	= mass density of fluid	ML^{-3}
66.	ρ_s	= mass density of solid	ML^{-3}
67.	ρ_w	= mass density of water	ML^{-3}
68.	τ	= period of time	T
69.	τ_w	= shear stress at wall	$ML^{-1}T^{-2}$
70.	ψ	= sphericity	-
71.	∇	= $i \frac{\partial}{\partial x} + j \frac{\partial}{\partial y} + k \frac{\partial}{\partial z}$ = vector operator del or nabla	-
72.	∇^2	= $\frac{\partial^2}{\partial x^2} + \frac{\partial^2}{\partial y^2} + \frac{\partial^2}{\partial z^2}$ = Laplacian operator	-

ABBREVIATIONS

1. centimeter	cm
2. cubic centimeter	cc
3. cubic feet	cu ft
4. cubic feet per second	cfs
5. degree(s) Celsius	°C
6. feet	ft
7. gallon(s)	gal
8. gallon(s) per minute	gpm
9. gram(s)	g
10. horse power	HP
11. hour(s)	hr
12. inch(es)	in.
13. micrometer(s)	μm
14. milligram(s) per liter	mg/l
15. milliliter(s)	ml
16. millimeter(s)	mm
17. minute(s)	min
18. nanometer	nm
19. parts per million	p.p.m.
20. pound(s)	lb
21. revolutions per minute	rpm
22. root mean square	r.m.s.
23. second(s)	sec
24. square centimeter(s)	sq cm

25. square feet

sq ft

26. versus

vs.

LIST OF FIGURES

	Page
Fig. 1. Schematic view of dirty filter	78
Fig. 2. Shear forces and velocities on elemental volume of fluid	80
Fig. 3. Schematic layout of experimental apparatus	95
Fig. 4. Details of pilot plant filters	96
Fig. 5. Views showing mixing tank, chemical feeders, flowmeter and effluent rate controllers	97
Fig. 6. Iron removed from sand by physical abrasion test	117
Fig. 7. Head loss curves for run 3B, top 6 in. of filter media	132
Fig. 8. Variation of the ratio of effluent to influent iron with time	133
Fig. 9. Cumulative differential effluent iron vs. time, run 7	135
Fig. 10. Cumulative differential effluent iron vs. time, run 8	136
Fig. 11. Cumulative differential effluent iron vs. time, run 9	137
Fig. 12. Cumulative differential effluent iron vs. time, run 10	138
Fig. 13. Cumulative differential effluent iron vs. time, run 11	139
Fig. 14. Cumulative differential effluent iron vs. time, run 12	140
Fig. 15. Cumulative effluent quality index vs. porosity, series 2, 12 in. depth	143
Fig. 16. Cumulative effluent quality index vs. porosity, series 2, all depths	145

Fig. 17.	Cumulative effluent quality index vs. porosity, series 1, 12 in. depth	146
Fig. 18.	Cumulative effluent quality index vs. expansion, series 3, 18 in. depth	147
Fig. 19.	Cumulative effluent quality index vs. expansion, series 3, all depths	148
Fig. 20.	Expansion-porosity characteristic for top 3 in. of graded sand	150
Fig. 21.	Cumulative initial effluent index vs. porosity, series 1 and 2	151
Fig. 22.	Cumulative initial effluent index vs. expansion, series 3	152
Fig. 23.	Initial effluent quality vs. time of valve closure, runs 13-15	154
Fig. 24.	Head loss increase vs. porosity, series 1	156
Fig. 25.	Backwash water quality vs. washwater volume, series 1	159
Fig. 26.	Backwash water quality vs. washwater volume, series 1	160
Fig. 27.	Backwash water quality vs. washwater volume, series 1	161
Fig. 28.	Terminal backwash water quality vs. porosity, series 1	163
Fig. 29.	Backwash water volume vs. porosity, series 1	164
Fig. 30.	Backwash water equality vs. washwater volume, series 2	166
Fig. 31.	Backwash water quality vs. washwater volume, series 3	167
Fig. 32.	Terminal backwash water quality vs. porosity, series 2	168
Fig. 33.	Backwash water volume vs. porosity, series 2	169
Fig. 34.	Terminal backwash water quality vs. expansion, series 3	170

Fig. 35. Backwash water volume vs. expansion, series 3	171
Fig. 36. Iron removable by physical abrasion test vs. expansion, runs 20 and 21	172
Fig. 37. Sieve analyses of graded sand and the top 3 in. layer	186

LIST OF TABLES

	Page
Table 1. Analysis of University tap water	106
Table 2. Comparative analyses of sand after 19 runs	119
Table 3. Experimental design for series 2	123
Table 4. Backwash procedures for graded sand	127
Table 5. Effluent quality index and porosity for series 2	142
Table 6. Head loss increases from run A to B, uniform sand, series 2	155
Table 7. Head loss increases from run A to B, graded sand, series 3	158
Table 8. A summary of optimum backwash and porosity	175

1. INTRODUCTION

'It is true that nature begins, as it were, with argument and ends with experience, but nevertheless we must follow the contrary way; as I have said, we must commence with experience and strive by means of it to discover truth. In the examination of physical problems I begin by making a few experiments -----, and then I show why it is that bodies are forced to act in the described manner.' Thus, in clear and classic terms did Leonardo da Vinci delineate the fundamental philosophy of the scientific method-experiment and analysis or practice and theory or in da Vinci's words, experience and argument.

The backwashing of rapid sand filters has had years of experience, however, only today do we stand at the threshold of a time wherein we can possibly augment experience with argument and hence use the scientific approach. In contrast to the voluminous work in filtration, the study of backwashing sand filters has received little attention throughout the history of rapid sand filtration, except for a sporadic burst of research in the late 1920's and early 30's. Even though studies in backwashing have been limited, it is a well known fact that most maintenance problems in filtration plants are an offshoot of backwashing effects.

This study is a theoretical as well as experimental study on determining the optimum expansion of sand filters during backwash. The problem is probed from a fundamental point of view, especially in developing the theory which predicts the existence of an optimum condition. It is impossible to obtain a deep insight into the mechanisms of

backwashing without delving substantially into the analogous subjects of turbulence and fluidization of which we know far more. However, it should be remembered that we still do not have an entirely satisfactory self-contained theory of turbulence, and fluidization is still a subject in its primary stage of growth.

It needs to be emphasized that the present study is centered around expansion for optimum backwash. For a more complete understanding of the general characteristics of fluidization and its application to backwashing, this study needs to be supplemented by the writer's previous work (2). The present study evolved from the previous work, and the earlier study provides a comprehensive introduction to the fundamentals of fluidization and backwashing. In it will be found a review of various features of fluidization, such as (i) terminology and fundamental behavioral patterns, (ii) uniformity of particle distribution in particulate fluidization, (iii) particle size segregation effects, (iv) two-component fluidization, (v) the mechanics of particle and bubble motion in aggregative fluidization, (vi) air scouring and three-phase systems and (vii) fluidization for optimum backwashing. Some interesting results emerging from this literature review were: (i) abnormalities like channelling which cause most filter maintenance problems can be controlled; (ii) the concept of sand grains being cleaned principally by abrasion with one another while in the fluidized state has little foundation; (iii) particle size stratification is an intrinsic property of the fluidized state and occurs at all diameter ratios and at all velocities; (iv) an air-scoured filter is a triple-phase system having similarities

to an aggregatively fluidized bed; and (v) the scales and intensities of turbulence maximized at an expanded porosity of 0.65-0.70.

As evident, the present study concentrates and develops in detail the particular problem of optimum backwash which was treated from an overview point of view in the previous work. It will be presumed that the other aspects of fluidization are known to the reader of the present work and it is not intended to cover aspects treated in the previous study, unless they are directly relevant to optimum backwash. However, significant results of the previous work are used in this study.

This study can be introduced by the following single sentence. It deals with developing a theory, and providing experimental verification of the prediction from the theory, that there is an optimum expansion for a filter bed during backwash; the study culminates by providing a tentative rational approach for designing backwashing systems, such that the filter operates optimally.

II. OBJECTIVES AND SCOPE OF STUDY

This study can be defined in general terms as a fundamental, theoretical and experimental study of the backwashing of sand filters. In specific terms, its primary all important objective is to show theoretically as well as experimentally that an optimum expansion of a sand filter does exist during backwash and that this expansion can be predicted, can be calculated for purposes of design and can also be rationalized in terms of the fluid mechanical theories of turbulence and the hydrodynamic forces within the fluidized bed.

In order to accomplish this objective the following studies are made in the various sections.

A. Theoretical

(i) A review of the statistical theory of turbulence and its application to eddy diffusion (turbulent diffusion) in fluidized beds; this provides basic background for understanding the behavior of backwashed filter beds.

(ii) A review of the literature in fluidization which indicates that an optimum in the turbulence parameters occurs in the region of expanded porosity of 0.65-0.70. This review also includes a subsection which critically analyzes the only other known study on backwashing of filters which probes the problem on an extensive theoretical and experimental basis.

(iii) Development of a new mathematical theory for backwashing from which it can be deduced analytically that a functional maximum of

the hydrodynamic shear exists in the region of optimum backwash, namely porosity = 0.65-0.70.

B. Experimental

(i) The experimental study investigates whether the optimum backwash predicted theoretically can be achieved while backwashing a filter sand under normal operating conditions. Five different criteria are used to evaluate the effectiveness of the backwash: (a) Cumulative effluent quality in the run following backwash, (b) initial effluent quality in the run following backwash, (c) head loss increase in the run following backwash, (d) the terminal backwash water quality during backwash and (e) the backwash water volume during backwash. Initially, these studies are made on twelve dual runs (dirtying run followed by a run after backwash) with 12 inch depth filters of uniform sand of 0.548 mm average size. Each run is made in a pilot plant filter apparatus which has three 6 inch diameter plexiglass filters. The suspension filtered is produced by the addition of ferrous sulphate to University tap water which has a high alkalinity.

(ii) The above studies are then repeated for six dual runs on a typical graded sand used in filters. This sand has an effective size of 0.45 mm and a uniformity coefficient of 1.47 and is 18 inches deep. In addition to the five criteria indicated above for evaluation of effectiveness of wash, an additional criterion based on the amount of iron which is physically removable from samples of the backwashed sand is also used.

Based on the experimental study, a simple mathematical model for designing optimum backwash systems for graded sand is proposed. The model uses the expansion model developed by the writer of this dissertation in an earlier study (2, 3).

III. A REVIEW OF THE THEORIES OF TURBULENCE- PHENOMENOLOGICAL AND STATISTICAL

A. A Capsular Summary

This summary is provided at the very outset, to provide a descriptive condensation of the material covered in this chapter and to emphasize the significant threads of development that need to be understood and remembered. The intent is also to stress the fact that the chapter is written in such a fashion that it is possible to approach the material via two routes: (i) a detailed understanding of the mathematical equations and developments, or (ii) a general understanding of the content by reading the descriptive material and assuming the mathematical developments to be valid. Though the first route is the ideal, nevertheless, the second is amply sufficient to progress towards the following chapters which are the more important. The theory developed in the following chapters does not involve any of the advanced mathematical notation used in this chapter. It is impossible to adequately describe and understand turbulence without using vector algebra and tensor analysis; however, by restricting the treatment to be semi-quantitative, only an elementary knowledge of vector algebra is used and tensors have been avoided. This chapter is a stepping stone to the following chapters wherein the important ideas of optimum backwashing are developed.

The entire field of fluid dynamics is principally founded on the Continuity (Eq. 1), Navier-Stokes (Eq. 3) and Energy equations. These are mathematical statements of the conservation of mass, momentum and energy. Reynolds found that by assuming a turbulent velocity to be

composed of a fluctuating velocity u , superposed on a mean velocity \bar{U} , and using certain averaging laws it is possible to obtain an analogous equation to the Navier-Stokes equation (Eq. 12) for the mean velocities of a turbulent flow. However, this equation had an extra term (Reynolds stress or eddy stress) which had similar characteristics to fluid stresses, and its solution required an extra equation. Several alternative hypotheses based on intuitive and physical ideas of turbulence gave this extra equation; these various hypotheses lead to the phenomenological theories of turbulence. One of these theories (Boussinesq's theory) gives rise to the important concept of eddy viscosity (Eq. 13). This concept can be extended by analogy to an eddy diffusion coefficient or eddy diffusivity which will describe turbulent field dispersions. The mathematical equation formulated is similar to that for molecular diffusion. The determination of quantitative values for eddy diffusivity provide the principal evidence for the maximum in the turbulence characteristics at the expanded porosity of 0.65-0.70 in a fluidized bed. Though a phenomenological theory provides a definition for eddy diffusivity, actual measurements of its value can be easily obtained from Taylor's theory of statistical turbulence.

The solutions resulting from the phenomenological theories (Prandtl's mixing length theory, Von Karman's similarity hypothesis) principally yield the velocity and eddy stress distributions in turbulent fluid fields. For the specific case of a turbulent flow in a pipe, these theories identify a boundary layer where viscous stresses predominate, a transition region where viscous and eddy effects are important and a turbulent core where eddy viscosity and eddy stresses are dominant.

These conclusions are of significant importance in understanding the characteristics of a particulate fluidized bed or a backwashed filter.

In order to develop a more fundamental approach to understanding turbulence and in order to find solutions to Reynolds equation (Eq. 12) for turbulent motion, Taylor proposed the statistical theory. It is based on the fundamental idea that a high degree of correlation exists between the velocities at two points within an eddy. Using these correlation functions in Reynolds equation leads to the famous closure problem in turbulence theory which is under active research even today. However, this aspect is not important in the present study.

Using the basic idea of the correlation function (Eqs. 19 and 20), Taylor developed a theory for the turbulent dispersion or diffusion of particles from a fixed point source. This theory yields an equation for the eddy diffusivity (Eq. 38) which is the most relevant equation of this review. It is commonly used to study the characteristics of turbulent dispersion in particulate fluidization. The equation also yields the scales of turbulence. The mathematical development of this theory has been presented in some detail in this chapter. Thus, quantitative values of some of the parameters of turbulence can be obtained by experimentally plotting this equation (Eq. 38). It is by this means that optimum diffusion in particulate fluidization was shown to be at a porosity of 0.65-0.70. This is one of the principal facts on which this entire dissertation is based.

B. The Basic Equations of Turbulence

1. General

It is perhaps pertinent to point out at this stage that the pure fluid velocities encountered during fluidization under backwashing conditions are insufficient to provide a turbulent fluid field; however, the interaction of the particle and fluid fields within the fluidized bed do provide a system closely approximating the basic formulation of a turbulent fluid field and is hence amenable to analysis by the same theories of turbulence (14, 39, 40). The following review is developed principally from an extensive condensation of the relevant material in the texts by Hinze (42), Brodkey (14), Bird, Stewart and Lightfoot (13), Curle and Davies (28), the collection of classic papers on the statistical theory by Friedlander and Topper (36), and other papers (58, 68, 69). It does not pretend to provide an up-to-date review of the literature in the field of turbulence; however, the following review is an essential prerequisite, for understanding the literature in fluidization as well as the theory of backwashing developed in the subsequent chapters. The material covered has rarely been dealt with in the field of sanitary engineering. Thus, the main purpose has been to cull and collate the material so that this dissertation can be read as a unified whole. It is impossible to understand momentum, mass transfer and diffusion in a particularly fluidized bed without understanding turbulence itself.

2. Introduction to turbulence

Hinze (42) modified a definition of turbulence given by Taylor and Von Karman for more precision. He states that,

Turbulent fluid motion is an irregular condition of flow in which the various quantities show a random variation with time and space coordinates, so that statistically distinct average values can be discerned.

The initial development of turbulence or the transition from laminar to turbulent motion is noteworthy. It has been shown that its development is continuous and it does not occur suddenly at a particular velocity (14). The problem has been analyzed from stability considerations. A qualitative picture of the changes as it develops in pipe flows is as follows. When laminar flow predominates it has been shown that eddies formed at the entrance to the system are dampened out. At the initial transitional zone, two dimensional waves are formed and then linearly amplified. These waves then develop into three dimensional waves culminating in turbulence spots at localized points. These turbulence spots or minute eddies then propagate and fill the entire flow field causing turbulence. If the turbulence has quantitatively the same structure in all parts of the flow field the turbulence is said to be homogeneous; in more definitive terms, especially for use in tensor analysis, it means that the system is invariant to axis translation. If the statistical features of turbulence have no directional preference then the turbulence is isotropic. Under these conditions, no average shear stress can occur and consequently, no velocity gradient of the mean velocity.

The earliest attempts to formulate a simple mechanism for turbulence resulted in the phenomenological theories, such as (i) Boussinesq's theory of eddy viscosity, (ii) Prandtl's mixing-length theory, (iii) Taylor's vorticity-transport theory and (iv) Von Karman's similarity hypothesis. It is now generally recognized that these phenomenological theories are inadequate to explain the mechanisms of turbulence. But, because of a lack of a general solution to the turbulence problem, these methods are still essential for practical use in engineering analysis such as in transport phenomena. The present hope for a more rational understanding of turbulence lies in the area of the statistical theory of turbulence.

The transport of any transferable quantity (energy, momentum and mass) by random fluid motion is diffusive in nature. Thus, the transport process is necessarily greater in turbulent flow than in nonturbulent flow. A solution to the turbulent transport problem requires a solution in terms of the turbulent velocity field and given boundary and initial conditions. A complete solution to the transport problem requires a complete knowledge of the functions describing turbulence; this is lacking even today.

It is customary in the treatment of fluid mechanics to distinguish between the Eulerian and Lagrangian descriptions. The Eulerian approach describes the system with respect to a co-ordinate system fixed in reference to the solid boundaries; in contrast, the Lagrangian description is an analysis of the system by focusing attention on a given fluid particle as it moves through the flow field.

3. The Continuity and Navier-Stokes equations

The mathematical expression for the basic physical concept of the conservation of mass results in the Continuity Equation.

In vector form,

$$\frac{\partial \rho}{\partial t} = - (\nabla \cdot \rho U) \quad (1)$$

where,

$$U = iU_x + jU_y + kU_z = \text{velocity vector}$$

$$t = \text{time}$$

$$\rho = \text{mass density}$$

$$\nabla = i \frac{\partial}{\partial x} + j \frac{\partial}{\partial y} + k \frac{\partial}{\partial z} = \text{vector operator}$$

$$\nabla \cdot U = \frac{\partial U_x}{\partial x} + \frac{\partial U_y}{\partial y} + \frac{\partial U_z}{\partial z} = \text{div } U$$

For an incompressible material, the density is constant and $\frac{\partial \rho}{\partial t} = 0$, hence the equation of continuity reduces to,

$$\nabla \cdot U = 0 \quad (2)$$

or alternatively,

$$\frac{\partial U_x}{\partial x} + \frac{\partial U_y}{\partial y} + \frac{\partial U_z}{\partial z} = 0$$

The expression $(\nabla \cdot U)$ is frequently denoted by $\text{div } U$, or divergence of the velocity, meaning an excess of outward over inward flow.

The basic physical concept of the conservation of momentum is expressed mathematically by the Navier-Stokes Equation.

In vector form the equation for a Newtonian fluid is,

$$\rho \frac{DU}{Dt} = -\nabla p + \frac{1}{3} \mu \nabla(\nabla \cdot U) + \mu \nabla^2 U + \sum_s \rho_s F_s \quad (3)$$

where,

p = pressure

F_s = external force per unit mass acting on species s

s = species s

μ = viscosity

$$\nabla^2 = \frac{\partial^2}{\partial x^2} + \frac{\partial^2}{\partial y^2} + \frac{\partial^2}{\partial z^2} = \text{Laplacian operator}$$

$$\frac{D}{Dt} = \frac{\partial}{\partial t} + (U \cdot \nabla) = \frac{\partial}{\partial t} + U_x \frac{\partial}{\partial x} + U_y \frac{\partial}{\partial y} + U_z \frac{\partial}{\partial z}$$

= substantial derivative

The elegance and brevity of the vector notation and an illustration of the equation for cartesian co-ordinates is shown by writing the x-component equation as follows,

$$\begin{aligned} & \rho \left[\frac{\partial U_x}{\partial t} + U_x \frac{\partial U_x}{\partial x} + U_y \frac{\partial U_x}{\partial y} + U_z \frac{\partial U_x}{\partial z} \right] \\ &= - \frac{\partial p}{\partial x} + \frac{1}{3} \mu \frac{\partial}{\partial x} \left(\frac{\partial U_x}{\partial x} + \frac{\partial U_y}{\partial y} + \frac{\partial U_z}{\partial z} \right) \\ &+ \mu \left(\frac{\partial^2 U_x}{\partial x^2} + \frac{\partial^2 U_x}{\partial y^2} + \frac{\partial^2 U_x}{\partial z^2} \right) + \sum_s \rho_s F_s \end{aligned} \quad (4)$$

An analysis of the origin of the terms in the Navier-Stokes Equation, Eq. 3 and various possible simplifications are essential for a

proper interpretation of the terms in the later development of the theory of turbulence. The left hand side denotes the mass per unit volume times the acceleration. The first term on the right hand side arises from forces due to the pressure gradient while the last term is due to external forces like gravity. The second and third terms arise from internal forces due to normal and shear stresses on the element considered.

If the fluid is incompressible, then from Eq. 2, $(\nabla \cdot U) = 0$ and the only term in Eq. 3 due to internal forces will be, $\mu \nabla^2 U$, which has the same form as Fick's law of diffusion. Equation 3 still remains a non-linear partial differential equation with no general solution.

The approximation is often made in the Navier-Stokes equation of neglecting the inertial terms; say when the Reynolds No. (ratio of inertial to viscous forces) is small. Under conditions of no external forces, this leads to,

$$\rho \frac{\partial U}{\partial t} = - \nabla p + \mu \nabla^2 U \quad (5)$$

This is the basic equation for laminar viscous flow or creeping motion and specific cases like Stoke's law maybe obtained from it.

If the assumption of zero viscosity is made, Eq. 3 reduces to,

$$\rho \frac{DU}{Dt} = - \nabla p + \sum_s \rho_s F_s \quad (6)$$

This is the Euler equation of motion for ideal flow and applies to fluids when the Reynolds No. is high, or where the viscosity is low and the main focus of attention is in the main fluid stream away from

the boundary layer. When only gravity is acting there are five equations with five unknowns and the equations can be solved in principle for given boundary conditions. Most two dimensional potential flows are treated under these conditions.

4. The Reynolds equations for turbulent motion

The Navier-Stokes equation should be valid for turbulent motion too, since it is essentially an application of Newton's Second Law to an element of a continuum at a particular instant. However the difficulty in analytical treatment is due to the fluctuating velocities, thus some statistical averaging is essential for meaningful analysis.

Let the instantaneous velocity be written as the sum of an average velocity, \bar{U} and a fluctuating velocity, u . Thus,

$$U = \bar{U} + u \quad (7)$$

Reynolds (58) formulated certain averaging techniques, which though not universally rigorous, do apply for quantities having sufficiently numerous random fluctuations superposed on statistically distinct mean values.

Consider two quantities, $A = \bar{A} + a$ and $B = \bar{B} + b$, where the over-score implies means. Then the following properties hold,

$$\overline{\bar{A} + a} = \bar{A} + \bar{a} = \bar{A} + \bar{a}, \text{ hence } \bar{a} = 0$$

$$\overline{\bar{A} B} = \bar{A} \bar{B} = \bar{A} \bar{B}$$

$$\overline{\bar{A} b} = \bar{A} \bar{b} = 0$$

$$\begin{aligned}\overline{AB} &= \overline{(\overline{A} + a)(\overline{B} + b)} = \overline{\overline{A} \overline{B}} + \overline{ab} + \overline{A b} + \overline{B a} \\ &= \overline{A} \overline{B} + \overline{ab}\end{aligned}\quad (8)$$

Equation 8 being the important result derived.

If A and B are vectors, such as a velocity $U = iU_x + jU_y + kU_z$, then the term \overline{UU} involves nine components of the form, $\overline{U_x U_x}$, $\overline{U_x U_y}$, $\overline{U_x U_z}$, etc. Defining the velocity in the form of Eq. 7 yields for one of these products,

$$\overline{U_x U_z} = \overline{U_x} \overline{U_z} + \overline{u_x u_z} \quad (9)$$

It should be noted that $\overline{u_x u_z}$ is not necessarily zero, even though $\overline{u_x}$ and $\overline{u_z}$ are zero.

Consider the equation of continuity Eq. 1. Using the above averaging techniques and assuming density fluctuations are possible as in compressible fluid flow, so that $\rho = \overline{\rho} + \tilde{\rho}$,

$$\frac{\partial \overline{\rho}}{\partial t} = -\nabla \cdot \overline{\rho U} = -\nabla \cdot (\overline{\rho} + \tilde{\rho})(\overline{U} + u)$$

hence,

$$\frac{\partial \overline{\rho}}{\partial t} = -\nabla \cdot \overline{\rho} \overline{U} - \nabla \cdot \overline{\rho u} \quad (10)$$

Comparing this equation with Eq. 1 it is seen that the averaging procedure introduces an extra term into the equation.

However, for incompressible flow, $\tilde{\rho} = 0$, therefore $\bar{\rho} = \text{constant}$ and Eq. 10 reduces to the identical form as Eq. 2,

$$0 = -\nabla \cdot (\bar{\rho} \bar{\mathbf{U}}), \text{ i.e. } (\nabla \cdot \bar{\mathbf{U}}) = 0$$

Consider the Navier-Stokes Eq. 3, written in the alternate form as in Brodkey (14),

$$\rho \frac{D\mathbf{U}}{Dt} = \rho \frac{\partial \mathbf{U}}{\partial t} + (\nabla \cdot \rho \mathbf{U}\mathbf{U}) = -\nabla p + \mu \nabla^2 \mathbf{U} + \sum_s \rho_s \mathbf{F}_s \quad (3a)$$

Substituting the variables in terms of their average values and their fluctuations, and then averaging the entire equation,

$$\begin{aligned} \rho \frac{\partial}{\partial t} \overline{(\bar{\mathbf{U}} + \mathbf{u})} + \nabla \cdot \rho \overline{(\bar{\mathbf{U}} + \mathbf{u})(\bar{\mathbf{U}} + \mathbf{u})} &= -\nabla \overline{(p + \tilde{p})} \\ &+ \mu \nabla^2 \overline{(\bar{\mathbf{U}} + \mathbf{u})} + \sum_s \rho_s \overline{\mathbf{F}_s} \end{aligned}$$

Therefore,

$$\rho \frac{\partial}{\partial t} \bar{\mathbf{U}} + \nabla \cdot (\rho \bar{\mathbf{U}} \bar{\mathbf{U}}) + \nabla \cdot (\rho \overline{\mathbf{u}\mathbf{u}}) = -\nabla \bar{p} + \mu \nabla^2 \bar{\mathbf{U}} + \sum_s \rho_s \bar{\mathbf{F}}_s$$

$$\text{i.e. } \rho \frac{\partial}{\partial t} \bar{\mathbf{U}} + \rho (\bar{\mathbf{U}} \cdot \nabla) \bar{\mathbf{U}} + \rho (\bar{\mathbf{U}} \cdot \nabla) \bar{\mathbf{U}} = -\nabla \bar{p} + \mu \nabla^2 \bar{\mathbf{U}} + \sum_s \rho_s \bar{\mathbf{F}}_s - (\nabla \cdot \rho \overline{\mathbf{u}\mathbf{u}})$$

Since $\nabla \cdot \bar{\mathbf{U}} = 0$, the equation reduces to,

$$\rho \frac{\partial}{\partial t} \bar{\mathbf{U}} + \rho (\bar{\mathbf{U}} \cdot \nabla) \bar{\mathbf{U}} = -\nabla \bar{p} + \mu \nabla^2 \bar{\mathbf{U}} + \sum_s \rho_s \bar{\mathbf{F}}_s - (\nabla \cdot \rho \overline{\mathbf{u}\mathbf{u}})$$

$$\text{or } \rho \frac{D\bar{\mathbf{U}}}{Dt} = -\nabla \bar{p} + \mu \nabla^2 \bar{\mathbf{U}} + \sum_s \rho_s \bar{\mathbf{F}}_s - (\nabla \cdot \rho \overline{\mathbf{u}\mathbf{u}}) \quad (12)$$

Equation 12 called the Reynolds equation for incompressible turbulent motion has several interesting features. It is exactly analogous to Eq. 32 shown above for non-turbulent motion except for the last term, $\overline{v \cdot \rho u u}$. This term has nine components, six of which are different and the term is associated with a stress called a Reynolds stress, eddy stress or a turbulent stress. The averaging procedure has made the equation indeterminate due to the fluctuation terms; however, it can be solved in a number of specific cases.

C. The Phenomenological Theories

The basic problem sought to be solved in these theories was to obtain some functional relation for the Reynolds stress, $\overline{\rho u_x u_y}$ by assuming some mechanism for turbulence. Thus, we note their hypothetical basis and the case for their inadequacy. It needs also to be noted that all the above development has been based on a Lagrangian point of view, i.e., by following the paths of particles.

Boussinesq sought to relate the Reynolds stress to an apparent viscosity which he called eddy viscosity by analogy with molecular viscosity, by the following relation,

$$\overline{u_x u_y} = - \mu_{\text{eddy}} \left(\frac{d\overline{U}_x}{dy} \right) \quad (13)$$

where,

$$\mu_{\text{eddy}} = \text{eddy viscosity.}$$

The above Eq. 13 is extremely important in the following development. By a similar analogy the eddy diffusion coefficient can be defined by the following equation.

$$J = e \left(\frac{d\bar{\rho}}{dy} \right) \quad (14)$$

where,

J = mass flux

e = eddy diffusivity for mass

The diffusion due to eddies is assumed to act in addition to that due to molecular effects. The concept of eddy diffusivity is applied in the solution for the backwashed filter bed. Though many problems in engineering can be solved using it, the fact that the eddy diffusivity is not constant from system to system makes it a rather inadequate concept. The analogies between transport of mass, momentum and energy has resulted in the use of the above concept to solve a number of important engineering problems. However, the analogies between mass and energy on the one hand, and momentum on the other often break down in specific applications. This is due to the fact that one cannot have a rigorous analogy between scalar and vector quantities.

All the other phenomenological theories also hypothesized on the turbulent stress developed above. Prandtl intuitively assumed that the eddy stress are related to a fixed length l , which he called the mixing length. He qualitatively assumed that this length characterized the average size of eddies in the turbulent fluid field.

Prandtl's theory yields the following equation,

$$\frac{d\bar{U}}{dy} = \frac{U^*}{ky} \quad (15)$$

where,

$$U^* = \sqrt{\frac{\tau_w}{\rho}} = \text{friction velocity}$$

$k = \text{constant}$

$\tau_w = \text{shear stress at the wall}$

To obtain this equation Prandtl assumed that the viscous stress was negligible in comparison to the eddy stress which was constant in the entire flow field. The above equation yields the logarithmic distribution of velocity with respect to distance for turbulent flow. The equation cannot be used near the wall.

Taylor developed the vorticity-transport theory, again assuming that the viscous terms are negligible.

Von Karman's similarity hypothesis assumed that viscous effects predominate only in the vicinity of the wall and obtained a relation between the velocity gradients at two points of the velocity field and the mixing length.

All the phenomenological theories provide the following important conclusions for a turbulent field in pipe flows, which are extremely relevant to the backwashing theory developed later where the cleaning action is hypothesized on the basis of shear stresses near the particles and mass diffusion in the main fluid flow channels.

(i) A viscous sublayer (boundary layer) exists next to the pipe wall where turbulence is negligible and the shear stress is equal to that at the wall.

(ii) At the centre of the flow region exists a turbulent core, where eddy viscosity and turbulent stresses predominate and the effect of shear stresses due to molecular viscosity are negligible.

(iii) In between the turbulent core and the viscous sublayer exists a buffer zone where both eddy and molecular effects are both important. Thus viscous as well as turbulent stresses play dominant roles.

Further details of the above theories and the best velocity distribution laws for each of the areas, are dealt with in detail in Brodkey (14).

D. The Statistical Theory of Turbulence

The previous development and the phenomenological theories brings to focus the crux of the problem in turbulence; namely, the necessity for additional relations for solving the Reynolds equation. In particular, relations for solving the fluctuating velocity terms or the Reynolds stresses are required. Additional relations are obtained by treating the problem with rigorous statistical theory, on the basis that the fluctuations are sufficiently numerous and random.

An intuitive physical model of turbulence describes it as consisting of the superposition of ever-smaller size of eddies or alternatively as the superposition of ever-smaller periodic motions. However this process must necessarily have a lower limit where the viscous effects of real fluids predominate over the eddying motion. The upper limit to the size of the eddies is dependent on the bounds of the system. It has been shown that the larger eddies transfer their energy to smaller eddies and these in turn to still smaller eddies until viscous effects

predominate. All the eddies have certain quanta of kinetic energy associated with them. Using Fourier analysis it is possible to allocate a certain quantum of the total energy to each distinct frequency. The size of the minimum eddy corresponds to the maximum frequency that occurs in the turbulent motion. This distribution of frequencies is called an energy spectrum.

Taylor (68) in 1935 was the first to propose the fundamental idea of the statistical theory; namely, if we consider two points in the turbulent field separated by a distance smaller than the eddy diameter, then a high degree of correlation exists between the velocities at these two points at a particular instant. If the points are several eddies apart, little correlation can be expected.

1. Some basic concepts and definitions

The definition of turbulence implies that if the time of observation is long enough, the statistical characteristics will repeat in time as well as space.

If τ is a period of time long enough to include a sufficient number of fluctuations to be able to compute a stable mean value \bar{U} , then

$$\text{Temporal mean velocity, } \bar{U} = \frac{1}{\tau} \int_{t-\frac{\tau}{2}}^{t+\frac{\tau}{2}} U dt \quad (16)$$

The instantaneous velocity U , has already been defined in Eq. 7. The violence or intensity of turbulence is defined by the root-mean-square value of the fluctuating velocity as,

$$u' = \sqrt{\frac{u^2}{2}} \quad (17)$$

where,

u' = r.m.s. of fluctuating velocity

$u = U - \bar{U}$ = fluctuating velocity

The intensity or relative intensity is defined as the ratio of the root mean square fluctuating velocity to the mean velocity.

$$\text{Intensity of Turbulence} = \frac{u'}{U} = \frac{\sqrt{\frac{u^2}{2}}}{U} \quad (18)$$

Homogeneous turbulence implies that, u'_x is constant for all values of x . Similarly, for u'_y and u'_z . Isotropic turbulence means that all values of the r.m.s. velocities are equal.

$$\text{i.e.} \quad u'_x = u'_y = u'_z \quad \text{for all } x, y \text{ and } z$$

Isotropic homogeneous flow by its very nature has no cross velocity terms of the type $\overline{u_x u_y}$, $\overline{u_x u_z}$ and $\overline{u_y u_z}$ and hence no Reynolds stresses occur in the Reynolds Eq. 12.

Consider a statistical property of the random variable, velocity u , at two points separated by a distance r . The Eulerian correlation function $R_E(r)$ is defined as,

$$R_E(r) = \frac{\overline{u(x)u(x+r)}}{u'(x)u'(x+r)} \quad (19)$$

For isotropic turbulence the fluctuating velocities are equal and Eq. 19 reduces to,

$$R_E(r) = \frac{\overline{u(x)u(x+r)}}{u'^2} \quad (19a)$$

A similar correlation function can be defined for a Lagrangian system for isotropic turbulence,

$$R_L(t) = \frac{\overline{u(t)u(t+\tau)}}{u'^2} \quad (20)$$

where,

$$R_L(t) = \text{Lagrangian correlation function.}$$

Eq. 20 can be simplified to,

$$R_L(t) = \frac{\overline{u_{t_1} u_{t_2}}}{u'^2} \quad (20a)$$

The covariance $\overline{u_{t_1} u_{t_2}}$ represents the average for a number of particles

of the product of the velocity at a time t_1 , and its velocity after a time t_2 . For large values of $(t_2 - t_1)$ there is no correlation between

u_{t_1} and u_{t_2} and $\overline{u_{t_1} u_{t_2}} = 0$. For a small time $(t_2 - t_1)$ the velocity of

the particle at t_2 will resemble that of the particle at time t_1 . This idea is the cornerstone of Taylor's theory.

The length scale of turbulence can be interpreted in a crude manner as the average size of the turbulent eddies or the size of the packet of fluid all of which has the same velocity. It has been defined in several alternate ways.

For a Lagrangian system the length scale L_L is defined as,

$$L_L = T_L u' \quad (21)$$

where,

$$T_L = \text{Lagrangian time scale of turbulence}$$

The Lagrangian time scale T_L is defined as,

$$T_L = \int_0^{\infty} R_L(t) dt \quad (21a)$$

Similarly, for Eulerian system the integration is carried out over the entire space system as,

$$L_E = \int_0^{\infty} R_E(r) dr \quad (22)$$

where,

$$L_E = \text{Eulerian scale of turbulence.}$$

The above definitions are directly used in the models developed by Hanratty et al. (40) and Handley et al. (39) for describing the diffusional characteristics of particulate fluidized beds. A turbulent field can be described by equations with the double correlations defined in Eqs. 19, 20 and by similar triple correlations. The rather complex random wave form can be reduced to an equivalent set of sine waves of various amplitudes and frequencies by a Fourier transform. For isotropic turbulence the Fourier transforms exist as finite quantities when integrated over all space and no approximations are needed.

Taylor (69) was the first to analyze the one-dimensional energy spectrum using Fourier transforms. The analysis can be extended to three dimensions, however the notation becomes complex without using tensors. For purpose of illustration the one dimensional Taylor treatment is briefly recorded. The following is essential for understanding the briefly reported work of Tesarik (70) who calculated the scale of turbulence as well as the energy spectrum function $F(n')$, for conditions similar to backwashing.

Let the frequencies of the waves between n' and $(n' + dn')$ make a contribution $\overline{u^2} F(n')$ to the mean value of $\overline{u^2}$.

Hence,

$$\int_0^{\infty} F(n') dn' = 1 \quad (23)$$

where,

n' = frequency of sine wave

$F(n')$ = fraction of total energy of turbulence in
energy spectrum.

Consider Eq. 20.

Assuming, $u = \phi(t) = \phi(x/\bar{U})$, Eq. 20 for the Lagrangian correlation is of the form,

$$R_L(t) = \frac{\overline{\phi(t)\phi(t + \frac{x}{U})}}{\overline{u^2}}$$

It can be shown (69) that,

$$\int_{-\infty}^{\infty} \phi(t) \phi(t + \frac{x}{U}) dt = 2\pi^2 \int_0^{\infty} (I_1^2 + I_2^2) \text{Cos}(\frac{2\pi n' x}{U}) dn \quad (24)$$

where,

$$I_1 = \frac{1}{\pi} \int_0^T u \text{Cos } 2\pi n' t dt$$

$$I_2 = \frac{1}{\pi} \int_0^T u \text{Sin } 2\pi n' t dt$$

T = time sufficiently long to obtain average values of fluctuations.

Using the Fourier Integral Theorem,

$$R_L = \int_0^{\infty} F(n') \text{Cos}(\frac{2\pi n' x}{U}) dn \quad (25)$$

$$F(n') = \frac{4}{U} \int_0^{\infty} R_L \text{Cos}(\frac{2\pi n' x}{U}) dx \quad (26)$$

In other words, the correlation coefficient R_L and $\frac{\overline{UF(n')}}{\sqrt{8\pi}}$ are

Fourier transforms of one another. Thus, if $F(n')$ is observed R_L can be calculated and vice versa.

The above functions and definitions, the relative intensity, the correlation functions, the scale of turbulence and the energy spectrum form the basic tools of the statistical theory. The application of these concepts to the Reynolds Eq. 12 results in the famous Von Karman-Howarth equation for isotropic turbulence (14, 36). This equation

cannot be solved, though the terms in it can be experimentally measured. The difficulty in the solution is that due to non-linearity, if an equation is obtained with a double velocity correlation, then it has inertial terms of the third order. If an equation of the third order is formed then it has terms of the fourth order. This gives rise to the closure problem of turbulence theory. An infinite set of dynamical equations can be formed with the set being indeterminate by one unknown. The reduction of the indeterminate set of equations by various approximations and empirical approaches to obtain solutions, form a large part of the work done in the statistical theory. The material is not relevant to the present study and will not be reviewed here. Complete details can be found elsewhere (14, 42).

2. Turbulent dispersion or diffusion

The terminology defined above and the basic concepts developed will now be applied to the specific problem of turbulent diffusion. An insight into the mechanism of turbulent diffusion is the prime purpose of the above review of turbulence theory. It has been found that the particulates fluidized bed (14, 39, 40) and similarly, the backwashed filter bed (70) can be well described by the statistical turbulence equations of Taylor's theory of diffusion.

The fundamental mechanics of a turbulent field is due to fluctuating fluid velocities and an ever decreasing system of eddies. The particulates fluidized bed is a system wherein the constantly moving suspended solid system causes analogous fluctuating fluid velocities in the fluidizing medium. Furthermore, it has been shown (4, 48, 65) that

the fluidized system is inherently unstable and small disturbances in the distribution of particles, or in other words porosity fluctuations, tend to rise through the bed and grow. Since there are circulation effects too, the system is comparable to the fluid field with various eddies. Thus, the diffusion characteristics of the two systems are physically similar.

Consider a Lagrangian system of co-ordinates, i.e. the co-ordinates of position and velocity along a path, in a uniform isotropic turbulent field. Consider the divergence, spread or dispersion of particles from a fixed point source in a steady field by eddying motion.

In the above field consider the displacement X and velocity u along the x -axis. The intensity $\overline{u^2}$ is constant, since the field is isotropic. Let u_t and u_{t_1} be the values of u at time t and t_1 respectively.

From Eq. 20a, the definition for the Lagrangian correlation function, gives

$$R_L(t) = \frac{\overline{u_t u_{t_1}}}{\overline{u^2}}$$

Hence,

$$\int_0^{t'} \overline{u_t u_{t_1}} dt_1 = \overline{u^2} \int_0^{t'} R_L(t) dt_1 \quad (27)$$

Let $(t_1 - t') = T$, and since $R_L(t)$ is an even function of t , Eq. 27 maybe written as,

$$\int_0^{t'} \overline{u_t u_{t_1}} dt_1 = \overline{u^2} \int_0^{t'} R_L(T) dT$$

But,

$$\int_0^{t'} \overline{u_t u_{t_1}} dt_1 = \overline{u_t \int_0^{t'} u_{t_1} dt_1} = \overline{u_t X} = \overline{uX} \quad (28)$$

where,

$$X = \int_0^{t'} u_{t_1} dt_1 = \text{displacement of fluid particle in time } t'$$

From Eqs. 27 and 28,

$$\overline{u^2} \int_0^{t'} R_L(T) dT = \overline{uX} = \overline{\frac{1}{2} \frac{dx^2}{dx} \frac{dx}{dt_1}} = \frac{1}{2} \frac{dX^2}{dT}$$

Integrating,

$$\overline{X^2} = 2 \overline{u^2} \int_0^t dT \int_0^{t'} R_L(T) dT \quad (29)$$

Equation 29 is the relation obtained by Taylor.

Consider the integration by parts, $\int V du = Vu - \int u dV$,

where

$$du = dT \text{ and } V = \int_0^{t'} R_L(T) dT.$$

Hence,

$$\begin{aligned} \int_0^t dT \int_0^{t'} R_L(T) dT &= [T \int_0^{t'} R_L(T) dT]_0^t - \int_0^t T R_L(T) dT \\ &= t \int_0^t R_L(T) dT - \int_0^t T R_L(T) dT \end{aligned}$$

$$\text{i.e.} \quad \int_0^t dT \int_0^{t'} R_L(T) dT = \int_0^t (t - T) R_L(T) dT \quad (30)$$

Substituting Eq. 30 in Eq. 29,

$$\overline{X^2} = 2 \overline{u^2} \int_0^t (t - T) R_L(T) dT \quad (31)$$

This well known result was first obtained by Kampe de Feriet and is quoted in most texts on turbulence (14, 42). The properties of $R_L(T)$ are: $R_L(0) = 1$ since the correlation function has to be 1. Since the system is homogeneous the function $R_L(T)$ is symmetric about the origin; however, no correlation exists at large values of T , therefore $R_L(\infty) \rightarrow 0$.

Consider the case,

$$R_L(0) \rightarrow 1 \text{ as } T \rightarrow 0$$

Integrating Eq. 31 with these approximations,

$$\overline{X^2} = 2 \overline{u^2} \int_0^t t dT = \overline{u^2} t^2$$

Therefore,

$$\sqrt{\frac{\overline{X^2}}{2}} = t \sqrt{\frac{\overline{u^2}}{2}} \quad (32)$$

Thus as $t \rightarrow 0$, diffusion is directly proportional to the time. For large values of t , $R_L(t) \rightarrow 0$, thus $\int R_L(T) dT \rightarrow \text{constant}$. In Eq. 31, the second term becomes small compared with the first term, hence,

$$\overline{X^2} = 2 \overline{u^2} \int_0^t R_L(T) dT \approx 2 \overline{u^2} t \cdot \text{constant}$$

therefore,

$$\sqrt{\overline{X^2}} = \text{constant} \cdot \sqrt{t} \quad (33)$$

Thus for large times the dispersion is proportional to the square root of the time.

For the root mean square displacement $\sqrt{\overline{X^2}}$ at intermediate times, the functional dependence of $R_L(T)$ upon T must be known.

It is convenient to assume,

$$R_L(T) = e^{-T/T_L} \quad (34)$$

where,

T_L = a constant, the Lagrangian Scale of Turbulence defined by Eq. 21 and regarded as the average lifetime of eddies, or the average time length of undeflected particle paths.

Substituting Eq. 34 in Eq. 31 and integrating for a general time t ,

$$\overline{X^2} = 2 \overline{u^2} \int_0^t (t - T) e^{-T/T_L} dT$$

For integration by parts, consider

$$\begin{aligned}
 \int_0^t (t-T)e^{-T/T_L} dT &= \int_0^t (t-T) \frac{d}{dT} (-T_L e^{-T/T_L}) dT \\
 &= [-(t-T)T_L e^{-T/T_L}]_0^t + \int_0^t T_L e^{T/T_L} \frac{d}{dT}(t-T) dT \\
 &= tT_L - T_L \int_0^t e^{-T/T_L} dT \\
 &= tT_L - T_L [-T_L e^{-T/T_L}]_0^t \\
 &= tT_L - T_L^2 (e^{-t/T_L} - 1)
 \end{aligned}$$

Thus,

$$\overline{X^2} = 2 \overline{u^2} T_L^2 \left[\frac{t}{T_L} - (1 - e^{-t/T_L}) \right] \quad (35)$$

For large times t , $e^{-t/T_L} \rightarrow 0$ and Eq. 35 reduces to,

$$\overline{X^2} = (2 \overline{u^2} T_L) t - 2 \overline{u^2} T_L^2 \quad (36)$$

Equation 36 is a straight line with slope $(2 \overline{u^2} T_L)$ and intercept on the ordinate $(2 \overline{u^2} T_L^2)$. Hence, the intercept on the abscissa is T_L . Thus by plotting the diffusion characteristics at large times t , ($t > 10 T_L$) and extrapolating the straight line section to the abscissa it is possible to measure the scale of turbulence T_L and hence

calculate L_L . This technique was used by Hanratty et al. (40) and Handley et al. (39) to study the diffusion in particulate fluidized beds. It has been found that there is excellent agreement between the theory developed above and experiments (14, 39, 40, 42).

One of the most frequently used parameters to describe turbulent diffusion is the eddy diffusivity E . It represents the average spread of some property of a physical system and by direct analogy with molecular diffusion from a fixed point it can be defined as,

$$E = \frac{\overline{X^2}}{2t} \quad (37)$$

It should be noted that E is not a constant as molecular diffusivity is, but rather is a function of time t .

Combining Eqs. 35 and 37,

$$E = \overline{u^2} T_L \left[1 - \frac{T_L}{t} (1 - e^{-t/T_L}) \right] \quad (38)$$

Hanratty et al. (40) developed this equation for their studies of diffusion in particulate fluidized beds. The above equation shows that the eddy diffusivity reaches an asymptotic value for large times t (large compared to T_L), that is at large distances from the source of diffusion.

For large t , $e^{-t/T_L} \rightarrow 0$ and $\frac{T_L}{t} \rightarrow 0$, hence

$$E = \overline{u^2} T_L \quad (39)$$

From Eqs. 17 and 21a,

$$L_L = T_L u' = T_L \sqrt{\frac{u^2}{2}}$$

Hence Eq. 39 reduces to,

$$E = L_L \sqrt{\frac{u^2}{2}} \quad (40)$$

The above equation which represents the limiting value of the eddy diffusivity as defined by Eq. 37 is also frequently used as a definition for the eddy diffusivity E . This equation can also be obtained by analogy with mixing length theory. The definition of eddy diffusivity as given by Eq. 40 was used by Cairns and Prausnitz (16, 17) in their studies of mixing in liquid fluidized beds. The above development shows that the definitions of eddy diffusivity by Eqs. 37 and 40 are consistent with one another, both having dimensions of $L^2 T^{-1}$.

Most correlations for mixing and diffusion phenomena are described by the non-dimensional Peclet group defined as,

$$Pe = \frac{Ud}{E} = \frac{Ud}{L_L \sqrt{\frac{u^2}{2}}} \quad (41)$$

A maximum eddy diffusivity results in a minimum Peclet Number.

Thus, the maximum diffusion or spreading in a system is characterized by a minimum Peclet Number. Alternatively, on the basis of the definition for eddy diffusivity, systems having the same value of the r.m.s.

fluctuating velocity $\sqrt{\frac{u^2}{2}}$, will have a maximum eddy diffusivity, if the scale of turbulence is a maximum.

The above concepts are the ones used to provide the frequently noted experimental result that most turbulence parameters (eddy diffusivity and scale of turbulence) maximized around a porosity of 0.65-0.70 in particulates fluidized beds. This is the central result used in this thesis to determine the optimum condition for backwashing.

For a complete, current and more advanced review of turbulent dispersion reference should be made to Corrsin's review paper (27).

An attempt has been made in the above review to provide a coherent but concise development of turbulence theory as required for analyzing the literature in fluidization and developing a theory for optimum backwashing in the chapters to follow. During the course of presenting turbulence theory, the material having greatest significance to the literature quoted in the following chapters has been noted.

IV. LITERATURE REVIEW

The literature review is being developed, initially within the self contained fields of sanitary and chemical engineering with the final sections intermingling the ideas from both fields. The first section deals with all the literature in the sanitary engineering field. The second, critically analyses Ulug's work on backwashing. The third and fourth sections review the literature in chemical engineering, though some overlapping of ideas is inevitable; the third section describes the development of the idea of the predominance of hydrodynamic forces in fluidized beds in comparison to collisional forces, while the fourth section reviews the literature which reveals the fact of maximization of most turbulence parameters at the expanded porosity of 0.65-0.70. This study essentially concentrates on the optimum expansion for backwash, hence, the literature reviewed is directly pertinent to this topic. The writer has previously reviewed the other concepts of fluidization and their application to backwashing (2); the previous study is an essential introductory supplement to the present work.

A. The Sanitary Engineering Literature

1. Filter backwashing

Perhaps one word more than any other which brings to mind slow sand filters is "schmutzdecke". In fact it was the cause of nearly a decade lost to filtration progress as many authorities argued its significance in filtration through a deep granular bed. It was believed as a corollary from slow sand filtration that the dirty coating on the grains in a rapid

filter improved bacterial removal and backwashing which removed all of this coating was assumed to be detrimental. This assumption was probably one of the factors which lead to low backwash rates, 8-15 in. rise per minute (6-11 gpm/sq ft). The lower rates did not cause sufficient expansion and auxiliary means of agitation was provided with mechanical rakes or air scour (31). Air scour systems with low velocity water wash caused problems of mud balls, clogging of strainers and gravel displacement and air scour disappeared from the U. S. water treatment scene circa 1900.

Hulbert and Herring's (46) excellent work in 1929 laid the foundation for backwashing practice in the United States and the oft quoted rule of thumb of 50 percent expansion for effective backwashing. Some of the conclusions of this study are worthy of record even today.

(i) They recommended the use of a high velocity wash and that sand expansion be used as the index of filter washing while earlier criteria was the rise of water in inches per minute.

(ii) They suggested that 50-60 percent expansion of the sand provided satisfactory results in preventing mud-ball formation, shrinkage of the filter sand and consequent cracking.

(iii) They indicated that bacterial removal efficiency was unaffected by the lack of a coating on the sand.

(iv) They showed that the expansion characteristics of the sand in a 3/4 inch diameter model filter and the actual filter were the same.

When first reported the above seemed to be the panacea for all ills of the filter; but Hudson (44) and Baylis (8) continued to report that even 50 percent expansion did not eliminate mud-ball formation. These

workers were the initiators of the use of surface wash systems in the 1930's. On the basis of fundamental theoretical considerations (negligible collisional effects) the writer of this thesis believes that surface wash systems do have significant advantages in improving the cleanliness of the sand during backwashing. There was a lull in research related to backwashing in the two decades following the above era.

In the fifties, Baylis (9, 10, 11) and Hudson (45) continued to report on the washing of filters and their experiences at the Chicago Filtration Plant. They repeatedly stressed that most maintenance problems were an offshoot of backwashing effects. They sought to explain qualitatively the formation of "sand boils", "jet action", "sand leakage", "gravel mounding" and traced the origin of all these to the effects of backwashing. Baylis also suggested (9) without any experimental evidence that 20-25 percent expansion of the sand may be sufficient for cleaning.

Fair and Geyer (33, p. 679) sought to associate the maximum scouring action in backwash with the point of minimum fluidization of the portion of the bed which had been penetrated by the floc.

Johnson and Cleasby (49) made a plant scale study and showed how the effluent quality in the run following backwash could be used for purposes of evaluating the effectiveness of the wash. They also showed that the backwash rate that produced 16-18 percent expansion was the best rate for the conditions studied. It should be noted that this was the maximum rate studied and the basis for selecting this rate as the optimum is questionable. Two other conclusions drawn in the study were

noteworthy. (i) They indicated correctly, that the shear on larger grains was larger for the same wash rate and (ii) they incorrectly stated that other cleaning mechanisms like collisions in the fluidized state were important.

Rimer (60) in a comparative study of single and trimedia filters and their associated backwashing effects concluded that, for a conventional filter the rate of filtration did not significantly affect the backwash rate; however, for the multi media filter increased filtration rates required larger wash rates. He also noted that the best backwash for the trimedia filter was a two stage sequential wash. One for fluidization of the coal layer and a subsequent wash which over-expanded the coal layers while washing the sand layers. The possible danger of carrying away the lighter media under the overexpanded conditions was mentioned. Rimer's results (60) can be elegantly explained by the theory of optimum backwash to be developed in a later chapter.

Two of the very few studies which have probed backwashing from a fundamental theoretical view were done by Camp (19) and Camp et al. (20). The first study dealing principally with filtration, nevertheless had a considerable section on the hydraulics of backwashing. The written discussion of this paper by Tesarik (70) and its closure by the author were noteworthy contributions which are directly related to this dissertation.

Tesarik (70) reported on the studies he had made of applying the theories developed in the field of turbulence to backwashing. The theories mentioned are developed in the previously recorded review of turbulence. This is the only known report in the sanitary engineering

literature of the use of turbulence theory to study the behavior of backwashed beds. He computed the mean square variations of velocity components (see Eq. 17 of this thesis) in a fluidized bed of spheres 0.56 mm in size with a mass density ρ_s of 3.008 g per cc and found them approximately equal to the approach velocity V of 4 cm per sec. Consequently, he stated that the degree of turbulence in a fluidized bed of sand or anthracite is high in comparison to the flow of clear fluid. Tesarik also made studies on the Eulerian correlation function (Eq. 19a of this thesis). Based on flow visualization he showed that the average size of eddies given by Eq. 22 of this thesis was approximately 0.7 cm.

That is, as in Eq. 22,

$$L_E = \int_0^5 R_E(r) dr \approx 0.7 \text{ cm}$$

Tesarik then used Taylor's analysis of the energy spectrum as developed in Eqs. 23 to 26, to determine the spectrum curve in the above mentioned fluidized bed. Using the Fourier integral theorem as in Taylor's theory, he determined the spectrum curve. The energy spectrum showed that the fluctuations with the lowest frequencies n' , less than 3 vibrations per sec, chiefly influenced the behavior of the fluidized bed.

Camp (18) in the closure of the above discussions studied the velocity gradients in a filter during backwashing, in order to shed some light on the magnitude of the adhesive forces. For the mean velocity gradient within the pores, he gave the following equation.

$$G = \sqrt{\frac{giV}{\nu\epsilon}} \quad (42)$$

where,

$$G = \frac{dV'}{dz} = \text{mean velocity gradient in the pores}$$

$$i = \frac{dh}{dz} = \text{hydraulic gradient in direction of flow}$$

ϵ = porosity

V = superficial fluid velocity

$$V' = \frac{V}{\epsilon} = \text{average fluid velocity within the pores}$$

$$\nu = \frac{\mu}{\rho} = \text{kinematic viscosity}$$

g = acceleration due to gravity

The writer of this thesis wishes to strongly focus attention on this equation, for it forms one of the fundamental equations in the mathematical theory of optimum backwashing developed by the writer in one of the following chapters.

The results quoted by Camp when using Eq. 42 are also of the greatest significance in this thesis. The mean shear stress S within the pores of the filter is given by,

$$S = \mu \frac{dV'}{dz} = \mu G \quad (43)$$

where,

S = mean shear stress

Using Eqs. 42 and 43 Camp (18) calculated the mean shear stresses during filtration, at the start and end of a run, and during backwashing. He found that the shear stress at the start of filtration was 2.17 dynes per sq cm and at the end of a similar run it was 8.88 dynes per sq cm. During backwashing the shear stress was 2.8 dynes per sq cm. These values caused Camp to hypothesize that the floc sheaths during filtration were resting on the grains with little adhesion and that the tensile strength of the floc was sufficient to resist the shearing forces. Further, he noted that the shear stress at the pore wall is 1.412 times the mean shear stress. For the purpose of comparing these values of shear stress with coulombic and molecular bonds, including Van der Waals forces, he computed the energy equivalent of the shear stress as 1.2×10^{-9} Kcal per mole of water. On the basis of this figure, Camp concluded that the number of molecular bonds per square centimeter must be very small indeed.

The second paper by Camp et al. (20) was devoted entirely to backwashing. The paper studied the backwashing operation theoretically as well as experimentally. Several interesting facts were noted in the paper. The authors suggested that the rubbing of grains together was a negligible factor in cleansing, because nearly all the energy of the wash water was required to suspend the grains. The writer of this thesis drew this same conclusion with considerably more evidence using the literature in fluidization (2). This fact also forms one of the basic hypotheses of this dissertation. It was found that air wash caused a decrease in the height of the fluidized bed. They showed that no breakdown of the floc sheaths covering the grains occurred even at

the end of a run when the shear force was the greatest, as evidenced by the fact that the head loss continued to increase because of continued deposits, albeit at sharply decreased rates. They also studied the cause and removal of mud-balls and concluded that the chief cause for mud-ball formation was inadequate fluidization. Air wash did help in smaller fragmentation of the mud-balls, but their removal from the bed required wash rates far beyond those used in practice. The paper suggested that, on the basis of the theory developed and the experimental procedures delineated, the backwash rates and the media to be used should be selected on the basis of pilot plant studies.

The only other study of major proportions was Ulug's work (71). The work described a theoretical and experimental study of backwashing. The theoretical work was based on developing the classical hydrodynamical equations as applied to a fluidized bed. Using Camp's formulae for the shear stress Eqs. 42 and 43, and modifying it to $[(\text{mean shear stress}) / \sqrt{\text{approach velocity}}]$, he concluded that an optimum wash rate resulted at an expansion of 25-30 percent, for a bed composed of uniform glass ballotini of 0.90 mm. On the basis of some of the literature in fluidization and the fact that in developing the equations for a backwashed bed no significant forces due to collisional interactions were detectable, he concluded that there were few collisions of particles in the fluidized state. Some of the experimental techniques used in the study were noteworthy. Studies were made on the settling velocities of particles, the hydraulics of backwashing, the analysis of backwashing based on flow visualization using a cine camera and determination of the efficiency of washing by data collection on the removal of suspended

solids and wash water turbidities. The study is a noteworthy contribution to a fundamental approach to backwashing and since it overlaps many areas of this study, it has been critically analyzed in more detail in a subsequent section of this dissertation.

The importance of backwashing in the operation of water treatment plants and the paucity of knowledge in the fundamental mechanisms of backwashing is best evidenced by the following reports and papers (6, 41, 43). The first reference is a collage of discussions of the operation of backwashing systems in fifty treatment plants all over the U.S.A. It indicated some significant statistics. Most plants reported a backwash water usage of 2 percent. The frequency of wash varied from as short as 8 hours to as long as 900 hours with most plants washing at frequencies of 68 hours. The time of wash was most often determined by the head loss across the filter. A significant reportage was that 76 percent of the plants used a surface wash with the normal backwash. It was reported that, of all the processes in a water treatment plant, filter backwashing was the most variable in respect of frequency, technique, control, cost, as well as effectiveness. For a 10-million gallons per day plant producing water at \$100 per million gallons, a reduction in use of wash water from 2.5 percent to 1.5 percent could reduce annual operating costs by nearly \$5500. A considerable number of operators indicated that most filtration problems were caused by incorrect backwashing, and the use of surface wash and evenly distributed wash-water significantly improved filter performance. These reports indicate; (i) the importance of backwashing, (ii) the lack of fundamental knowledge which has resulted in wide variation in washing techniques,

and (iii) the tendency to move towards surface wash systems to improve backwashing performance.

The lack of knowledge in the mechanics and the mechanisms of backwashing has resulted in papers purporting to correct the ill effects of backwashing using baffles etc., in the backwash water above the fluidized bed (41, 43). Even the operators noted above, have found through experience that even distribution of the washwater improves the washing operation. Thus, uniformity control in backwashing can only be achieved at the distribution system of the washwater.

The above review spotlights the current status of knowledge in backwashing in the sanitary engineering field. It clearly shows that even though one of the chief causes of operating problems in filters is the backwashing process, only a limited amount of study has been devoted to it (6, 9, 10, 11, 45) in comparison to studies in filtration. However, recent studies (2, 20, 70, 71) indicate an encouraging movement towards more fundamental approaches. These studies have brought to light several facts of importance.

(i) They have exposed the myth (5, 6, 33) that particle collisions and abrasion are significant in comparison to the hydrodynamic forces (2, 20, 71). A review of the considerable literature in fluidization which supports this conclusion is given in one of the following sections.

(ii) Even though the actual fluid velocities in a backwashed bed are in the transitional regime, the interaction of the fluid and particle fields create a turbulent fluid regime, which is amenable for treatment by the statistical theory of turbulence (2, 70, 71).

(iii) In the final analysis, the fluidized bed is an unsatisfactory means of achieving ideal cleansing of the media and additions like surface wash and air wash are becoming increasingly important (2, 6, 9, 10, 11, 20).

(iv) The most notable trend in recent papers has been the search towards developing rational criteria for optimizing the backwashing operation within the constraint of (iii) (2, 49, 71). This dissertation is specifically directed towards this end.

2. A critique of Salim Ulug's work on backwashing

At the University of London, Ulug made a noteworthy contribution to the study of backwashing filters in 1967 (71). Some mention of his work has been made in the previous section. The breadth and scope of Ulug's work is sufficiently significant that it warrants a critical analytical review in a separate subsection. The study was both theoretical as well as experimental.

In the theoretical section, he developed equations starting with the basic differential equations of fluid mechanics; namely, the relations of conservation of mass, (Eq. 1 of this thesis) momentum (Eq. 3 of this thesis) and the equation of state. The expanding fluidized bed was considered analogous to a continuous elastic medium of vanishing compressibility, in which the propagation of disturbances is infinite. Ulug treated the entire bed as a macroscopic system with the solid and liquid phases treated together as a single system. The analysis closely followed that of Murray (56) who also developed similar equations for a fluidized system. However, the approximation made by Murray that

$\rho_f \ll \rho_s$, enabled him to simplify the equations and obtain analytical solutions for the case of aggregative fluidization. Ulug presented the flow equations without attempting any mathematical solution.

The pertinent variables were then collected and dimensionless groups were formed. The complex hydrodynamic system was represented by a general relation of the form,

$$\lambda' = \text{Constant} \times (\text{Re}')^m \quad (44)$$

where

λ' = modified friction factor

Re' = modified Reynolds number

m = empirically measured exponent

Though Eq. 44 was shown in the above simple form, the modified dimensionless numbers λ' and Re' were formed by assuming the incorporation of several parameters like, a porosity function, viscous resistance coefficient and inertial resistance. Using an analogy of flow around spheres, Ulug finally obtained an empirical equation of the form,

$$\frac{8}{\pi} \frac{F_D}{N d^2 \rho_f \left(\frac{V}{\epsilon}\right)^2} = 3.426 \times 10^6 \left[\frac{\frac{V}{\epsilon} d \rho_f}{\mu} \right]^{-2.95} \quad (45)$$

where,

F_D = Total drag force on system

N = total number of particles in bed

d = length characteristic of granular media.

The above expression does not have general validity, it only holds for Ulug's experiments. Though the technique can be adopted for any system, it implies that a pilot plant has to be operated for determining the empirical constant 3.426×10^6 , and measurements must also be made to determine the total drag force on the system. The above equation can then be explicitly determined and it gives a relation between the superficial velocity and the porosity. Since the relation between porosity and velocity which we are setting out to determine can simply and easily be made on the pilot plant apparatus itself there is no need for the above development. The development of the above theory does have some value as an intellectual exercise, however, it has little use as an analytical or design equation, since it is necessary to obtain empirical constants for every system for which it is to be used. The writer of this thesis has presented a far simpler generalized model for direct use in design office practice (2, 3). A considerable part of Ulug's thesis consists of the theoretical work in developing the above Eq. 45 and the experimental determination of the empirical constants in the equation. Ulug studied the terminal settling velocities as a function of the hindered settling velocities for glass ballotini using the same method as Richardson and Zaki (59). They found that the superficial velocity V was related to the terminal settling velocity V_s of the particles composing the bed by the relation

$$\frac{V}{V_s} = \epsilon^{2.8}$$

The sections of the thesis that are more directly relevant to this study will now be analyzed in some detail. Ulug, in developing the basic differential equations, omitted the term arising from particle collision pressure, on the basis of the arguments presented in the fluidization literature (1, 48, 55, 56, 61, 62) that appreciable noise and increases in temperature due to such collisions were absent. He then found that these equations were applicable for investigating the mean shear stress on the grains and the mean velocity gradients within the pores of the system on the basis of Eq. 42. He found no significant forces or reactions not accounted for, and hence concluded that these forces of collision are negligible, for the system of particle sizes often used in filtration. Thus, Ulug's work provides additional evidence for the fact that collisional effects are negligible in back-washed filter beds.

In another phase of the study, the actual movements of individual particles were studied using cine films, similar to the technique used by Handley et al. (39). A detailed study was made on the statistical parameters of the particle velocities by analyzing the collected data with a digital computer. The particles studied were generally, those close to the wall of the 3.5 inch internal diameter filter and all showed a downward velocity. This confirms other studies made in fluidization (2) which indicate circulation patterns going up at the centre and down at the walls. These patterns are more predominant for small diameter systems as used in this study. Though the author measured values of the r.m.s. velocities $u(x)$ and $u(x + r)$ as in Eqs. 17-20, he has not tried to use any of the turbulence theories developed in an

earlier chapter of this thesis for analyzing the data. However, he did conclude as Tesarik did (70) that the particle fluctuating velocities were of the same order of magnitude as the approach velocities of the fluid. The author of this thesis studied all the velocity diagrams given by Ulug and noted that there were only a very few step wise sudden changes in the velocities of the particles. Though this analysis was not made by Ulug it provides impressive evidence of the fact that negligible particle collisions occur in the fluidized state.

In the final section of the dissertation, Ulug completed the study by applying the experimental data and the conclusions drawn from the above mentioned sections to determine the degree of bed cleanliness attained by applying different wash rates to the experimental bed after it was made dirty by a filtration cycle.

The dirtying run at 2 gpm/sq ft was made by filtering 160 liters of a suspension of fullers earth of concentration 200 p.p.m., through a 30 inch bed of uniform glass ballotini spheres of 0.9 mm diameter and 2.95 g/cc density. Seven runs were made on the single filter and the duration of the washing cycle was kept the same (12 minutes) in each backwashing cycle. The filter was washed at 10, 20, 25, 30, 35, 40 and 50 percent expansion in a series of seven runs. During the filtration runs, measurements were made of (i) the time variation of effluent quality, (ii) the measurement of the amount of accumulated solids at different layers of the filter bed by withdrawing samples of water, and (iii) the total head loss in the bed. During backwashing the following measurements were taken: (i) total solids removed from the filter bed during 12 minutes of backwashing, (ii) the time rate of change of

turbidity of the backwash effluents and (iii) the time rate of change of turbidity at different layers of the bed, which was measured by withdrawing samples of wash water at the desired layer. The solids removed from the filter were determined by analyzing the solids concentration in the total wash water used which was collected in a storage tank.

Ulug determined the efficiency of washing by making a mass balance on the suspended solids, by measuring the total solids retained in the filter and the total solids removed by the backwash water. He found that the percent removal of solids in backwashing increased continuously from 42.55 percent at 10 percent expansion to the maximum 91.62 percent at 50 percent expansion. He also found that most solids were removed within the first two minutes of wash. He determined efficiency of wash by dividing the percent removal, by the total wash water used in liters during 12 minutes, and hence obtained 25-30 percent expansion as the optimum wash.

Samples were taken during the backwashing cycle at various levels and times for turbidity measurements. From the total turbidity remaining in the filter at a given time, measured by withdrawing samples during the backwash, the percent removal of turbidity was calculated and plotted against the volume of wash water passed. The time change of turbidities of the wash water in the filter bed at different levels and different expansions was also plotted. From an analysis of these results, Ulug again concluded that 25-30 percent expansion was indeed the optimum. His results indicate that the retained turbidity in the bed at 50 percent expansion was more than that retained at 25-30 percent expansion.

In order to give a theoretical explanation for the observed result of 25-30 percent expansion as the optimum, Ulug determined the maximum shear stress per unit approach velocity for the system. By plotting $[(\text{shear stress}) / \sqrt{\text{velocity of approach}}]$ against expansion he found that this parameter gave a maximum at 25 percent expansion.

A critical and careful analysis of Ulug's work will indicate several inconsistencies in the analyses, which lead him to the invalid conclusion of optimum expansion of 25-30 percent. These expansions give porosities of the order of 0.52-0.54.

(i) If as shown, optimum expansion is 25 percent for a uniform system it clearly means that for a graded sand system to have the analogous hydrodynamical conditions for optimum cleaning, the expansion should be 25 percent at the top sections of the bed, since most solids are removed in these layers. This would lead to total bed expansion of the order of 5 percent, since the larger particles at the lower layers may not be even fluidized; this has been shown to be quite inadequate and one of the chief causes for mud-ball formation (6, 10, 20, 46, 49).

(ii) When a filter is washed, assuming turbulent diffusion is the controlling mechanism of cleaning at the initial stages of the wash, then as shown by Eqs. 32 and 33 the diffusion of particles will be initially proportional to time t , and subsequently to \sqrt{t} . Thus, washing the filter for the same time (12 mins) for different expansions can only result in the efficiency of wash being less effective per unit volume of wash water for the larger expansions, towards the end of the washing time. In fact, Ulug himself noted that most of the

solids were removed during the first two minutes of each wash. If the total suspended solids removed are then divided by the total volume of wash water, it will indicate an initial increasing efficiency and then a deteriorating efficiency at the higher expansions of 40 and 50 percent. Hence giving an invalid optimum at 25-30 percent expansion. For a valid analysis, the same volume of wash water must have been used or the suspended solids removed in equal volumes of total water should have been compared at the different expansions. The result of 25-30 percent expansion as the optimum should have been expected on the basis of the experimental procedure.

(iii) There seems to be some discrepancy in the results as reported on the percent removal of turbidity. According to the mass balance of the total suspended solids it was shown that the maximum removal of suspended solids (91.62 percent) was achieved by backwashing at 50 percent expansion for 12 minutes. This is a rational result, since this wash utilized the greatest amount of wash water. However, the turbidity of samples of water taken from the bed during this wash, seem to be much greater than the turbidities at the other expansions at the same times, whereas we would expect the turbidities to be diminished too. The author of this dissertation hypothesizes that this was because the 50 percent expansion run was probably the last run to be made. Thus, the media was coated continuously on each run and the last run had to deal with the largest amount of accumulated matter. This conclusion is not pure conjecture, it is based on experimental evidence which will be presented later in this thesis. No experimental details on how each run was started have been presented by Ulug. This shows

the problems of using a single filter to make comparative studies. It would be much better to use a set of filters simultaneously as in the present study. If a single filter were used, then new media or identical media should have been used for all the runs to avoid this type of error.

(iv) The final critical comment is on the theoretical prediction. It appears that Ulug has sought to relate how the shear stress can be modified to conform to the experimental evidence of 25-30 percent expansion being the optimum. This is possibly the reason for the selected parameter, $[(\text{shear stress})/\sqrt{\text{approach velocity}}]$. Purely on an analytical basis, if the shear stress is the primary parameter controlling the cleaning mechanism then we would expect that better cleaning will result by the higher shear stress. The only way an optimum will result is if the shear force itself reaches an optimum or a maximum. The present study provides a complete theory indicating that this maximum of shear occurs at a porosity of 0.65-0.70, and showing how well it is confirmed by the experimental evidence. Ulug has calculated the shear stress based on the same equation as that which will be used by the author of the present study for his optimum theory, namely, Camp's Eq. 42. Ulug has also shown that the shear force increases continuously throughout the expansions from 10 percent to 50 percent, which is also a confirmation of the theory to be developed in the latter sections of this thesis.

The above, rather detailed analysis of Ulug's work had to be presented to make it quite clear that the evidence he has presented is not a contradiction of the present study. A superficial analysis might lead one to assume as proven fact, the single sentence saying 25-30 percent

expansion was optimum and present it as a contradiction of the present study. However, the evidence as presented by Ulug leaves room for criticism, especially that section of the study which deals with the optimum backwash. This criticism, however, does not in any way imply that the study itself was less valuable. As already stated it is really the only known study of backwashing of a substantial scale.

B. The Fluidization Literature

1. Predominance of hydrodynamic forces in cleaning mechanism

The basic hydrodynamic behavior of a fluidized bed is frequently forgotten in trying to explain the removal of impurities from the grains of a filter sand during backwashing. Fair and Geyer (33, p. 676) mention that "substances adhering to the filter grains are dislodged... by the rubbing together of the suspended grains". Babbitt et al. (5, p. 494) state that the "purpose of such expansion is to cause the sand grains to rub against one another".

From purely theoretical grounds it should be expected that the suspension of particles in a rising stream of fluid requires a field of flow around each particle thus negating the concept of a number of particles rubbing together when fluidized. Considerable direct evidence (61, 62, 72) as well as most correlations (2, 53, 59) are based on the assumption that the particles are uniformly distributed within the beds. Thus, experimental verification of these correlations implies that the assumption of uniform distribution is reasonably valid. Further qualitative support of the above assumption is the fact that particle attrition

(73, p. 258) is negligibly small in fluidized beds and also the fact that however well filters are backwashed, sand growth by layers of deposited material frequently occurs in significant amounts. Johnson and Cleasby noted a growth from 0.43 mm to 0.65 mm in 14 years at the Ames plant (49).

The most significant work which removed the above from the realm of postulates to that of fact is Rowe's studies of "Drag forces in hydraulic models of fluidized beds I, II" (61, 62). He showed in a fundamental study that the drag forces on spheres arranged in regular arrays is extremely sensitive to the separation between the particles. The required modification to the drag coefficient for a single particle C_D , due to neighboring particles was effectively to multiply it by $(1 + \frac{0.68}{\delta})$, where $\delta = \frac{x}{d}$, dimensionless spacing of the particles based on the particle diameter, where x = clear distance between particles. Particles in various close packed arrays, ($\delta = 0.1 - 1.1$, $d = 0.5$ in.) were found to be subjected to a drag 68.5 times greater than that on an isolated particle for the same superficial velocity of the fluid (62). The value of the drag coefficient given by the above expression when $\delta = 0.01$ is 69 and was considered to refer to the terminal condition (61).

Rowe's studies showed that small local changes of particle concentration were unstable, because they required a very large change in the velocity distribution. A local decrease in particle concentration of 3 percent required the velocities to be doubled. It can be seen that as $\delta \rightarrow 0$, the drag coefficient $\rightarrow \infty$, however the expression does not

apply for $\delta = 0$. The studies indicate the existence of lateral repulsive hydrodynamic forces between particles; these became extremely large as the spacing between particles was reduced. Thus physical contacts between particles in fluidized beds were extremely limited and the particles were uniformly distributed in the fluid field. Rowe clearly indicates that his development does not eliminate the existence of particle contacts and concentration effects, but only that they cannot persist and their effect is negligible. Adler and Happel (1) have also indicated that solid-solid frictional effects in the low porosity range of fluidized beds where they should be most significant were inconsequential.

In a study of the stability of particulate fluidization, Jackson developed general equations of motion for a fluidized assembly of identical particles (48). In discussing the equations of motion, he neglected terms due to the direct interaction by collision, and justified it in two ways. Firstly, if collisions between particles were of comparable importance to drag forces than the number of particles per unit volume would be expected to decrease with height above the bed support, in the same way as the pressure of the atmosphere decreases with height above the earth's surface. Secondly, a posteriori justification was provided by the fact that the equations of motion obtained by neglecting collisions gave a good qualitative account of the main phenomena of fluidization.

Murray (55) summarized Jackson's arguments, and also gave some of the other reasons for the fact that negligible particle collisions occur in fluidized beds. He stated that,

Collision forces, which are a form of particle pressure, are also small, since, if such a term were important it would probably increase with n_p (n_p = number density of the particles). This would result in a gradation in n_p from the surface into the bed from zero to a finite value, this is not observed. The surface appears to be a discontinuity. Furthermore, observation of particle flow round a bubble by X-ray techniques seems to show little or no contact interference between neighbouring particles. Also, if collisions were frequent, the noise would be noticeable, which is not the case.

Though Murray was chiefly concerned with aggregative fluidization, it is a well known fact (2, 29, 55, 73) that the fluidized section of the bed outside the bubbles is very similar to a particulate fluidized bed at minimum fluidization. The hydrodynamical behavior of the continuous phase is, hence, similar to that of a particulate fluidized bed.

In a recent two-dimensional study (which may not effectively extrapolate to three dimensions) using a mono-layer of fluidized particles, Volpicelli et al. (72) indicated the presence of inhomogeneities in particle distribution within the bed. They presented photographic stills from their motion picture study of the fluidized beds. A study of these photographs by the author of this thesis showed that particle contacts are rare, which confirms Rowe's studies. Their studies must be interpreted with caution since they used steel balls and water as one of their systems; this system will exhibit marked aggregative tendencies. This study also indicated that particle flow patterns switch from a circulation regime to a regime of quasi-random motion as the voidage increases. This characteristic, confirmed by other workers too, has important implications in the development of criteria for backwashing at optimum rates.

In a recent Russian theoretical study, on the pseudo-turbulent diffusion of particles in homogeneous suspensions using tensor analysis, turbulence equations were developed for a two-phase system by Buevich and Markov (15). In a discussion on the collisional dissipation of energy the authors stated that particles under going collision have step-changes in velocity which will always be small for dilute suspensions. They also said that the collisions of particles suspended in a liquid are characteristically very gradual and there are no step-wise changes in the particle velocities. The latter being due to significant increases in the pressure in the liquid layer between the particles as they approach each other, and the need for "squeezing out" this layer before direct contact of the particles occurs. An analogous effect also occurred as particles approach a solid wall and in lubrication processes, when the lubricating liquid in the gap between bearing and slider played the part of this liquid layer. Hence, they concluded that any model of energy dissipation based on elastic collisions will be in error by at least an order of magnitude.

Ruckenstein (63) developed a physical model for a homogeneous (particulate) fluidized bed, using the equation of motion of one particle which is part of an ensemble of particles in interaction with a fluid. The equation is established by neglecting the interaction by collision of the particles of the ensemble.

All the above evidence in the fluidization literature pinpoints one single fact; that, the effect of collisional interactions between particles in the fluidized state is comparatively insignificant. This fact, now becoming more and more accepted in the sanitary engineering

literature (2, 3, 20, 71) indicates, that the age old argument whether abrasions between particles or the hydrodynamic shear forces are the predominant cleaning mechanism, will finally be laid to rest. This conclusion is also one of the basic assumptions of the theory developed by the author of this thesis in a later chapter.

2. Particulate fluidization and optimum turbulence

Analyzing a filter being backwashed, qualitatively, will indicate that at minimum fluidization individual particles have no motion and frequently the fluid motion is streamline, hence cleaning of the media will be negligible; at the other extreme overexpansion of the bed will also reduce the cleaning action due to large separations between particles. This macroscopic analysis indicates that somewhere between the two extremes lies an optimum condition which we seek.

The review of the literature quoted in this section indicates a striking phenomenon discovered in particulate fluidization research; namely, the existence of a maximum value for most turbulence parameters at a porosity of 0.65-0.70. This was the fact that originally lead the author towards inferring that the elusive condition of optimum backwash would probably be centered around this porosity. This entire dissertation revolves around proving, theoretically and experimentally, this hypothesis.

Considerable evidence was collated in a previous section to show that particle abrasions or collision are inconsequential in a fluidized bed. This fact leads immediately to the deduction of two very important hypotheses: (1) our present mode of cleaning filters by fluidization

has an intrinsic weakness in the process itself; and (ii) the most that can be achieved from the process is to backwash at flow rates which will produce the maximum turbulence and the maximum shear in the fluid-particle field, for this is the principal mode of cleaning. Alleviating the first weakness needs an invention which will revolutionize filtration technology. The second problem is far more tractable both theoretically as well as experimentally with the systems we have at present and the knowledge we have in fluidization.

Hanratty, Latinen and Wilhelm (40) were the first to use Taylor's turbulence equations, Eqs. 27 to 36, to describe the diffusion of a tracer dye in particulates fluidized beds. They established the mixing parameters—eddy diffusivity (Eqs. 37 and 40), and the scales and intensities of turbulence (Eq. 21a, Eq. 18). The experimental studies were made in a 5.40 cm Lucite tube, by admitting methylene blue dye from a central location to the bed of fluidized particles. Four different systems consisting of glass spheres of diameter 0.47 mm, 0.93 mm and 3 mm, as well as silica spheres of 1.84 mm were used for the solids in the bed. In all runs except two, a constant expanded bed height of 20.3 cm was maintained and the porosity was adjusted by changing the amount of solids in the bed. Two types of sampling traverses, radial and centerline were used to measure the spreading of the dye.

The time scale of turbulence was measured from the x-axis intercept of Eq. 36 written in Eulerian form,

$$\overline{x^2} = (2 \overline{u^2} T_L) \approx 2 \overline{u^2} T_L^2$$

where,

z = coordinate in direction of flow.

The intensity of turbulence $\frac{\sqrt{u^2}}{\bar{U}}$, was determined by measuring the initial slope of the $\frac{\sqrt{X^2}}{z}$ vs. z curve, similar to Eq. 32. The limiting value of the eddy diffusivity was evaluated from the slope of the $\frac{\sqrt{X^2}}{z}$ vs. z curve at very large values of z .

The results indicated that the theoretical equations of Taylor's theory of turbulence were applicable for diffusion in a particulate fluidized bed. A minimum Peclet Number (i.e. maximum eddy diffusivity) was found for all particle sizes and corresponded to a porosity of 0.70. This maximum eddy diffusivity was directly related to the maximum in the length scale of turbulence, which also occurred at this porosity. The intensity of turbulence increased continuously for all porosities. For the bed of 3 mm spheres the maximum scale of turbulence was approximately 4 mm.

Hanratty et al. did not attempt to provide a quantitative explanation for the minimum Peclet Number at the porosity of 0.70. Qualitatively explaining the observed phenomenon in terms of the random-walk model they stated,

Mixing in a packed bed was found to be explainable in terms of a random-walk model, and it is suggested that a dense fluidized bed retains elements of this mechanism. The distance a fluid element must side step in order to pass around a particle decreases as the bed is expanded. Eventually, at a fraction void of 0.70, a fluid element may begin to flow past solid particles without the necessity at each level of flowing laterally in order to evade a particle. Beyond the critical fraction void, in dilute beds, the turbulence is particle generated and the eddy diffusivity

is a direct function of particle population, leading to an increase in the Peclet Number as the velocity is increased.

Cairns and Prausnitz (16, 17) studied macroscopic mixing and longitudinal mixing in solid liquid fluidized beds. The studies in longitudinal mixing were made by determining the electrical conductance break-through curves using very small electrical conductivity probes with a step-function input of salt-solution tracer. The principal advantage of the conductivity method was that it enabled continuous monitoring and hence the tracing of transient velocities in the system. Longitudinal eddy diffusivities were determined for 1.3 and 3.0 mm lead spheres and 3.2 mm glass spheres in 2 and 4 inch diameter beds at a distance of 5 bed diameters from the injection point.

The analysis of the data was based on a statistical model developed by H. A. Einstein in connection with the motion of pebbles in a water stream. The model gives an easy and rapid method of determining the Peclet groups from the experimental data. The longitudinal eddy diffusivities were determined for various solids to column diameter ratios, various radial positions and various void fractions. The results were consistent with the fact that the fluidized bed was considered as a transition between a packed bed and an open tube. It was found that the ratio of longitudinal to radial eddy diffusivity E_l/E_r was approximately 20 to 30. Thus, the rate of longitudinal mass transfer was very much greater than the radial transfer.

In all cases a maximum of the longitudinal eddy diffusivity occurred at a porosity of 0.65 to 0.70. This maximum was much more pronounced for the lead sphere system than for the glass sphere system.

On defining the Peclet group in terms of the diameter of the solids in the system, a minimum Peclet Number occurred at a porosity of 0.7 in all cases. However, for the glass sphere system an asymptotic minimum value was reached for all porosities greater than or equal to a porosity of 0.7. The authors concluded that the eddy diffusivity was strongly affected by the density and concentration of particles in fluidized beds and a maximum in the mixing properties occurred at a fraction voids of 0.7.

In the study reported later the authors investigated macroscopic mixing (17) with a similar experimental set up. They measured the frequency distribution of fluctuations and the correlation coefficients at two points separated by a known distance. From the mixing data, radial eddy diffusivities, scales of turbulence and intensities of turbulence were measured.

Since mixing-length theory suggested that the mixing process in fluidized beds was analogous to molecular diffusion, a similar analytical model for a steady state system in cylindrical co-ordinates was used for analysis of the data. The results showed that the scale of turbulence maximized at a porosity of 0.70. A plot of the Peclet Number indicated a minimum corresponding to this same porosity. Detailed visual records of the behavior of the solids and the fluid was also noted. It was found that the most active particle motion occurs in the range of $\epsilon = 0.70$; the motion of the particles changing from a circulation pattern to that of random motion. This change in flow pattern was also noted by Volpicelli et al. (72), as recorded

before, in their studies of a monolayer of particles in the vertical plane.

Lemlich and Caldas (52) studied the heat transfer characteristics from the wall to the fluid within a particulates fluidized bed. They used a bed of glass spheres fluidized by water and found that the heat transfer coefficient maximized at a transition between two regimes of flow. The lower regime indicated limited axial mixing, while considerable mixing was evident in the temperature profiles at the higher rates of flow. The maximum heat transfer coefficient occurred at porosities of 0.66 and 0.81 for solid particles of diameter 0.50 and 0.29 mm respectively.

Handley et al. (39) studied the mechanics of fluid and particles in a particulates fluidized bed using unusual experimental techniques. They obtained a transparent solid-liquid system using soda glass (density = 2.50, refractive index = 1.52) and methyl benzoate (density = 1.08, refractive index = 1.52). An opaque white glass tracer particle having the same properties as the transparent soda glass was used and the motion of this particle was studied by cine photography. A similar technique was used in Ulug's studies of flow visualization as recorded earlier.

Fifty histograms of displacement vectors measured from projected stills, showed a mean zero solids velocity and the standard deviations were independent of radial or vertical positions in the bed. The mean zero solids velocity means that a single particle over a sufficient length of time does not have a velocity. This is to be expected from the fact that the solids in a fluidized bed do not have a finite

velocity over a long period. Thus, particle motion was random and homogeneous although isotropic conditions were not obtained. They then applied Taylor's random walk type statistical analysis (36, 68, 69) which was developed in a previous chapter, to the motion of the particles as well as the fluid regimes. Their data was analyzed using Eq. 35 and the Lagrangian time scale determined by means of the extrapolated intercept on the x-axis.

The results showed that the r.m.s. of the turbulent fluid velocity $\sqrt{\frac{u}{2}}$, passed through a maximum at some voidage between 0.44 and 0.75; the extrapolated graph indicated a value near 0.70. The r.m.s. of the turbulent particle velocity too, similarly, passed through a maximum at a voidage between 0.44 and 0.75. Using fluid dynamic pressure measurements (made with a pitot meter) they also found that the vertical turbulent fluid velocity component passed through a maximum at $\epsilon = 0.68-0.70$. Unfortunately, due to the experimental limitation requiring transparency, the authors did not investigate sufficient systems expanded to porosities less than 0.65.

In one of the pioneering studies in fluidization, McCune and Wilhelm (54) determined mass transfer characteristics by measuring the partial dissolution of spherical and flake-shaped naphthol particles in a fluidizing stream of water. It was found that the mass transfer characteristics for 1/8 inch pellets maximized around a porosity of 0.70-0.75.

In a recent study, Galloway and Sage (37) using an instrumented copper sphere within a packed bed of spheres studied the local thermal

transfer from the instrumented sphere. Using the data of McCune and Wilhelm (54) and Rowe (61, 62), they established a boundary layer model based on the behavior of thermal and material transfer from single spheres and cylinders in turbulent fluid streams. The studies showed that a maximum mass transfer occurred at a fraction voids of 0.70 for fixed beds. Extending the use of the model for fluidized beds with literature data, they showed, that the maximum mass transfer correlated with the maximum turbulence at the expanded porosity of 0.70.

Except for the qualitative observation of changing flow fields the researchers have not sought to explain why this maximum occurred at this porosity. Probably the answer to this lies in Jackson's studies (48). Jackson probed the fundamental mechanics of the fluidized bed and concluded that particulate and aggregative fluidization were both mechanically unstable systems. The instability manifested itself as traveling waves of increasing amplitude. His theory predicted that disturbances similar to those of bubbles in aggregative systems would also develop in particulate fluidized beds. However, for particulate systems these disturbances are of the same order of magnitude as the size of the solids in the system and do not develop to a noticeable extent, except in very deep beds. The visual observations of Cairns and Prausnitz (17) previously described in this dissertation, were mentioned by Jackson as evidence for the results he deduced from his stability study. As additional evidence he also referred to the papers by Slis et al. (65) and Kramers et al. (51).

In the study by Slis et al., they determined the propagation of a discontinuity in the porosity by a sudden change in the fluidizing

velocity. They showed that the boundary between the old and the new porosity broadens or remains sharp, depending on whether the porosity was increased or decreased. It was found that the velocity of small porosity disturbances was given by,

$$U_{\Delta\epsilon} = U_s n (1 - \epsilon)^{n-1} \quad (46)$$

where,

$U_{\Delta\epsilon}$ = velocity of propagation of small porosity
disturbance

n = expansion coefficient in Richardson and Zaki's
equation

The above function has a maximum around $\epsilon = 0.65-0.70$ and the porosity function is similar to the shear stress function developed by the author of this thesis in a later chapter.

Kramers who was a co-author of both papers (51, 65), studied in the second paper (51), the longitudinal dispersion of liquid in a fluidized bed. The study used a similar experimental set up as that used by Cairns and Prausnitz (16) except that Kramers et al. used very deep beds (12 meters and 6 meters) and fluidized glass spheres of diameters 0.50 mm and 1.0 mm (51). In order to avoid any external influences they took great care to eliminate, as far as possible, all visible systematic eddies. In fact the tubes used for the bed were purchased as a single piece and had no connections or protuberances.

The results indicated (51), a hump in the longitudinal diffusivity E_L at a porosity of 0.7 for the 0.50 mm particles. However at

porosities greater than 0.75, the value of the diffusivity continued to increase. For the 1.0 mm system the hump at the porosity of 0.7 was barely perceptible. Analyzing these results in terms of the reported maxima of Cairns and Prausnitz's studies (16, 17) the authors concluded that the eddy diffusivity was composed of two parts. One part was supposed to be due to the eddies produced by individual particles and this contribution passed through a maximum at the porosity $\epsilon \approx 0.70$. The other part which strongly increased at higher values of porosity was thought to be connected with the presence of local porosity fluctuations which were seen to travel upwards through the bed.

In discussing the above paper, Beek (12) reported on theoretical attempts which were made in order to explain both mechanisms. Using statistical turbulence theories and considering fluctuations in porosity, velocity and concentrations, he developed an equation of the form,

$$\frac{E}{V_s d} = c_1 \bar{\epsilon}^{(n-1)} + c_2 [(n+1)\bar{\epsilon} - (n-1)][n\bar{\epsilon} - (n-1)]\bar{\epsilon}^{(n-1)} \quad (47)$$

where,

$$\bar{\epsilon} = \epsilon - \epsilon' = \text{mean porosity}$$

$$\epsilon' = \text{fluctuation in porosity}$$

$$c_1, c_2 = \text{constants to be determined empirically}$$

By suitably choosing c_1 and c_2 , Beek was able to find a good fit for the data. The values of c_1 and c_2 were strongly dependent on the Reynolds Number. The first term in the equation was predominant at the lower

porosities, while the second term dominated values of the diffusivity at the higher porosities.

All the above studies have considered a solid phase and a pure fluidizing liquid. In order for the above results to be directly applicable to backwashing, it is necessary to assess, whether, the presence of a number of small floc particles in the liquid phase, will affect the turbulence parameters. Precisely this question, the effects of solids on turbulence in a fluid, was studied by Kada and Hanratty (50). Using the same technique as that used by Hanratty et al. (40) to study turbulent diffusion in fluidized beds, mentioned previously in this thesis, Kada and Hanratty studied the effect of solids concentration of 0.13 to 2.5 percent by volume on the turbulent dispersion characteristics of a pure fluid. They found that one of the chief variables affecting the system was the slip velocity, which was the difference between the particle and fluid velocities in the direction of flow. For the systems studied the slip velocity was equal to that of the free fall velocity. It was found that glass particles of diameters 0.10 mm and 0.38 mm and concentration of 1.5 percent and 1.7 percent by volume had no effect at all on the turbulent dispersion characteristics of the fluid. One of the principal conclusions of the study was that for systems with small slip velocities the effect of solid concentrations upto 1.5 percent had no effects at all on the dispersion characteristics. This study provides the final argument for applying the results of the studies reviewed in this chapter to the backwashing of filters.

The evidence recorded above is impressive, since several studies have confirmed the central result. The impressiveness lies in the fact that totally different experimental techniques used to study different, but hydrodynamically related characteristics, namely, scales of turbulence, eddy diffusivities, Peclet numbers, particle and fluid motions, mass transfer and heat transfer effects, all yielded the surprising fact of maximization at a porosity of approximately 0.65-0.70. The very few studies which have sought to explain the reason for this maximization of the turbulence parameters, indicate that the diffusivity is probably due to two factors. One is due to the eddies associated with the particles and the other is due to porosity fluctuations which travel up the bed.

C. A Summary

The essential conclusions of the entire literature review can be summarized as follows.

(i) Filter backwashing is one of the operations in water treatment plants which has caused the most amount of maintenance problems, but it has received the least study, especially in its fundamental characteristics.

(ii) Considerable evidence exists in the fluidization literature that particle collisions in the fluidized state are of negligible consequence compared to the hydrodynamic effects. This fact is also being realized in the sanitary engineering field and as a corollary it implies that the present mode of cleaning a filter is inherently unsatisfactory.

(iii) The fluidization literature abounds with evidence that the fluid and particle fields in particulate fluidization can be described by the statistical turbulence theories, even though the actual fluid velocities are not in the turbulent regime. It has been found that most turbulence parameters had a maximum at an expanded porosity of 0.65-0.70. It is hence hypothesized by the author of this dissertation that, within the constraint that fluidization is not an excellent process for cleaning, the best cleaning that can be achieved is by expanding the bed to these porosities.

(iv) Only qualitative and semi-quantitative attempts have been made to unravel the reasons for the optimum in the turbulence parameters. These have been based on the assumption that dispersion is caused by (a) eddies around individual particles and (b) the movement of porosity fluctuations through the bed.

The theory developed for optimum backwashing in the next chapter is entirely new and original, however it draws sustenance, principally from the conclusions and results reported and summarized in this section of the dissertation.

V. THEORY OF OPTIMUM BACKWASHING

The following is an original theory of backwashing developed from the results reviewed in the previous chapters and also using additional concepts in filtration.

A. The Formulation of the Physical Model

1. An introduction to filtration

Consider a filter at the end of a filtration run and prior to backwashing. It is generally accepted among research workers that the mechanism of particle removal during filtration involves two steps: transport and attachment. Straining, interception, diffusion, sedimentation, inertial and hydrodynamic effects all contribute towards the transport mechanism. The attachment mechanisms or as some refer to it, attachment-detachment mechanisms are still not completely understood or universally accepted. But most investigators have agreed that attachment of particles to grain surfaces or to previously deposited particles are due to molecular forces (London-Van der Waals) that are operative at very close range (47). Hence adsorption of suspended particles to the surfaces of the filtering medium has been proposed by many workers as being a principal mechanism (47). Camp on the basis of shear strength calculations (18, 20) suggested that the number of molecular bonds involved in adhesion of the floc to the grains had to be extremely small. He suggested that the floc sheaths during filtration were resting on the grains like a cap with little adhesion, but with sufficient tensile strength to resist the shearing forces during filtration. The

filter sand and the solids removed from the water form a porous matrix through which even at the end of the filter run the flow is laminar (25).

Due to gradations in the sand as well as increased removals at the top, the matrix is more dense at the surface of the filter than at greater depths. Excellent reviews of filtration with far more details can be found in the published works of Cleasby (23), Baumann and Oulman (7), O'Melia and Crapps (57) and Ives (47).

2. The backwashed filter

On the basis of the accepted theories of filtration it is hypothesized that the solids deposited in the dirty filter be considered to consist of two portions. The first portion is due to the interaction of the electrical double layers of the media and the suspended solids being removed, and also due to molecular cohesive forces (Van der Waals forces). This results in the adsorption of floc particles on the media and on previously deposited particles. The second portion can be considered to consist of suspended solids deposited in the pores with negligible cohesion between adjacent particles. This division is rather arbitrary and the extent to which each portion dominates the solids removal, greatly depends on the characteristics of the solids being filtered. However for a number of systems the second portion is chiefly due to solids being deposited within the pores by various physical means such as straining, sedimentation, etc. The experimental work of Cleasby et al. (26) and Cleasby (24) lends support to this assumption, since even very small changes in filter flow rate caused material to be flushed out of the filter. A schematic drawing of the

dirty filter is shown in Fig. 1. It is further hypothesized that during the initial stages of backwashing the loose matrix breaks up into small particles and forms a suspension of very light solids in the liquid phase. Some evidence for this hypothesis can be found in the paper by Edeline, Tesarik and Vostrcil (30) and Cleasby's dissertation (24). Iron floc was found to have densities of 1.001 to 1.004 g/cc and dimensions of 20 to 100 μ . Hence applying the results of Kada and Hanratty's experiments (50) the backwashed suspension can be said to have turbulence characteristics identical to that of a pure liquid. This follows because of the low density and small slip velocities of the floc particles.

During the later stages of backwashing the solids that tend to be removed are those around the particle. Since only hydrodynamic forces are involved in this cleaning it can be expected that the removal of adsorbed particles will be small. Thus it can be postulated, on the basis of the fluidization literature reviewed, that the initial dispersion of the settled material is due to turbulent dispersion within the fluidized bed which reaches a maximum at porosities of 0.65-0.70. Towards the end of backwashing the boundary layer adjacent to the coated particle becomes the significant section for removal of filtered flocs and shear forces at the boundary are the principal cause for removal of the solids. Even though shear forces will probably predominate the cleaning mechanisms at the later stages of cleaning, it needs to be remembered that the turbulence characteristics and the hydrodynamic shear forces are inextricably bound together and both contribute towards cleaning the filter at all stages of backwashing. It is necessary to reemphasize that in both types of cleaning mechanisms described,

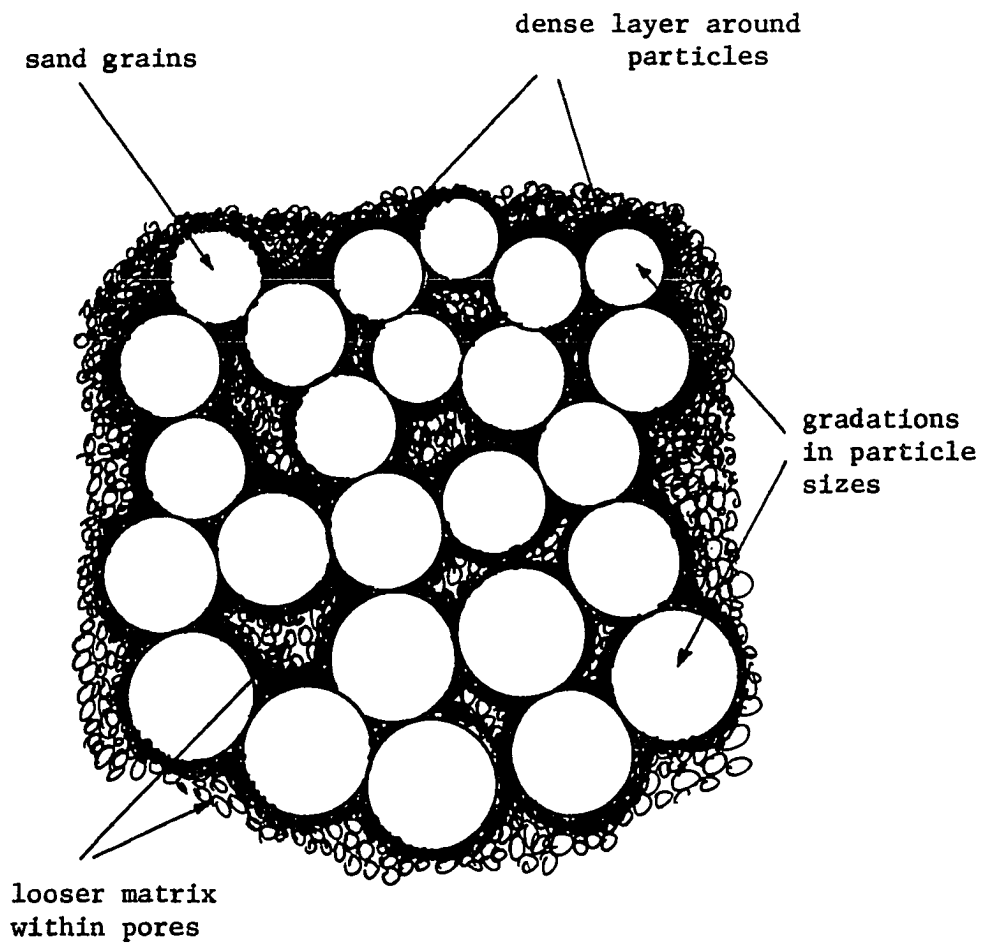


Fig. 1. Schematic view of dirty filter

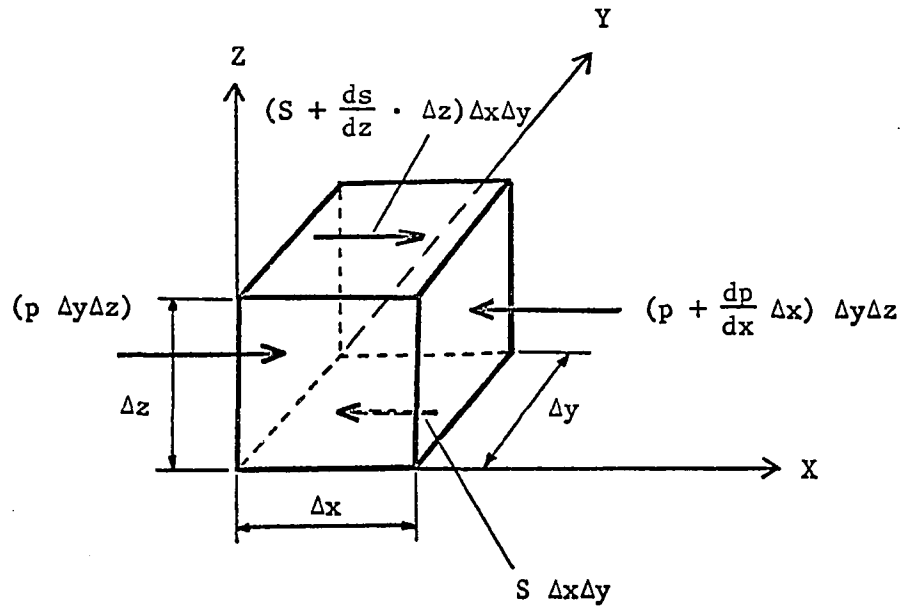
abrasion and collisions between particles do not significantly contribute towards the cleaning of the filter.

B. A New Mathematical Theory for Optimum Backwashing

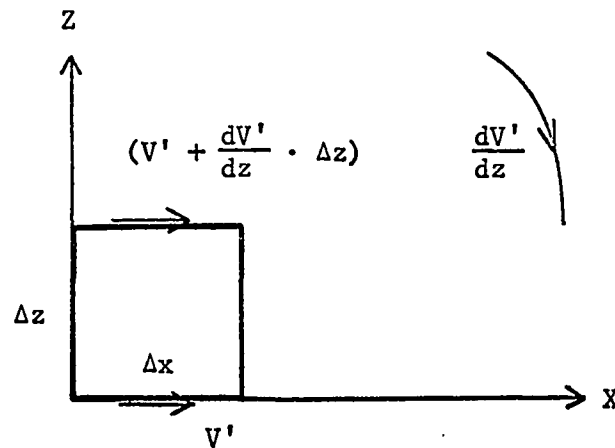
It has been shown in the previous section that filter cleaning during backwash is due to the turbulence of the fluidized bed and hydrodynamic shear forces. The voluminous fluidization literature quoted, has shown that turbulent diffusion is maximized at the porosity of 0.65-0.70. Some mathematical theories have sought to identify this maximum with the eddies around particles and the fluctuations in porosity which travel up the fluidized bed.

The following new theory shows that hydrodynamic shear forces in a fluidized bed reach a maximum at this porosity of 0.65-0.70, for most systems considered. Even if the turbulence parameters cannot be directly related to the shear forces at the present time, on the basis of the discussion in the previous section, the cleaning in a backwashed filter bed necessarily reaches an optimum with the maximum shear. Since shear and turbulence parameters are inseparably related it should be possible as a future extension of the theory, to obtain an analytical model which will relate the maximum in the hydrodynamic shear to the maxima in the turbulence parameters. This is also predicated on the fact that the actual fluid velocities in a fluidized bed are in the transitional regime and only the interaction with the solids produces a system having behavior similar to that of a turbulent field.

Consider a one dimensional analysis of the motion of an elemental volume of fluid as in Fig. 2. Let p = pressure intensity, S = shear



(a) FORCES



(b) VELOCITIES

Fig. 2. Shear forces and velocities on elemental volume of fluid

stress, V' = velocity and Δx , Δy and Δz be the dimensions of the cube.

The work done by shearing stresses is irreversible and is dissipated as heat. This loss in energy corresponds to what is frequently called head loss or friction loss in fluid flow problems.

Let the power dissipated by the torque composed of the shear forces due to S , be P_1 ,

$$\begin{aligned} P_1 &= \text{torque} \times \text{angular velocity} \\ &= (S\Delta x\Delta y)\Delta z \cdot \frac{\left(\frac{dV'}{dz} \Delta z\right)}{\Delta z} \\ &= S \frac{dV'}{dz} \Delta x\Delta y\Delta z \end{aligned}$$

By definition

$$S = \mu \frac{dV'}{dz}$$

therefore,

$$P_1 = \mu \left(\frac{dV'}{dz}\right)^2 \Delta x\Delta y\Delta z \quad (48)$$

Let the hydraulic gradient in the z -direction or the head loss per unit length be $\left(\frac{dh}{dz}\right)$.

Hence the power dissipated by the element of height Δz and area of cross section $\Delta x\Delta y$, moving with a velocity V' is,

$$P_2 = \left(\frac{dh}{dz}\right) \Delta z \cdot \Delta x\Delta y \rho_f g \cdot V' \quad (49)$$

Since the power dissipated by the shear forces corresponds to the head loss, Eqs. 48 and 49 give

$$\mu \left(\frac{dV'}{dz} \right)^2 \Delta x \Delta y \Delta z = \left(\frac{dh}{dz} \right) \Delta x \Delta y \Delta z \rho_f g V',$$

that is,

$$\left(\frac{dV'}{dz} \right) = \sqrt{\left[\frac{gV'}{\nu} \left(\frac{dh}{dz} \right) \right]} \quad (50)$$

Now, $\left[\left(\frac{dh}{dz} \right) \rho_f g V' \right]$ is the power dissipated per unit volume, say $\frac{P}{C}$, and G is the velocity or shear gradient defined as $\left(\frac{dV'}{dz} \right)$; hence Eq. 50 reduces to,

$$G = \sqrt{\left(\frac{P}{\mu C} \right)} \quad (50a)$$

Equation 50a is the familiar form of Eq. 50, originally derived by Camp and Stein (21) as the general power dissipation function in a three dimensional treatment. The derivation of Eq. 50a in condensed form is also presented in Fair, Geyer and Okun (34, pp. 22-12).

For a fluidized bed with a superficial velocity V , where $V' = \frac{V}{\epsilon}$ and the hydraulic gradient $\left(\frac{dh}{dz} \right) = i$, Eq. 50 becomes

$$G = \sqrt{\left(\frac{giV}{\nu \epsilon} \right)}$$

This is Eq. 42 mentioned previously as presented by Camp (18) for calculating the shear forces during filtration and backwashing.

Equation 50 will now be put in the form most useful for the following development of the theory of optimum backwashing.

$$S = \mu \frac{dV'}{dz} = \sqrt{[\mu g \rho_f \frac{V}{\epsilon} (\frac{dh}{dz})]}$$

that is,

$$S = [\mu g \rho_f \frac{V}{\epsilon} (\frac{dh}{dz})]^{\frac{1}{2}} \quad (51)$$

where,

S = shear intensity

V = superficial fluid velocity

$(\frac{dh}{dz})$ = head loss gradient

An important property of fluidized beds arises from the fact that particles suspended in a fluid require that the frictional drag of the fluid exactly counterbalances the pull of gravity. In effect, this leads to the requirement that the head loss across a fluidized bed must equal the buoyant weight of the particles. Two of the earliest researchers to report this well known property were Fair and Hatch (35). In differential form this result is,

$$dh \rho_f g = dz (\rho_s - \rho_f) g (1 - \epsilon)$$

that is,

$$(\frac{dh}{dz}) = \frac{(\rho_s - \rho_f)}{\rho_f} (1 - \epsilon) \quad (52)$$

The above Eqs. 51 and 52 and the following Eq. 53 form the principal equations of the optimum backwashing theory.

Richardson and Zaki's equation as modified by Amirtharajah and Cleasby (3) for graded and irregular particle systems is,

$$V = K \epsilon^n \quad (53)$$

where,

$K = f(V_s, \psi, d/D_t) = \text{constant for a particular system}$

$\psi = \text{sphericity}$

$D_t = \text{diameter of tube or bed}$

$n = \text{expansion coefficient in Richardson and Zaki's equation}$

The coefficient n is a function of the flow regime and the dimensions of the apparatus but is constant for a particular system. For the flow regimes of interest under filter backwashing conditions,

$$n = (4.45 + 18 \frac{d}{D_t}) Re_o^{-0.1} \text{ for } 1 < Re_o < 200 \quad (54)$$

where,

$$Re_o = \frac{\rho_f V_s d}{\mu} = \text{Reynolds Number}$$

A method of calculating Re_o from the minimum fluidization velocity and hence n from Eq. 54 is given in Amirtharajah and Cleasby (3).

Substituting Eqs. 52 and 53 in Eq. 51 gives

$$S = \left[\mu g \rho_f \cdot \frac{K \epsilon^n (\rho_s - \rho_f)}{\epsilon \rho_f} (1 - \epsilon) \right]^{\frac{1}{2}}$$

$$= [\mu g K (\rho_s - \rho_f) (\epsilon^n - 1 - \epsilon^n)]^{\frac{1}{2}}$$

that is,

$$S = \alpha \sqrt{(\epsilon^n - 1 - \epsilon^n)} \quad (55)$$

where,

$$\alpha = \sqrt{\mu g K (\rho_s - \rho_f)} = \text{constant for a particular system}$$

The above Eq. 55 is the basic equation of the writer's theory. It is a relation between the shear stress and the porosity in a fluidized bed.

Let us analyze this function by classical optimization techniques to determine the stationary points of the function as the porosity ϵ changes.

The simplest analysis is to consider the function S^2 .

$$S^2 = \alpha^2 (\epsilon^n - 1 - \epsilon^n)$$

Differentiating with respect to ϵ by treating S^2 as an implicit function,

$$\begin{aligned}
2S \frac{dS}{d\epsilon} &= \alpha^2 [(n-1)\epsilon^{n-2} - n\epsilon^{n-1}] \\
&= \alpha^2 \epsilon^{n-2} [(n-1) - n\epsilon]
\end{aligned} \tag{56}$$

For stationary points $\frac{dS}{d\epsilon} = 0$. Since $\alpha^2 \epsilon^{n-2}$ cannot be zero,

$$(n-1) - n\epsilon = 0$$

therefore,
$$\epsilon = \frac{(n-1)}{n} \tag{57}$$

Hence the maximum or minimum value of S is given by the value of S

when $\epsilon = \frac{(n-1)}{n}$.

Differentiating Eq. 56 again,

$$2S \frac{d^2S}{d\epsilon^2} + 2 \left(\frac{dS}{d\epsilon}\right)^2 = \alpha^2 \epsilon^{n-3} [(n-1)(n-2) - n(n-1)\epsilon].$$

When $\epsilon = \frac{(n-1)}{n}$, $\frac{dS}{d\epsilon} = 0$,

therefore,

$$\begin{aligned}
2S \frac{d^2S}{d\epsilon^2} &= \alpha^2 \left(\frac{n-1}{n}\right)^{n-3} (n-1) [(n-2) - (n-1)] \\
&= \alpha^2 \left(\frac{n-1}{n}\right)^{n-3} (n-1) [-1]
\end{aligned}$$

Since $S \neq 0$ and $n > 1$, therefore

$$\frac{d^2S}{d\epsilon^2} < 0 \text{ when } \epsilon = \frac{(n-1)}{n}.$$

Thus the stationary point is a maximum. Alternatively, the following simpler analysis gives the same result.

Consider the sign of $\frac{dS}{d\epsilon}$ as it passes through the stationary point.

From Eq. 56,

$$\frac{dS}{d\epsilon} > 0, \text{ for } \epsilon < \frac{(n-1)}{n}$$

$$\frac{dS}{d\epsilon} < 0, \text{ for } \epsilon > \frac{(n-1)}{n}$$

Hence the stationary point is a maximum.

It is shown in Chapter VIII of this thesis that the effective n for the top 3 in. of the graded sand is 3.54. For the uniform sand used in part of the current study $n = 3.3$.

For the graded sand maximum shear stress S occurs at,

$$\epsilon = \frac{(n-1)}{n} = \frac{(3.54-1)}{3.54} = 0.72$$

For the uniform sand,

$$\epsilon = \frac{2.3}{3.3} = 0.70.$$

Thus, a maximum shear stress S occurs in a fluidized bed at the porosity $\epsilon = \frac{(n-1)}{n}$, which corresponds to porosities of 0.70 - 0.72 for real sand systems. This is the main result of the optimum back-washing theory.

The above result derived entirely from the theory indicates that optimum cleaning of the filter by maximum hydrodynamic shear forces occurs at the porosity 0.70-0.72. This theory in combination with the literature cited in fluidization, which reviewed several experimental studies indicating an optimum diffusion at the porosity 0.65-0.70, provide an excellent theoretical framework for experimentally studying optimum backwashing. Detailed experimental studies which provide confirmation of this theory are presented in the later chapters of this dissertation.

It should be noted that the above theory is developed from three equations which are valid for all types of flow regimes in fluidization. Camp and Stein's equation is valid for viscous as well as turbulent flows since it only equates the energy dissipated by shear to the head loss. The constant head loss equation is valid for all fluidized beds and Amirtharajah and Cleasby's equation is a modified form of a power function of porosity which is valid for all shapes and sizes of particles. Hence the theory developed is applicable for all particularly fluidized systems in all regimes of flow.

The following is an extended analytical treatment of the above theory to determine how sensitive the maximum is to changes in porosity.

From Eq. 55,

$$S = \alpha [\epsilon^n - 1 - \epsilon^n]^{\frac{1}{2}}$$

therefore,

$$\frac{dS}{d\epsilon} = \frac{\alpha}{2} \frac{[(n-1)\epsilon^{n-2} - n\epsilon^{n-1}]}{[\epsilon^{n-1} - \epsilon^n]^{\frac{1}{2}}}$$

In terms of finite increments,

$$\Delta S = \frac{\alpha}{2} \frac{[(n-1) - n\epsilon]\epsilon^{n-2}}{[\epsilon^{n-1} - \epsilon^n]^{\frac{1}{2}}} \cdot \Delta\epsilon$$

Therefore,

$$\frac{\Delta S}{S} = \frac{1}{2} \frac{[(n-1) - n\epsilon]\epsilon^{n-2}}{[\epsilon^{n-1} - \epsilon^n]} \Delta\epsilon$$

Consider the ratio $\frac{\Delta S}{S}$, that is the ratio of the incremental change in shear to the shear, around the maximum value of S (i.e. at $(n-1) - n\epsilon = 0$).

It is seen that $\frac{\Delta S}{S} \rightarrow 0 \times \Delta\epsilon$.

This shows that the maximum value of S is very insensitive to changes in ϵ , or in simpler terms the curve of S vs. ϵ is very flat around the maximum. Thus the effect on the shear stress of changes in porosity around the maximum will be very small. A more rigorous analysis of sensitivities can be made by expanding the function S around the maximum in terms of a Taylor Series. However this degree of sophistication in analysis is unwarranted since simpler methods yield equally valid conclusions.

Some numerical values will reinforce the above analysis. Consider the values of S for the following values of ϵ when $n = 3.1$.

$$\begin{aligned} \text{At } \epsilon = 0.68, \quad S_{\max} &= \alpha [\epsilon^n - 1 - \epsilon^n]^{\frac{1}{2}} \\ &= \alpha [0.68^{2.1} - 0.68^{3.1}]^{\frac{1}{2}} \\ &= 0.378 \alpha \end{aligned}$$

$$\text{At } \epsilon = 0.60, \quad S = 0.368 \alpha$$

$$\text{At } \epsilon = 0.75, \quad S = 0.370 \alpha$$

Thus it is seen that nearly 12 percent change in ϵ produces only 2 - 2 1/2 percent change in S .

For backwash porosities of approximately 0.52 (i.e. 25 percent expansion) used commonly in practice, shear stress $S = 0.349 \alpha$. Thus change in shear stress from that at optimum is 7.8%. It needs to be emphasized that even though the change in shear stress maybe small it is quite possible that even very small changes in shear stress may have considerable effect on the cleaning action.

It is anticipated that the above theory can be extended to graded systems using a probability function to represent a graded bed. However this extension is not being pursued in the present study due to limitations in space. It is only by applying the theory for a graded system, as explained below, can the above theory be meaningful in practice.

As a fitting closure to the above theory, it is necessary to anticipate the results that can be derived by applying this theory

to backwashing in practice. The theory predicts an optimum in cleaning at a porosity of 0.70. Consider a uniform sand bed of depth λ_0 with a fixed bed porosity of 0.40. For the porosity to be 0.70 in the expanded state of depth λ' ,

$$\lambda' (1 - 0.70) = \lambda_0 (1 - 0.40)$$

therefore,

$$\lambda' = 2\lambda_0.$$

Hence the expansion required is nearly 100 percent. This can rarely be achieved in practice. However, for a graded system the particle diameters at the top of the bed are a fraction of the diameters in the deeper sections. Thus an expansion much smaller than 100 percent will cause the porosities to be 0.70 in the top layers. Since these layers are the ones that remove most of the suspended matter in filtration, it can be rationally expected that optimum cleaning of the top layers will produce the best cleaning for the system. Expansions higher than that producing the porosity of 0.70 in the top layers, will tend to increase the porosities of the layers on top but will simultaneously cause the lower layers to reach the optimum porosity of 0.70, hence we would expect only a negligibly small decrease in the optimum cleaning. This would cause a nearly asymptotic curve of optimum cleaning to be produced for graded systems. This effect for graded systems in addition to that due to the flat shear force-porosity relation indicates that the experiments need to be carefully designed so that rather small variations in cleaning efficiency can be detected. An exact theory for optimum cleaning of graded systems should seek the optimum balance

between the gradations in shear force caused by the gradations in particle size (increasing from top to bottom) and the gradation in removal of suspended matter (decreasing from top to bottom).

In conclusion, the above theory predicts the following characteristics of optimum backwashing.

(i) An optimum backwash for uniform systems is exactly predicted by the shear stress maximum at the expanded porosity of 0.70-0.72 for the sands normally used in filters.

(ii) This optimum is not very sensitive to changes in porosity and requires an expansion of about 100 percent for uniform systems.

(iii) More importantly, the optimum can be realized for the real graded systems at a much smaller expansion; however, an asymptotic behavior of the optimum can be expected as the flow rate is increased.

(iv) The theory shows that for systems having strong surface removal tendencies the optimum will be more specific than for systems having removals of suspended solids at deeper layers.

(v) Since anthracite coal has fixed bed porosities of 0.50, optimum cleaning of the coal layers can be achieved at expansions of about 67 percent for uniform coal systems, or much smaller expansions for graded coal systems.

(vi) The theory confirms the experimental result of Rimer (60) who found that best cleaning of multi-media filters was achieved by step wise expansion of the different layers.

(vii) The theory also predicts by analogy from the above, that step wise washing procedures, or a continuously increasing programmed

wash to obtain porosities of 0.70 for most of the layers, will probably give the cleanest filter.

VI. EXPERIMENTAL INVESTIGATION

A. Experimental Apparatus

1. General layout

A schematic layout of the experimental apparatus is shown in Fig. 3, and photographic details are given in Figs. 4 and 5. The arrows in Fig. 3 trace the path of water from the tap supply to the outlet drain for filter F3, during a filtration run. The main pilot plant consisted of the university tap water supply (hot and cold) blended in a thermostatically controlled mixing valve¹ A. The blended water passed through a centrifugal pump B, used as an inline booster. After being metered in the flowmeter C, the water passed through a dual outlet; one end of this outlet fed the supply water to the mixing tank D, while the other end provided the backwash water supply. Each of these outlets was used singly, and the pump B was only used during high rates of backwash since the normal tap pressure was sufficient for most uses.

The influent to the filters was mixed in tank D with the chemicals being added from constant head capillary feeders. The influent water was pumped from the mixing tank by a centrifugal pump E which was driven by a variable speed D.C. motor. This enabled influent control to be achieved. The main influent line trifurcated to the filters, via the filter valve system. The effluent from each of the filters F1, F2 and F3, passed through its own flowmeter and then discharged freely into a

¹Lawler Automatic Controls, Inc., Mt. Vernon, New York.

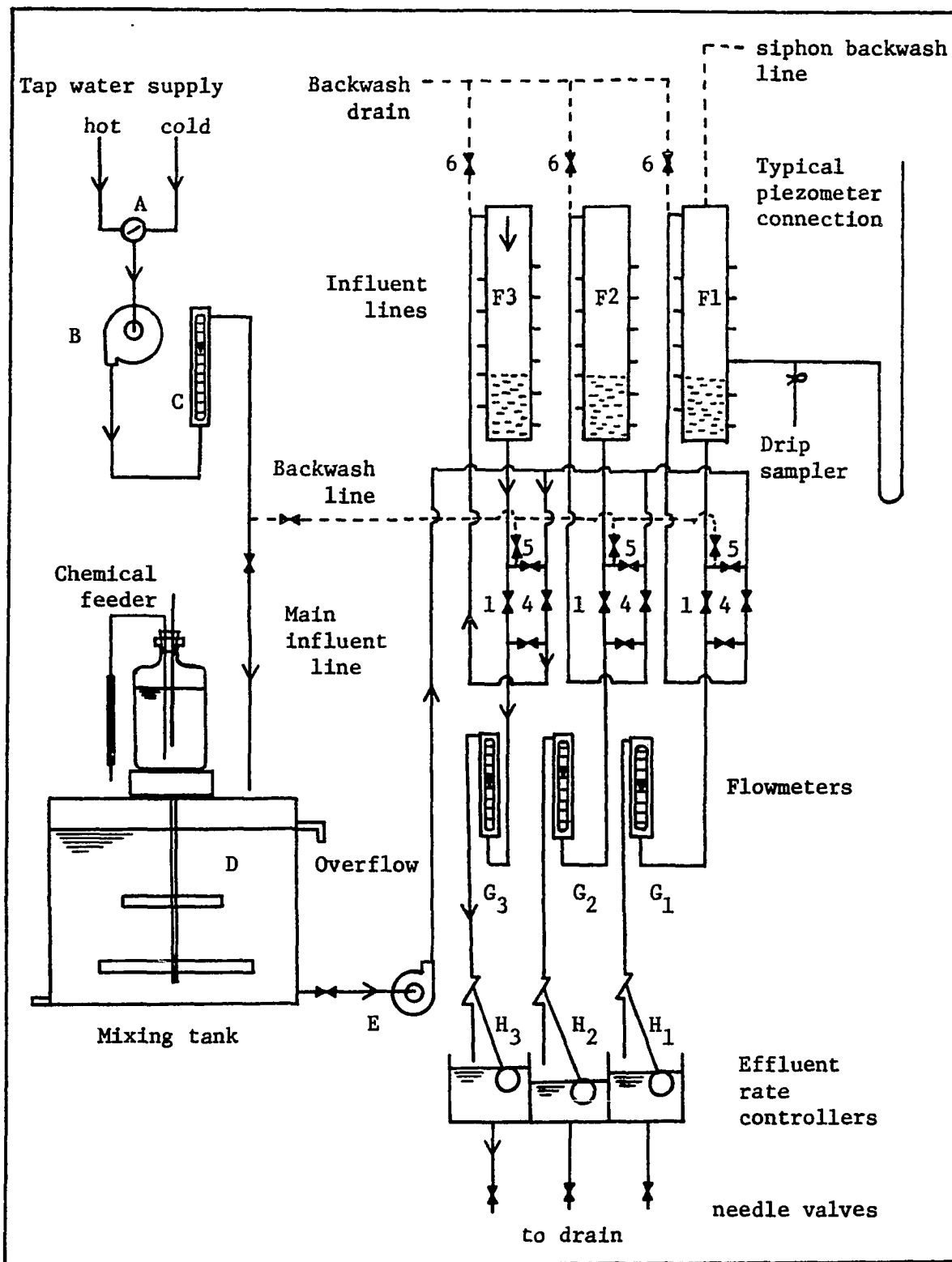


Fig. 3. Schematic layout of experimental apparatus

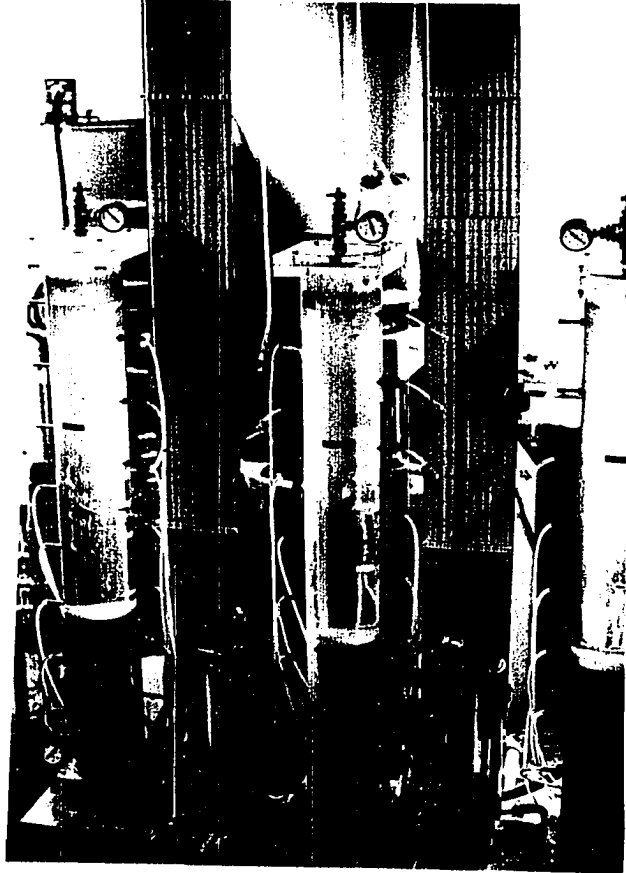


Fig. 4. Details of pilot plant filters

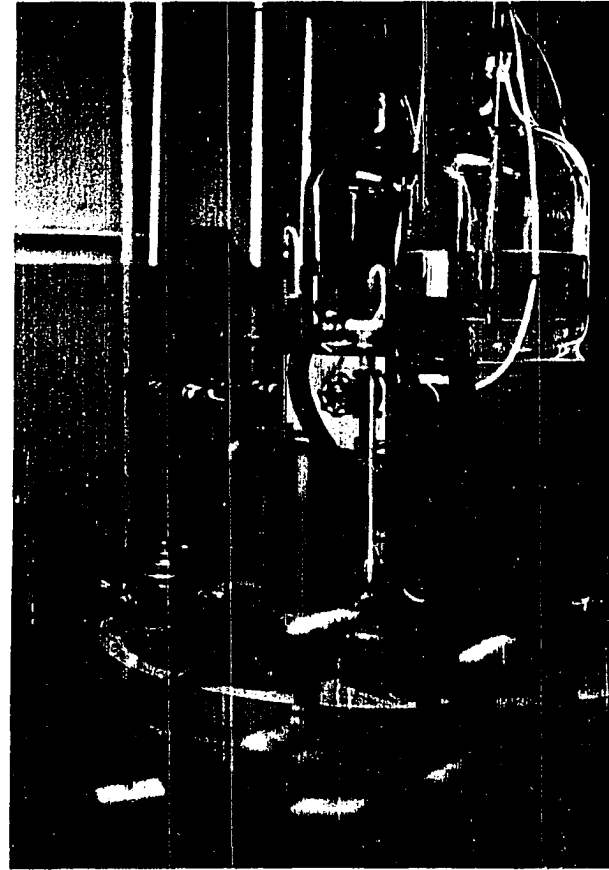
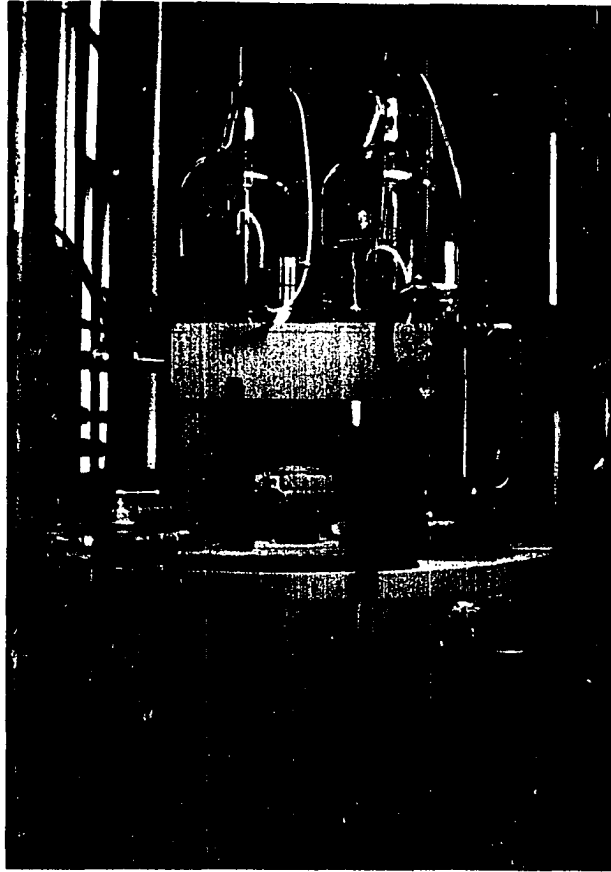


Fig. 5. Views showing mixing tank, chemical feeders, flowmeter and effluent rate controllers

float operated effluent rate controller. Eleven piezometer connections enabled the head losses to be determined at every 3 inch depth of the filter. The expanded height of the filters was determined by a scale placed along the side of the filter.

For backwashing the filters, blended tap water was used and metered in flowmeter C. The backwash line passed via the valve system, and discharged in a drain. The capacity of the backwash outlet line was insufficient to carry away the higher flows used in this study (nearly 38 gpm/sq ft) and also, filter media sampling was done during backwash requiring an open top in the filter. For these reasons, a siphon backwash line was used in addition to the normal backwash line.

2. Details of filters and appurtenances

a. Pilot plant filters The filters consisted of 6 in. inner diameter 1/2 in. thick plexiglass tubes 4 ft 5 in. deep with a 3 in. high calming section at the bottom. The water was fed through 59 orifices, 1/16 in. diameter, in a 1 in. thick underdrain plexiglass plate. The orifices were arranged as follows: 1 at the center, 6 spaced at 60° intervals on a circle of radius 5/8 in., 12 spaced at 30° intervals on a circle of radius 1 1/4 in., 16 spaced at 22 1/2° intervals on a circle of radius 1 7/8 in. and 24 spaced at 15° intervals on a circle of radius 2 1/2 in. Sets of orifices were staggered from one another so as to provide a uniform matrix of orifices on the entire plate. The calming section was filled with 1/2 in. diameter glass marbles. Two pressure gauges, one attached to the center of the calming section and

the other to the cover plate of the filter, were provided to serve as safety gauges to warn of dangerous build up in pressure.

The solid particles composing the bed were supported on two stainless steel meshes (No. 50 over No. 10) placed above the 1 in. thick plexiglass plate with the orifices. This plate rested on the calming section of glass marbles. Sixteen pressure taps were located on two rows on diametrically opposite sides of the filter. The height of the first pressure tap was 3 in. above the stainless steel meshes, while pressure tap No. 2 was diametrically opposite and at a height 6 in. above the meshes. The other taps were spaced in a line 6 in. from one another; thus, the pressure at every 3 in. depth of the fixed or fluidized bed could be read on water manometers. Further details including drawings of the calming section and the pressure taps have been presented previously (2).

Eleven of the pressure taps from each filter were connected, via glass T-connections to 4 mm glass tubes which were fixed to 10 ft long piezometer boards. The other end of the T-connection was provided with plastic tubing and a screw clamp. This outlet enabled flushing of the solids drawn into the manometer tubes and, more importantly, provided the means of obtaining continuous drip samples during filtration. The upper ends of the piezometer tubes were connected to a manifold header to permit the application of a small constant pressure on all tubes. The pressure was exerted by a rubber squeeze bulb at the beginning of each run to depress the water level in the tubes to approximately the middle of the board. This enabled reading the manometers during the progression of increasing head loss.

The height of the bed was measured by placing a scale against the filter resting on the top of the two one in. thick plates at the top of the calming section. Since the supporting meshes were at the middle of these two plates the zero height of the bed was 1 in. below the zero of the scale. All original readings in the data books were the actual heights of the bed, that is the scale reaching plus 1 in.

b. Slow speed mixing tank and chemical dosing apparatus A mixing tank 3 ft high and 3 ft 6 in. diameter, equipped with a slow speed paddle was used to provide the necessary detention time for completion of the iron precipitation reaction. Allowing 6 in. of freeboard, this 180 gal tank provided a 30 minutes theoretical detention time at a pumping rate of 6 gpm. All filtration runs were made at 7 gpm/sq ft and hence the tank provided a theoretical detention time of approximately 45 minutes. The tank had an overflow outlet which enabled a constant head to be maintained on the inlet of the pump E, thus maintaining uniform pumping rates. The lower drain allowed a constant bleeding out from the bottom sections of the tank small amounts of the mixed influent suspension, thus preventing an accumulation of any heavy floc at the bottom. A slight excess of inflow was provided to allow for the waste overflow and underflow water. The chemicals were added to the mixing tank from a constant head capillary feeder.

c. Pumps, motors and influent control A 1 1/2 in. outlet diameter, 1/3 HP, 3500 rpm close coupled centrifugal pump B¹ was used for back-washing.

¹Weinman Unipump, The Weinman Pump Manufacturing Co., Columbus, Ohio.

A 1 1/2 in. outlet diameter self priming centrifugal pump¹ was used to pump the influent water from the mixing tank to the filters. The pump was driven by a 2 in. X 3 1/2 in. pulley drive from a 1/3 HP D.C. motor equipped with a variable speed control². This system enabled the influent pumping rate to be increased simultaneously on all three filters by a gradual increase in the speed of the centrifugal pump. Thus influent control was achieved; and any changes in flowrate affected all three filters to the identical extent.

d. Flow meters The total flow to the mixing tank during filtration and the total backwash rates were metered by a rotameter C³ which had a range up to 13 gpm. Results and experimental details of a calibration test made on this flowmeter at 14°C, 38°C and a variable 14°C-18°C are presented elsewhere (2). Variations due to changes in temperature were not detectable in the tests.

The effluent from each filter passed through a rotameter suitable for water flow measurement from 0.2 to 2.0 gpm⁴. These flowmeters G₁, G₂ and G₃, were calibrated by determining the time to fill a liter measuring cylinder. Several readings were taken at 15°C, 25°C and 30°C. Variations were found from meter to meter as well as slight variations

¹Teel Self-Priming Centrifugal Pump, Model 1P746, Dayton Electric Manufacturing Co., Chicago, Illinois.

²Westinghouse Hi-Torque Speed Control with D.C. Motor, Westinghouse Electric Corporation, Springfield, Massachusetts.

³Fischer and Porter Precision bore flowmeter.

⁴Fischer and Porter Flowrators.

at different temperatures, apparently due to the deposition of small amounts of material on the inside of the glass tube or the float. All of the current experiments were conducted at 25°C. Before the start of each run the flowmeters were flushed with tap water and hence the accumulation of deposits on the insides of the glass tubes and the float was prevented. This procedure proved sufficient to keep the flowmeters clean throughout the studies.

e. Effluent rate controllers The effluent from each filter passed via each flowmeter into a float operated rate of flow controller. The controller maintained a constant rate of filtration by holding a constant head on a needle valve outlet. Each float chamber was 9 in. x 9 in. x 12 in. deep and the flowrate into each chamber was controlled by a 4 in. diameter copper float actuating a 3/4 in. float valve. As the head loss through the filter increased during a run the float valve would gradually open to maintain a constant filtration rate. These rate of flow controllers functioned remarkably well. Slight differences from filter to filter were adjusted by changing the needle valve settings. The slight decreases in flowrate which would result due to decreasing head on the outlet needle valve were eliminated by gradually increasing the speed of the influent centrifugal pump E, to maintain approximately constant pressure on the float valve. This dual influent-effluent control system enabled excellent control of flowrate to be achieved and also kept the flushing of deposited material to the very minimum. The system was based on combining the best of the different characteristics of influent and effluent control. This has been discussed in detail by Cleasby in his paper (22) on rate controllers.

f. Filter sand The sand used for this study was a granular filter sand¹. The original sand had an effective size of 0.455 mm, a uniformity coefficient of 1.52, a specific gravity of 2.648 and a porosity of 0.412. The graded sand used in the latter stages of the study was this original sand. The uniform sand used in the earlier stages of this study was prepared by sieving the sand in a Gilman set of U.S. Standard sieves on a mechanical shaker for 10 minutes. The uniform sand used was that sand, 100 percent of which passed sieve no. 30 and was retained on sieve no. 35. This sand had an arithmetic mean size of 0.548 mm or a geometric mean size of 0.545 mm on the basis of the adjacent sieve openings.

The actual filter beds of uniform sand were obtained by the following procedure. Each filter was filled up to a static depth of 15 in. and fluidized to an expanded height of 32 in. for 15 min. The top 6 to 8 in. of the fluidized sand was then siphoned off so as to obtain a static depth of 12 in. exactly. Head loss readings for every 3 in. depth of the bed during filtration at 6.6 gpm/sq ft, with clean tap water were compared. Then sand from each filter was remixed with the others so that finally identical head losses (within 0.1 cm) were obtained at all depths amongst all filters. It was also seen that use of a constant backwash valve closing time of 2 mins from an expanded height of 18 in. produced a depth of 12 in. exactly in all the filters. Considerable time and effort was spent in this regard and

¹Fine sand, from Northern Gravel Co., Muscatine, Iowa.

finally, identical uniform sands as far as practicable were obtained in the three filters.

A similar procedure was used to obtain the 18 in. deep graded sands. However, no siphoning off of the fines was done, and the graded sand from the supplier was directly used. Obtaining identical head losses in graded sand beds with clear water filtration was much more difficult and the best that could be achieved was differences of the order of 0.02 ft over the entire depth of 18 in., when filtering at rates of 7 gpm/sq ft. Since the total head losses were of the order of 1.34 ft, these differences were of the order of 1 1/2 percent and were considered sufficiently small. However, it needs to be emphasized that the experimental design was such that a duplication of runs was made on each filter at each expansion, hence even these minute errors were eliminated by the averages obtained on all filters.

B. Laboratory Analytical Procedures

1. Preparation and nature of influent suspension

The influent suspension was prepared by dripping a stock solution of ferrous sulphate ($\text{FeSO}_4 \cdot 7\text{H}_2\text{O}$) from a constant head capillary feeder to the mixing tank, into which a metered quantity of water (4.5 gpm) was added continuously. This flow rate was sufficient to apply to the three filters at 7 gpm/sq ft, and allowed a continuous bleed from the bottom of the mixing tank as well as continuous overflow. The stock solution of ferrous sulphate was prepared by dissolving 111.1 g of the iron salt in distilled water, containing 16.7 ml of concentrated hydrochloric acid and making up to 2 liters in a volumetric flask. This

solution had an iron concentration of approximately 0.2 M in an acid solution of strength 0.1 N. A drip rate of approximately 11 ml per minute of this stock solution gave an iron suspension of 7 mg/l when added to tap water at the rate of 4.5 gpm. Final adjustments to obtain this 7 mg/l of influent iron concentration were made by altering the head on the capillary feeder as well as the flowrate of tap water into the tank. With periodic checks on these variables it was possible to maintain a uniform influent suspension. Minor fluctuations in the chemical feeding rate did occur and were probably due to fluctuations in room temperature which caused the viscosity of the stock solution to change.

Table 1 gives a general analysis of the University tap water used in the studies. This is a hard well water of high alkalinity and total dissolved solids and of relatively constant quality. When ferrous sulphate in acid solution was added to this water a yellowish brown precipitate was formed. A sample of the suspension from the influent to the filters, after the normal detention in the mixing tank, was filtered through a 0.45 μm millipore filter and the filtrate was analyzed for any dissolved iron. It was found that within the accuracy of the equipment used no dissolved iron was detectable. This indicated that the precipitation was complete in the mixing tank. It should be noted that no aeration or addition of air was required for the formation of the precipitate. All the runs were made without the addition of any air. Cleasby found in his study (24), that the precipitated iron under aerated conditions had particle sizes ranging from 1-20 μm with a majority of the particles of the size 5 μm .

Table 1. Analysis of University tap water

Characteristic of water	Concentration-mg/l
Total dissolved solids	680
Total hardness as CaCO_3	365
Calcium hardness as CaCO_3	254
Magnesium hardness as CaCO_3	111
Total alkalinity as CaCO_3	270
Calcium as Ca^{++}	
Magnesium as Mg^{++}	27
Bicarbonate as HCO_3^-	330
Chlorides as Cl^-	17.5
Sulphates as SO_4^{--}	160
Fluorides as F^-	0.9
Manganese as Mn^{++}	0.0
Iron as Fe^{++}	0.03

The actual nature of the precipitate formed by addition of ferrous sulphate to high alkalinity waters has been the subject of considerable controversy during the last decade (24, 38, 64). It has been supposed by various workers that the precipitate could be ferric hydroxide, ferrous carbonate or a combined precipitate of both. Calculations based on chemical equilibrium indicate that the solubility of ferrous carbonate is much smaller than that of ferrous hydroxide ($\text{Fe}(\text{OH})_2$) for values of pH less than 9.5 and should precipitate first (34, p. 29-15).

However, the solubility of ferric hydroxide ($\text{Fe}(\text{OH})_3$) is much smaller than either of the above, and in the presence of oxygen the equilibrium calculations indicate that it should be the first to precipitate. But the principal controlling factor seems to be the kinetics of the oxidation reaction of ferrous hydroxide to ferric hydroxide in comparison with, the kinetics of the precipitation reaction of ferrous carbonate. The kinetics are probably such that a mixed precipitate of ferrous carbonate and ferric hydroxide is formed.

Singer and Stumm (64) under oxygen free laboratory conditions did produce a precipitate of crystalline siderite (ferrous carbonate) and verified its nature by X-ray diffraction analysis. They also determined a new value for the solubility product (pK_s) of ferrous carbonate, which indicated that the solubility of ferrous carbonate maybe nearly three times the value predicted by the pK_s value in the literature. They suggested that this incorrect value of pK_s may have been the cause for the controversy regarding the solubility of ferrous iron in carbonate bearing waters. During the present study, an X-ray diffraction analysis of the precipitate from the mixing tank did not conclusively indicate the presence of crystalline siderite. The diffraction pattern did produce a halo effect, with the maximum of the halo at the diffraction angle corresponding to the peak expected in the standard pattern for siderite. However, due to the semi-amorphous nature of the precipitate and possible oxidation at the solid surfaces by atmospheric oxygen, an exact identification of the precipitate by X-ray diffraction was not possible. A change in color from yellowish brown to dark brown was noticed in the precipitate upon exposure to the atmosphere, indicating

possible oxidation. It is suggested as a future project that wet chemical analyses be performed on the precipitate to identify its character more definitely.

2. Measurement of influent and effluent iron

The main series of experiments consisted of 18 runs, 12 made on uniform sand filters and 6 on graded sand filters. The influent and effluent qualities were evaluated on the basis of iron content. During these 18 runs nearly five thousand four hundred analyses for iron were made; thus a simple and accurate method of analysis was required.

During the initial series (run 1-run 6) the standard method in the water supply field, namely the 1, 10 - phenanthroline method was chosen. Three molecules of 1, 10 - phenanthroline chelate each ferrous ion to form an orange-red complex. The intensity of the color developed obeys Beer's law in the range of pH from 3 to 9, and hence the iron concentration can be determined colorimetrically. In the Standard Methods procedure (66) for total iron, it is necessary to dissolve and reduce the iron in concentrated hydrochloric acid and hydroxylamine, and also boil the solution to insure dissolution. The procedure was considerably simplified by using the patented single powder formulation¹ which dissolves and reduces the iron without any heating. Since very little interfering ions were present the results were unaffected by such interferences. The developed color was observed at 510 nm on a Beckman Model B spectrophotometer. The actual procedure was standardized as

¹Hach Chemical Company, Ames, Iowa - FerroVer.

follows: (i) Pipetted out 25 ml of water into a 50 ml erlenmeyer flask. (ii) Added two scoops of the FerroVer powder with a scoop of size 0.25 g, swirled the mixture and allowed to stand. (iii) At the end of 5 minutes, after the maximum color developed, read the percentage transmittance on the spectrophotometer. The actual concentration of iron was read on a calibration curve, called a standard calibration in this study. This calibration curve had zero transmittance for the dark current setting, and 100 percent transmittance through distilled water. The straight line calibration curve for FerroVer reagent had the following Eq. 57. Representing the calibration in this form enabled the raw data to be easily analyzed on the IBM 360 digital computer.

$$\text{Log}_{10} y_T = - 0.189 x_c + 2.000 \quad (57)$$

where,

y_T = percent transmittance

x_c = iron concentration in mg/l

Ewing in Instrumental methods of chemical analysis (32) analyzed the relative accuracy of readings based on Beer's law. It was shown that the relative error has a minimum at a transmittance of 36.8 percent; if the transmittance was greater than 90 percent or less than 3 percent, the relative error becomes greater than 10 percent, and it increases asymptotically to infinity at 100 percent and 0 percent respectively. Thus, readings of concentration of iron based on transmittances greater than 90 percent are subject to considerable error. Most of readings

of the final effluent quality from the full depth of 12 in. had transmittances between 85 and 95 percent, during the first series of runs 1-6. Also, the FerroVer reagent's sensitivity was limited by the molar absorptivity of 1, 10 - phenanthroline which is 11,100 liter-moles per gm-cm.

The above procedure for measuring the effluent iron had the following weaknesses. (i) The procedure for measuring the quantity of reagent using a scoop had possible errors from analysis to analysis. (ii) The transmittances of the final effluent at the 12 in. depth was too high. (iii) The molar absorptivity of phenanthroline limits the possible accuracy of small changes in iron concentration.

In order to alleviate these weaknesses the following modified procedure was used in all the runs after run 6 and it improved the accuracy of the analyses considerably. A new patented reagent¹, disodium salt of 3-(2-pyridyl)-5,6-bis(4-phenyl sulfonic acid)-1,2,4 triazine, hereafter called FerroZine having a molar absorptivity of 27,900 was used. This compound reacts with divalent iron to form a stable magenta complex species, which is very soluble in water and maybe used for the spectrophotometric determination of iron. The absorption spectrum of the complex has a sharp peak at a wavelength of 560 nm and is uniform in development over the pH range 4-10. Further details of interference studies and statistical data on multiple laboratory studies of FerroZine can be seen in Stookey (67).

¹Hach Chemical Company, Ames, Iowa - FerroZine.

The above reagent as a single solution formulation, FerroZine Solution 1¹ can be added directly to iron hydroxides or carbonates for reduction and dissolution. The procedure for analysis was to add 0.5 ml of FerroZine Solution 1 to 25 ml of water and reading the transmittance on a spectrophotometer after allowing 5 minutes for development of color.

In order to obtain increased accuracy of the transmittance readings on the spectrophotometer, the following new dual standard procedure, based on the method of ultimate precision as described in Ewing (32) was developed. Most of the effluent iron concentrations were of the order of 0.35 to 0.05 mg/l. By dissolving standard iron wire in acid, two standard solutions with concentrations of 0.10 mg/l and 0.30 mg/l of iron were made. These solutions were neutralized to a pH of 7.0 a few hours before the run. Every time a water sample was analyzed, the standard solutions were used for calibrating the spectrophotometer. Using the dark current and slit opening settings simultaneously, the 0.10 mg/l standard was set at 63 percent transmittance and the 0.30 mg/l standard was set at 25 percent transmittance. These settings can only be obtained by a trial and error procedure on the Beckman Model B. Once the spectrophotometer was adjusted to these settings the sample requiring analysis was read. Thus, most readings were obtained between transmittances of 80 and 20 percent and the relative error was reduced to levels below 2 percent. The procedure was rather difficult as every analysis required simultaneous analyses of the standard solutions too,

¹Hach Chemical Company, Ames, Iowa - FerroZine Solution 1.

with the color development time being kept constant at 5 minutes for the standards as well as the analyzed samples. It was found that analyzing a standard sample after addition of the reagent at times greater than 5 minutes (i.e. allowing the colored complex to stand, for say 30-60 minutes) tended to give slightly lower readings as time increased; hence, the above stated procedure was followed to avoid this small error. The calibration curve for these analyses was called the precision calibration and had the following equation,

$$\text{Log}_{10} y = - 2.005 x_c + 2.000 \quad (58)$$

The actual step by step experimental procedure was as follows: (i) Pipetted 25 ml of water samples from the three filters into 50 ml erlenmeyer flasks. (ii) Pipetted 25 ml of the standard solutions (0.10 mg/l and 0.30 mg/l) into two other 50 ml erlenmeyer flasks. (iii) Added 0.5 ml of FerroZine Solution 1 to each of the five flasks using a 1 ml pipette, and then started the stop watch. (iv) Swirled the contents of the flasks occasionally. (v) At the end of 5 minutes decanted samples from the flasks into spectrophotometer cuvettes. (vi) Set the spectrometer by trial and error so that the standard samples read 63 percent and 25 percent transmittances. (vii) Read the three samples of water from the filters. The readings were all taken within 6-8 minutes from the time of addition of the FerroZine. This precision calibration method nullified all the stated weaknesses of the FerroVer method considerably, and increased the accuracy of the effluent quality analyses in the second and third series of runs.

In addition to the effluent samples obtained from the full depth of the filters, continuous drip samples were also taken at various depths of the filter every half hour. These samples had considerably higher iron concentration and hence the standard calibration technique was sufficiently accurate for all these readings. For the runs 1-6 the calibration curve Eq. 57 for FerroVer reagent was used. A similar standard calibration curve for FerroZine reagent was plotted and used in the second (runs 7-12) and third series (runs 20-25) of runs. The standard calibration equation for FerroZine reagent was,

$$\text{Log}_{10} y_T = - 0.465 x_c + 2.000 \quad (59)$$

During the runs, the influent suspension was sampled every half hour. These samples had iron concentrations of 7 mg/l and hence they had to be diluted for obtaining readings within the range of the calibration curves. The samples were diluted in a ratio of 1:5 by adding 20 ml of distilled water to 5 ml of samples. These were then analyzed using the standard calibration technique and gave readings of approximately 22.5 percent transmittance using FerroZine reagent.

All the samples of influent and effluent were collected every half hour. Also, the initial effluent quality was analyzed at frequencies of nearly a minute during the first 10 minutes of a run to study the initial degradation and improvement of effluent quality. These samples were also analyzed by the FerroZine test using the standard calibration technique and if the concentrations were such that the percentage transmittance was less than 20, then dilutions were made to obtain sufficiently accurate readings.

As a further procedure for elimination of small errors, the cuvettes of the spectrophotometer were periodically checked with distilled water for zero errors. Corrections for these errors were made to all the readings. Whenever the errors amongst the cuvettes became larger than 2 small divisions on the transmittance scale, they were cleaned with acid and alcohol as recommended by the manufacturer.

3. Measurement of backwash water quality

While backwashing the filters after a dirtying run samples of the backwash water were collected periodically. These samples had considerable amounts of suspended iron floc, some as high as 800 mg/l. These samples were also analyzed using the standard calibration procedure detailed above; the samples being diluted to obtain reasonable readings on the spectrophotometer. Extra care was taken to see that the samples were thoroughly mixed, and all dilutions were made using volumetric pipettes and volumetric flasks.

4. Sand analyses using a magnetic stirrer wash

During the course of the research project it was realized that additional evidence of the effectiveness of backwash could be obtained by analyzing the amount of iron left as a coating on the sand after the wash. Not only would this provide comparative evidence for studying various expansions, but it would also prove beyond any shadow of a doubt, that abrasion in the fluidized bed was negligible. This of course, was already anticipated from theory and other experimental results quoted in the earlier chapters.

It was decided to evaluate two methods of washing the sand: (i) a physical wash and (ii) a chemical acid wash. At the end of run 19 which included the first two series as well as other studies, the uniform sands in all three filters had been subjected to, the same number and length of filter runs, as well as the same types of back-wash. It was hence realized that the coatings on the sands would in general, be of the same quantity and quality.

Each filter was fluidized, and using a long handled scoop three samples of sand were removed from the top layers of the fluidized bed. Each sample of sand removed by the scoop was approximately 25 g. This sand was washed from the scoop into a 250 ml beaker using exactly 100 ml of distilled water. The beaker had already been weighed, empty and dry. It was now weighed containing the sand, the water drawn by the scoop and the distilled water added. A 1 1/4 in. magnet was placed in the beaker with the sand and water, and the sand was washed by the magnetic stirrer for 10 minutes at a fixed speed setting. A standardized procedure was developed to move the rotating magnet to five different positions of the base of the beaker namely, North, South, East, West and center. The magnet was allowed to rotate at one position for 1 minute. Thus, each position was washed in two periods of 1 minute each. This procedure enabled all the sand in the beaker to be abraded and washed to the same extent. It was found that the distilled water turned quite dark and cloudy and considerable amounts of iron had been removed from the sand by abrasion between sand particles, as well as, by abrasion with the magnet. Photographs showing the sand and water, before and after the physical wash with the magnetic stirrer are shown

in Fig. 6. The supernatant iron suspension was stirred by the tip of a pipette and 25 ml were withdrawn and delivered into a 500 ml volumetric flask. Distilled water was added to make up to 500 ml and this diluted solution (1:20) was analyzed for iron concentration using the FerroZine standard calibration technique. The same procedure was followed for all nine samples.

The beakers containing the sand and the iron suspension (approximately 75 ml) were placed in an oven. The water in the beakers was evaporated and the beakers containing the dry sand were cooled to room temperature and weighed again.

From the above readings the amount of iron removed from the sand in mg/g can be determined from the following formula.

$$\text{Iron removed (mg/g)} = \frac{[\text{Conc. of iron in diluted solution (mg/l)}] \times [\text{Dilution Factor}] \times [\text{Weight of water (g)}]}{1000 \times [\text{Weight of sand (g)}]}$$

It should be noted that the weight of water in grams is assumed to represent the volume of water in ml, and it is the total water in the beaker including whatever water is drawn with the sand from the fluidized bed. This formula gives the iron removed from the sand, quite accurately.

The above was the procedure used in all the analyses run on samples of the graded sand during the third series, runs 20-25. However, due to limitations in time it was only possible to withdraw two samples of sand from each filter during backwashing. At the end of each sand analysis, and prior to the beginning of the subsequent run, the withdrawn samples

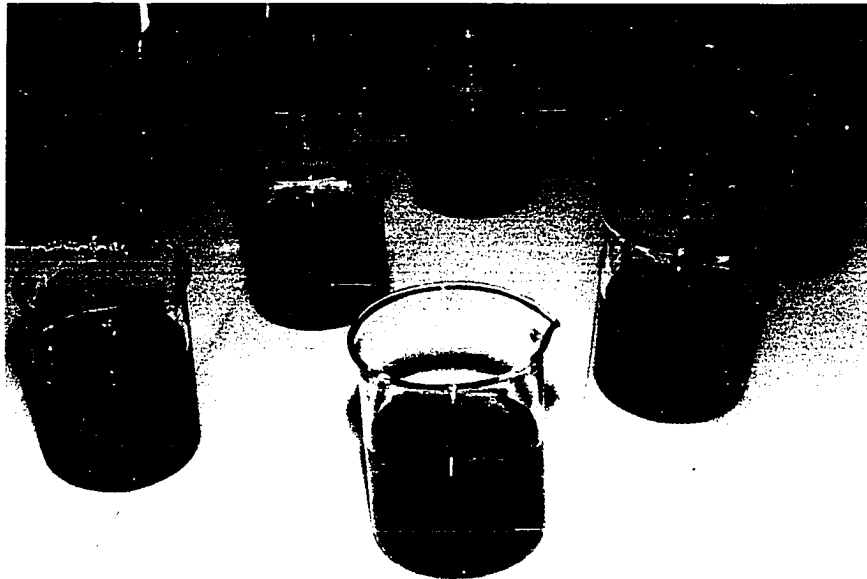


Fig. 6. Iron removed from sand by physical abrasion test

of sand were returned to their respective filters. Thus, the sand in all the runs was identical and no sand losses were allowed to develop.

For the purpose of comparison with an acid wash technique, the following extra analyses were run on the uniform sand samples taken from the filters after run 19. To each of the beakers containing the oven dried sand, 100 ml of 0.3 N sulphuric acid was added. The sand was washed again for 10 minutes using the magnetic stirrer and the standardized procedure already outlined. Five ml of the acid solution of iron was diluted to 1005 ml by the addition of 1 liter of distilled water and its pH was adjusted to 7.0 by the addition of 5-6 drops of concentrated potassium hydroxide. Twenty-five ml samples of the neutralized solution was analyzed for iron using the FerroZine reagent. Using the above readings the iron removed from the sand by the acid wash per gram of sand was calculated. A visual analysis of the sand indicated that the sand was quite clean after washing with the acid, in comparison with the physical wash only.

The comparative results of the physical and chemical wash are presented in Table 2.

The results show that the iron removed by the chemical wash is nearly ten times that from the physical wash; however, the results are consistently analogous and the ratios of iron removed by the chemical wash to that removed by the physical wash are reasonably consistent. Thus, there seems to be no advantage of using a chemical wash to that of a physical wash; also, there is a definite disadvantage in that the acid would tend to remove the entire coating on the sand and hence alter its surface characteristics from run to run. For these reasons

Table 2. Comparative analyses of sand after 19 runs

Filter No.	Sample No.	<u>Iron removed from sand (mg/g)</u>		<u>Ratio of iron removed</u>
		Physical wash	Chemical wash	Chemical wash/ Physical wash
1	1	0.0407	0.445	10.9
	2	0.0409	0.448	10.9
	3	0.0345	0.384	11.1
2	1	0.0494	0.526	10.7
	2	0.0578	0.595	10.3
	3	0.0537	0.554	10.3
3	1	0.0187	--- ^a	--
	2	0.0200	0.371	18.5
	3	0.0237	0.382	16.1

^aOmitted due to incorrect washing.

it was decided to use only a physical wash in all the analyses done on the graded sand during the third series from run 20-25.

C. Experimental Observations

1. Chronology and general descriptions of runs

Twenty-five runs, of which eighteen were dual runs were made. The dual runs consisted of a dirtying run designated "A", the backwash of A, and a filtration run designated "B". In the following, a reference to a run means the complete dual run. Runs A and B are designated as such. The first twelve runs (series 1: 1A, 1B to 6A, 6B. series 2:

7A, 7B to 12A, 12B) were made on filters with 12 inch depth uniform sands of 0.548 mm mean size. From the results to be presented later it will be seen that the initial effluent quality did not have a significant relation to the expansion during backwash. In order to study a hypothesis that the rate of backwash valve closure at the end backwash was the primary criterion affecting initial effluent quality, the runs 13 to 19 were made. These studies are not directly relevant to the theory of optimum backwash, except as a means of showing that initial effluent quality cannot be used as a parameter to evaluate backwash effectiveness; the results and experimental details of these studies are hence presented in a very condensed form. The runs in the series 1 and 2 were made at 7 gpm/sq ft and each run (A or B) lasted for approximately 5 hours. The runs, A or B had to be terminated due to the fact that the head losses developed were nearly 8 to 9 ft and this was the maximum differential heights that could be measured on the piezometer boards.

The reagent used for iron analysis in series 1 was FerroVer. In the first series of runs, the dirtying runs A were made on the first day, and the backwash and the filtration runs B were made on the following day. Since it was possible that some physical and chemical changes could have occurred in the solids removed, due to overnight standing, and also because in actual treatment plants backwashing is performed soon after a filter is removed from service, the two runs A and B, and the backwash of runs A in series 2 were made on the same day. Each dual run including backwash required about 15 hours and two experimenters were required to work continuously to take the readings and make the

analyses of iron. In run 1 the samples of water at depths other than the full depth of 12 inches, were collected by a single experimenter and kept for about 2 to 3 days before all the analyses were completed. It was found that iron in suspension tended to be deposited on the sides of the plastic sampling bottles and the effluent quality at 9 inch depth of the filter measured on a later date was better than the effluent quality measured at the 12 inch depth on the day the run was made. These results were invalid and were not used in the analyses. All iron analyses from run 2 onward were made within a couple of hours after sampling and rational readings were obtained. This could only be accomplished because two experimenters worked. The reagent used for series 2 and 3 was FerroZine.

The last six dual runs (run 20A, 20B through run 25A, 25B) were made on 18 inch depth graded sands with an effective size of 0.45 mm and a uniformity coefficient of 1.47. This set of runs was called series 3. These runs were made using identical procedures to that of series 2. However, in addition to ferrous sulphate, a non-ionic polyelectrolyte¹ was also added to the influent suspension to obtain a concentration of 0.10 mg/l of polyelectrolyte in the feed to the filters. The polyelectrolyte was added in the hope of magnifying the differences of backwashing at different expansions.

The runs 13 to 19 made to study initial effluent quality, had a dirtying run, a backwash and then the initial effluent quality was measured for the first fifteen minutes of the run after backwash.

¹Dow Chemical Company, Midland, Michigan - Separan.

The parameters used to study the effectiveness of backwash in all three series were, (i) initial effluent quality, (ii) head loss increase and (iii) cumulative effluent quality in the run following backwash, (iv) the backwash water quality during backwash and (v) the backwash water volume. For series 3 the additional parameter based on the iron which is physically removable from samples of the backwashed sand was also used. The variation of each of these parameters with porosity was studied at six different porosities of 0.55, 0.60, 0.65, 0.75 and 0.78 on each of the filters. The expansions needed to obtain these porosities for the uniform sand were approximately 33, 50, 70, 100, 140 and 190 percent respectively. Since each run was made on a bank of 3 filters and each series consisted of 6 runs, the effective number of points for each series was 18. The experiments was designed such that each filter was studied at the 6 different porosities during a series. Thus by considering all 18 readings of a series of 6 runs, the small variations between filters and the small variations from run to run were averaged out. Table 3 illustrates the format of the experimental design for series 2, and how the backwash at the different expansions was studied for the three filters F1, F2 and F3. A similar format was used for series 1.

For the series 3, the format of run 7 and 8 as shown in Table 3 for series 2 was repeated three times. This procedure was adopted to enable a particular run to be studied with the backwash expansions of 30, 50 and 75 percent or 15, 40 and 60 percent. This format avoided two adjacent expansions like 40 and 50 percent being studied in a single run and the differences for purposes of comparison were enhanced. This was

Table 3. Experimental design for series 2

Run number	Porosity during backwash					
	0.55	0.60	0.65	0.70	0.75	0.78
	Filter number					
7		F1		F2		F3
8	F2		F1		F3	
9	F1			F3		F2
10	F3	F2			F1	
11			F3	F1	F2	
12		F3	F2			F1

thought advantageous because of the anticipated smaller differences in effectiveness of backwash at different porosities for graded systems. The cause for the anticipated smaller differences in backwash for graded systems has been discussed in page 91 of this thesis.

The expansions needed to obtain porosities of 0.58 to 0.82 in the top layers of the graded sand ranged from 15 percent to 75 percent and these were much less than the expansions required for the uniform sand. All backwashing expansions were controlled on the basis of the expanded heights of the fluidized bed during backwash.

In order to reproduce identical conditions with a clean filter at the beginning of each dual run, the following standardized procedure was used for all runs. The filter was expanded to the anticipated optimum at a porosity of 0.70 and washed for 15 minutes. During the runs 1 to 10 the filters were washed twice before each run began, once

at the completion of the previous run and again immediately preceding the start of a run. However, from run 11 onwards in order to achieve identical conditions to that in a treatment plant, the solids removed in run B of the preceding run were not washed until the following run A. Immediately before the dirtying run A, the filter was expanded to the anticipated optimum at a porosity of 0.70 and washed for 15 minutes.

2. The check list procedure for backwashing

The procedure at the end of a dirtying run A, during backwash and at the start of run B was quite complex and involved several valve operations. A single valve incorrectly opened or closed would have completely ruined all the readings of a run. In order to avoid any errors and to standardize the procedure a check list operation was performed at every run. The following is the sequential check list operation used; the description should be read in conjunction with the schematic layout shown in Fig. 3.

- (i) At the end of run A, close lower drain outlets from the effluent rate controllers with rubber stoppers.
- (ii) Reduce the speed of influent pump E to zero and stop pump.
- (iii) Close all drip samplers.
- (iv) Close all valves 1 and 4 in filter valve system.
- (v) Close water supply inlet to mixing tank.
- (vi) Stop drip of chemicals to mixing tank.
- (vii) Adjust water levels by pouring or removing water in the chambers of the effluent rate controllers, so that the water levels are slightly higher than the equilibrium position at the start of a run.

(viii) Open all drain valves 6 from filters.

(ix) Open top covers of filters and fix siphon backwash line to filter which is to be washed.

(x) If high expansion is needed during backwash start pump B.

(xi) Backwash filters according to planned experimental design expansions by opening valves 5. Use standardized procedure for valve opening and closing: 1 min slow opening, 5 min wash and 2 min very slow closure. The two experimenters should start stop watches at the start of backwash.

(xii) One experimenter to take water temperature, backwash flow-rate in meter C, expanded height and piezometer readings during the 5 min wash time.

(xiii) Using a stop watch, the second experimenter to take backwash water samples from the top of the filter at preplanned intervals of time.

(xiv) While first experimenter is closing backwash valve (i.e. during last 2 min of wash), the second experimenter to flush out all the drip samplers. No backwash water samples should be taken during the flushing operation. After flushing the drip samplers to be adjusted to the correct drip.

(xv) Stop backwash pump B as soon as backwash on any filter for which it is used is completed.

(xvi) Fix covers to filters.

(xvii) Close all drain valves 6 from filters.

(xviii) Start flow of chemicals and open water supply inlet to mixing tank.

(xix) Open all valves 1 and 4 of filters.

(xx) Open outlets from effluent rate controllers by removing rubber stoppers.

(xxi) Start influent pump E and increase speed to noted setting to obtain required flows (for flows of 7 gpm/sq ft in filters, the speed setting was approximately 54).

(xxii) In order to obtain exact flows, make slight adjustments in outlet valves from rate controllers if required.

(xxiii) Adjust water levels in piezometer tubes to obtain the required readings of piezometers at start of run.

The above procedure was followed in all runs of series 1 and 2 as well as the runs 13 to 19. In the case of series 1 and 2 the time of backwash was the same for all expansions; for the graded sand studies of series 3 however, the operation was modified slightly. In series 3, the backwash at different expansions was done for different times, so that the same volume of washwater approximately 36 gallons was used during the total sequence of washing (i.e. valve opening, washing and valve closing). Also while the bed was fluidized, one experimenter collected two samples of the backwashed sand at different times. The samples were collected after approximately 10 gallons and 21 gallons of washwater had been used for backwash. A resume of the backwash sequences and the sand collection times for the graded sand at different expansions is presented in Table 4.

Table 4. Backwash procedures for graded sand

Expansion -percent	Porosity in top 3 in.	Wash sequence			Sand collection times	
		Valve opening -min	Wash time -min	Valve closure -min	Sample 1 -min	Sample 2 -min
15	0.58	1.0	10.5	2.0	4.5	9.0
30	0.67	1.0	6.5	2.0	3.0	6.0
40	0.70	1.0	5.0	2.0	2.75	5.0
50	0.74	1.0	4.0	2.0	2.5	4.5
60	0.77	1.0	3.25	2.0	2.0	3.75
75	0.82	1.0	2.75	2.0	2.0	3.5

3. Observations made during a run

The observations made during the course of a run can be grouped into two categories, (i) data for analysis and (ii) data for quality control. For series 1 and 2 the following readings were taken as data for analysis. During runs A:

(a) The initial effluent quality for each of the three filters at intervals of 1 min each for the first 10 min of a run.

(b) Piezometer readings at depths of 0 in., 3 in., 6 in., and 9 in. for each of the three filters at frequencies of a half hour.

(c) The effluent quality at the total depth of 12 in. for each of the three filters at every half hour. The samples were collected at the outlets flowing into the effluent rate controller chambers.

(d) The effluent quality at intermediate depths of 3 in., 6 in. and 9 in. for each of the three filters at intervals of every hour beginning with the first sampling at 0.5 hours after the run began. These samples were collected from the continuous drip samplers.

During backwash:

- (e) The heights of the expanded bed.
- (f) The backwash flowrate.
- (g) The piezometer readings at every 3 in. depth of the expanded bed.
- (h) The temperature of the washwater.
- (i) The backwash water quality from each filter at times of 0.5, 1.0, 2.0, 3.0, 4.0 and 5.0 min during the washing time of 5 min.

During runs B:

Similar readings as those taken during runs A, and indicated above by (a), (b), (c) and (d) were taken.

(For purposes of maintaining identical conditions from run to run, the following data were taken for purposes of quality control, during runs A and B.

(j) Influent iron concentration for one of three filters at frequencies of a half hour.

(k) The flowrate through the three filters was monitored and adjusted if necessary every half hour. Adjustments were only required during the latter halves of runs A or B.

(l) The room temperature and the water temperature were monitored every half hour. Any small changes of water temperature were adjusted.

A similar set of readings were taken during the series 3 for the graded sand, subject to the following modifications.

(a) In order to obtain the peak of the initial effluent quality curve, the samples of water were collected at 0.5, 1.0, 1.5, 2.0, 3.0, 4.0, 5.0, 6.0, 8.0 and 10.0 min respectively.

(b) Since the depth of sand was 18 in., piezometer readings were taken at 0 in., 3 in., 6 in., 9 in., 12 in. and 15 in.

(c) The effluent quality was measured at the total depth of 18 in.

(d) The effluent quality at intermediate depths was measured at 3 in., 6 in. and 12 in.

(i) The sampling for backwash water quality from each filter was variable depending on the duration of the washing sequences as shown in Table 4. However, the sample collection times were so preplanned that 7 samples were collected from each filter at times corresponding to usage of equal volumes of washwater.

4. Sieve analysis of expanded layers of fluidized bed

In order to evaluate the degree of segregation and the distribution of particle sizes in layers of the fluidized bed, the following experiment was made on the graded sand. The graded sand bed was fluidized to 50 percent expansion and allowed to stabilize for nearly 1/2 hour and then, approximately 3 in. layers of the fluidized bed were siphoned off. These sections of sand were then oven dried and cooled. The total dry volumes were measured and then representative samples from each layer for purposes of sieving were obtained by repeatedly reducing the total volume of each layer in a two way splitting sampler to about 500 grams.

Using the balance sand from each layer after selecting the 500 grams, bed porosities of each layer were measured by procedures described elsewhere (2). From the measured volumes and the expanded heights of the same layers, the porosity of each layer when the total bed expansion was 50 percent was also calculated. The samples selected for sieving, which weighed about 500 grams were sieve analyzed using a sieving time of 5 minutes. Further details and a discussion on the theory of sieving can be found in Amirtharajah (2). U.S. standard sieve nos. 12, 14, 16, 18, 20, 25, 30, 35, 40 and 45 were used in the analysis. The above sieve analyses of the 3 in. layer at the top of the bed has been used in a subsequent chapter to help formulate a design model for optimum backwash.

D. Data Analysis

In order to simplify the analysis of all the data, several short computer programs with simplotter subroutines were written in Fortran IV G. The programs utilized the raw data of the iron concentrations given in percent transmittances, converted them to concentrations in mg/l using the calibration equations 57 through 59 and then performed the required calculations on the IBM 360 computer of the university. The calculated results were then plotted graphically by the incremental plotter of the computer.

For purposes of quality control and to check the general form of the curves, the following curves were plotted for most of the runs: (i) head loss against time (ii) ratio of effluent to influent concentration against time (i.e. C/C_0 vs. t). Some typical results are

shown in Figs. 7 and 8. From the head loss curves it can be seen that the behaviour is reasonably linear for the uniform sand. The ratio of effluent to influent curves indicate that even after backwash at various expansions the variation from filter to filter is very small. Thus, for using the effluent quality as a parameter to indicate the effectiveness of wash needs a cumulative effluent quality curve as described by Johnson and Cleasby (49).

The main results of this dissertation presented in the next chapter were obtained chiefly from the above computer analyses.

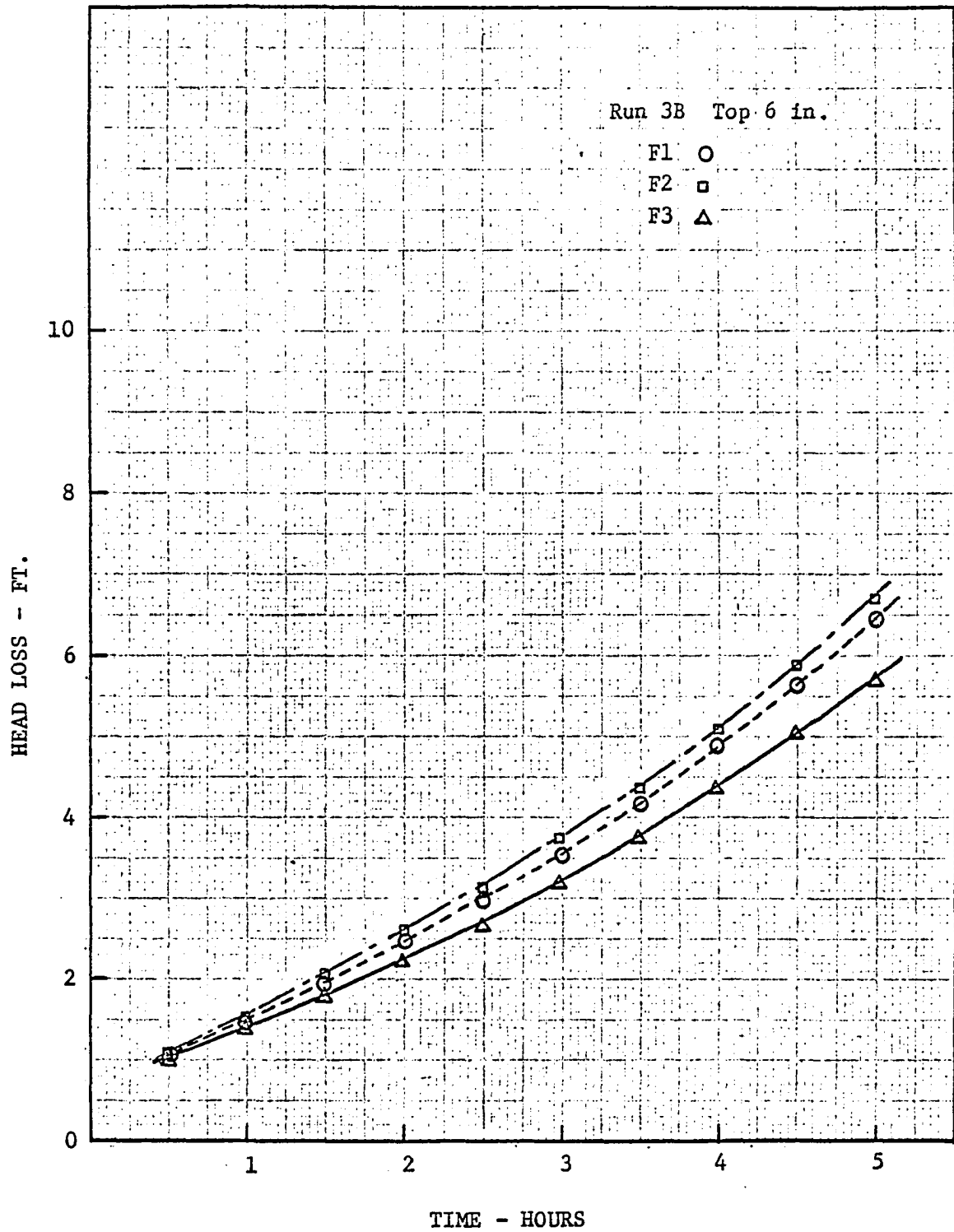


Fig. 7. Head loss curves for run 3B, top 6 in. of filter media

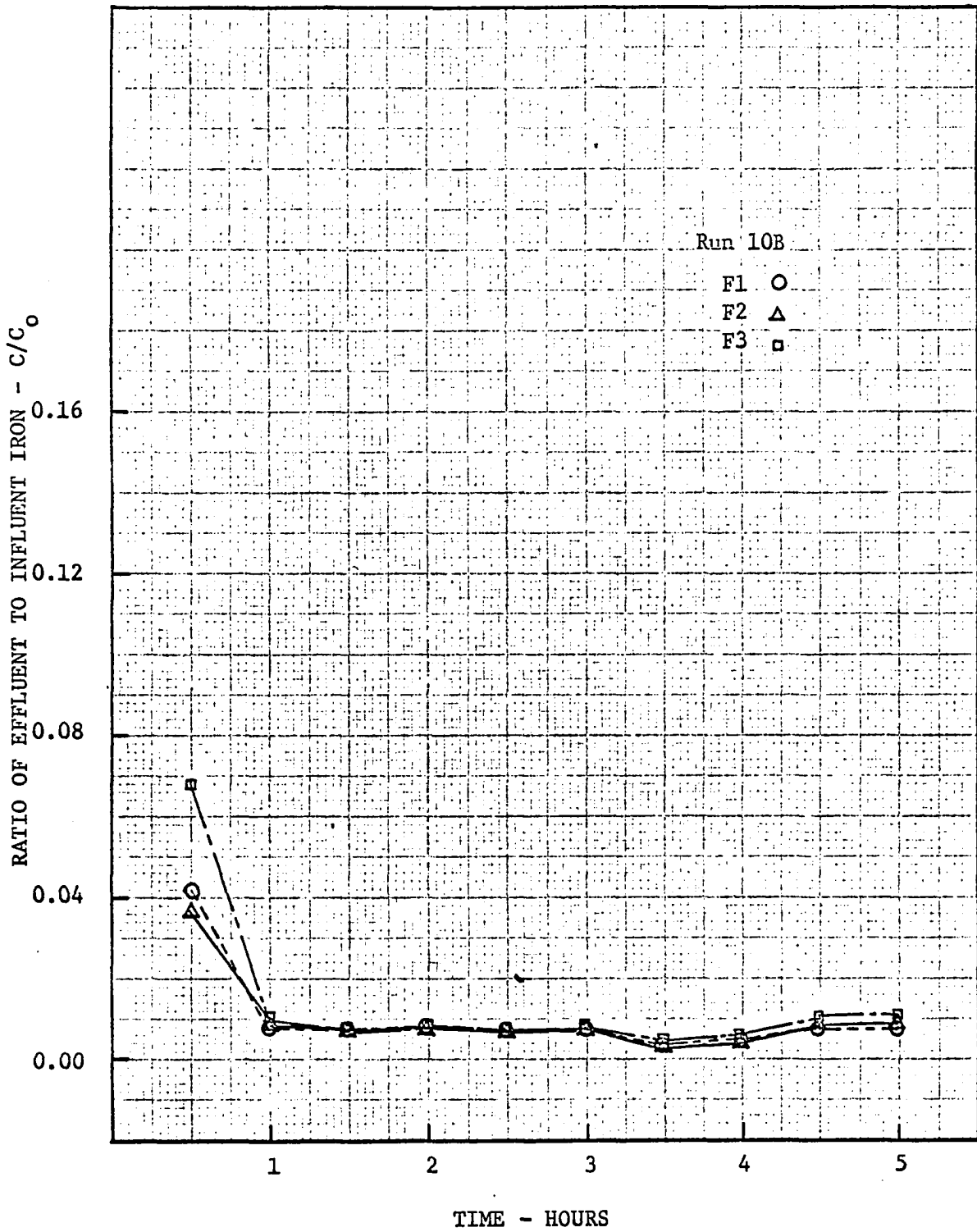


Fig. 8. Variation of the ratio of effluent to influent iron with time

VII. RESULTS AND ANALYSIS

A. Results

The following sections present the main results of this thesis. The results in each section indicate the variation of the following parameters with the porosity provided during the controlled backwash following the dirtying run: (i) effluent quality at various depths, (ii) initial effluent quality at full depth of filter, (iii) head loss increases, (iv) backwash water quality, (v) backwash water volumes and (vi) sand wash analysis. The parameters of effluent quality, initial effluent quality and head loss were the differences between the standard dirtying runs A and the subsequent runs B after backwash.

1. Cumulative effluent quality and porosity

The Figs. 9-14 show typical plots of the cumulative differential iron of the effluent with time (runs 7-12, series 2). The ordinate is the accumulated difference between the iron in the observation run B and the dirtying run A for the effluent from the full depth of the filter. If the ordinate is negative it means that the cumulative iron in run A was greater than that in run B or mathematically $\sum_{\text{time}} \text{Iron}$ (B-A) < 0. In each run all three filters were dirtied under identical conditions as explained in the previous chapter. The filters were then backwashed at different expansions and the quality was studied in the following run. Study of these figures towards the end of the run will indicate which filter performed the best in a particular run. The filter with the smallest positive, or the most negative cumulative iron

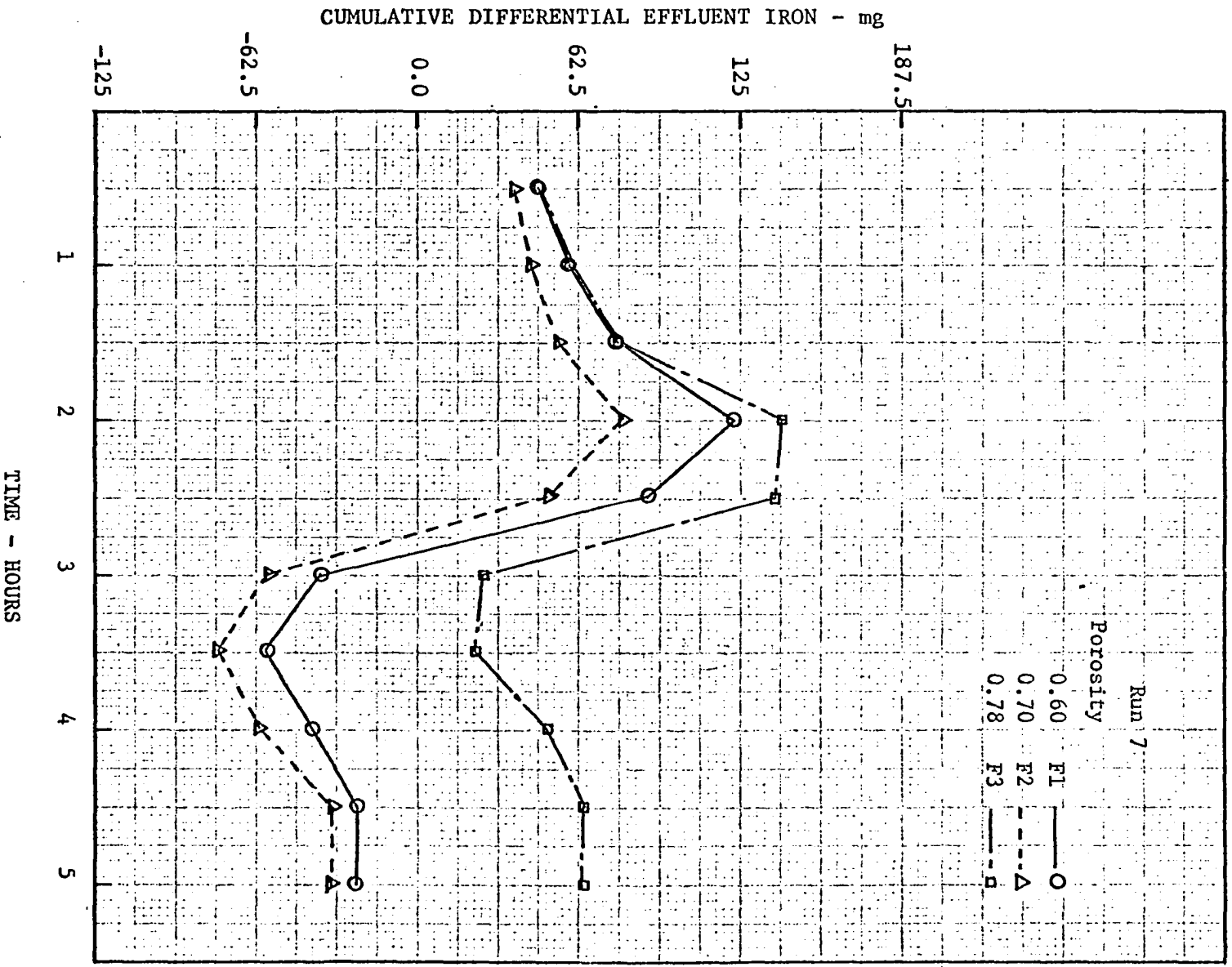


Fig. 9. Cumulative differential effluent iron vs. time, run 7

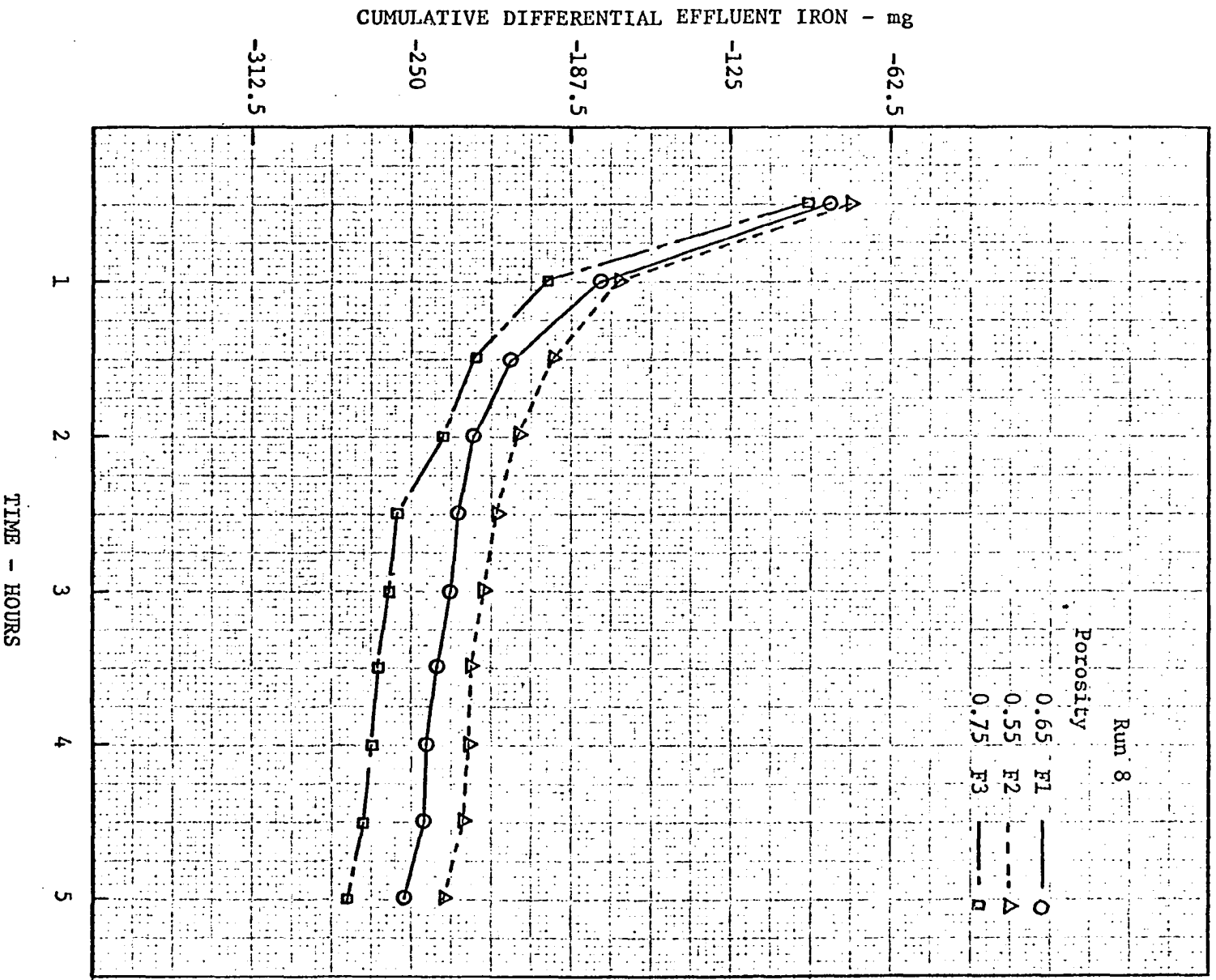


Fig. 10. Cumulative differential effluent iron vs. time, run 8

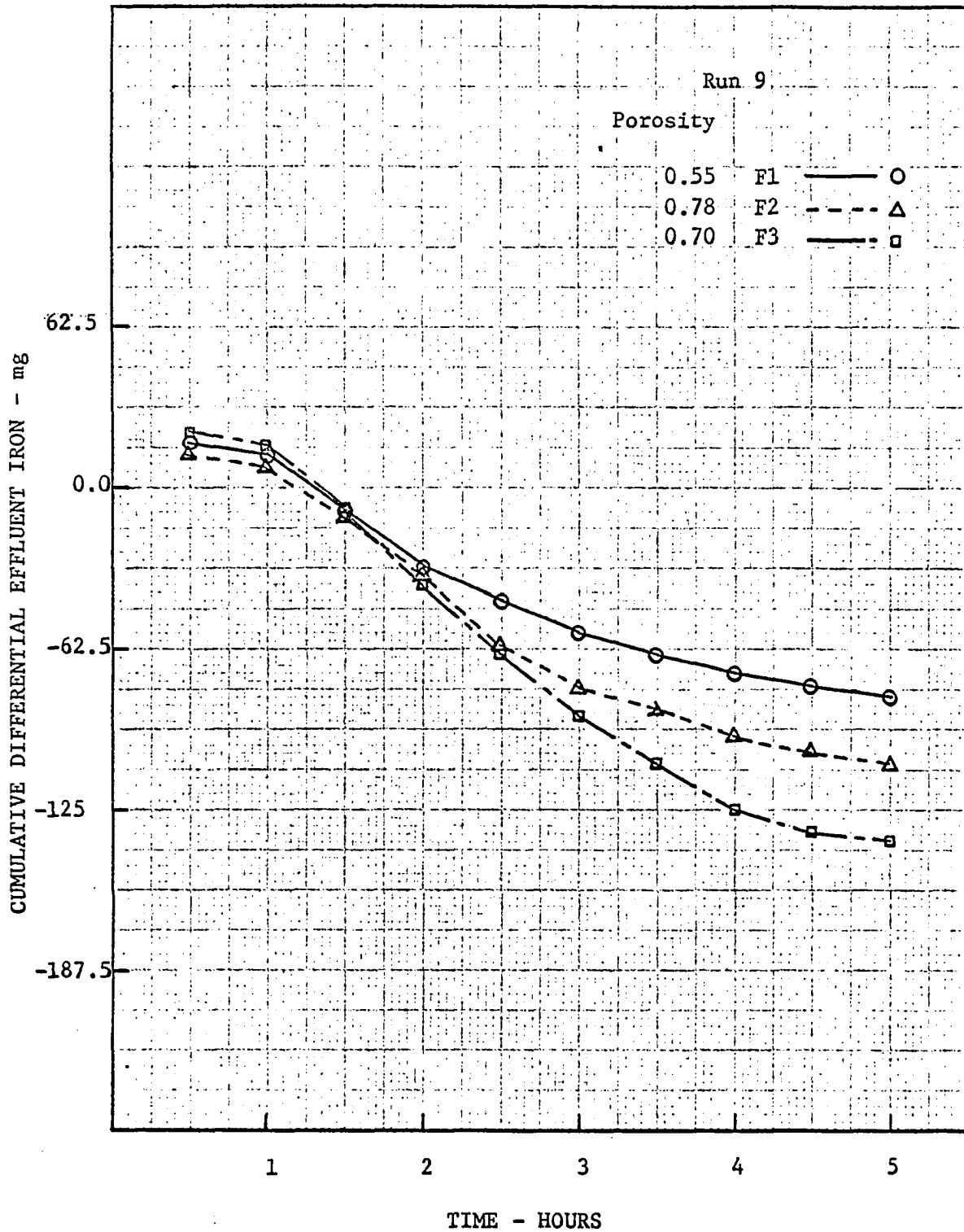


Fig. 11. Cumulative differential effluent iron vs. time, run 9

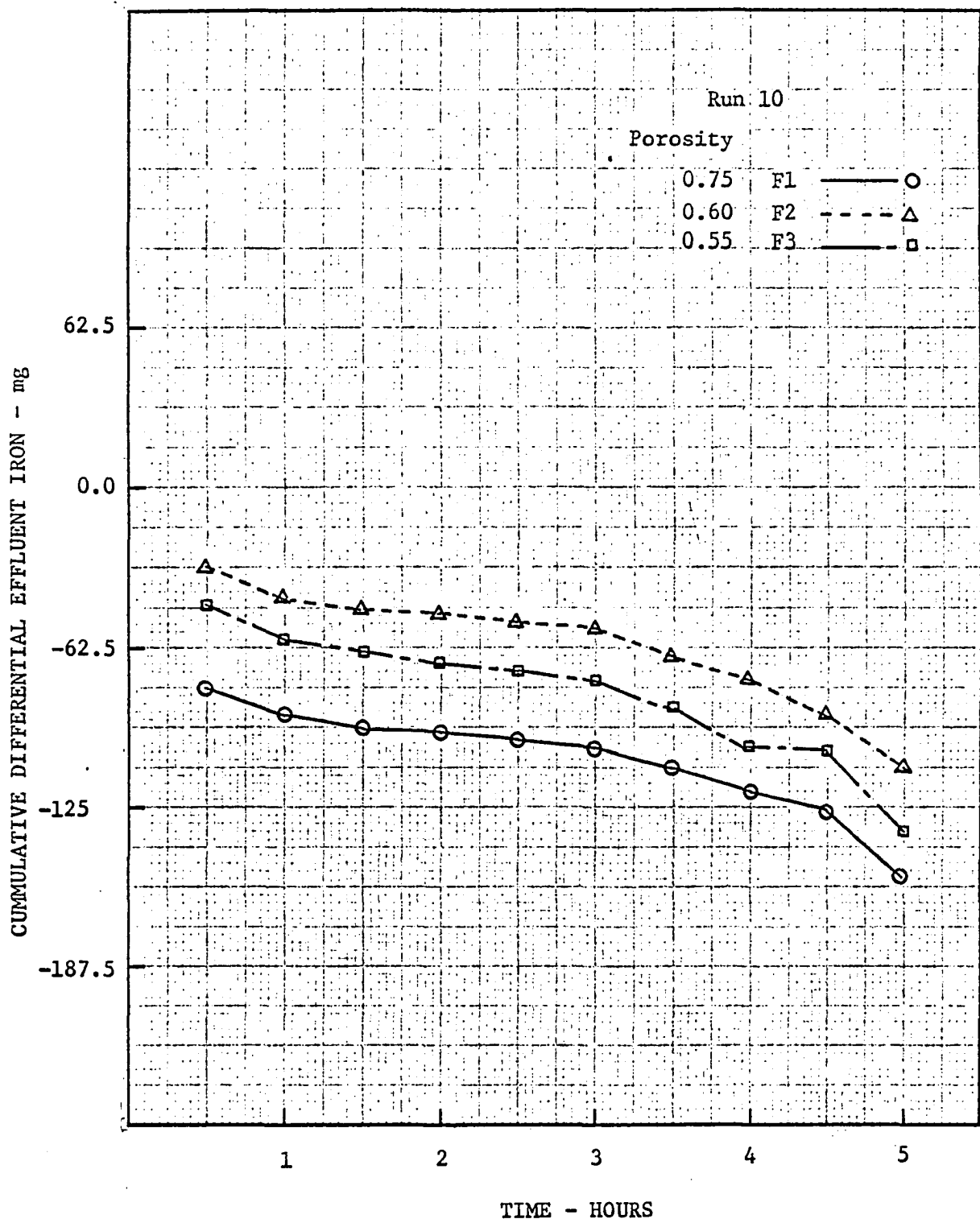


Fig. 12. Cumulative differential effluent iron vs. time, run 10

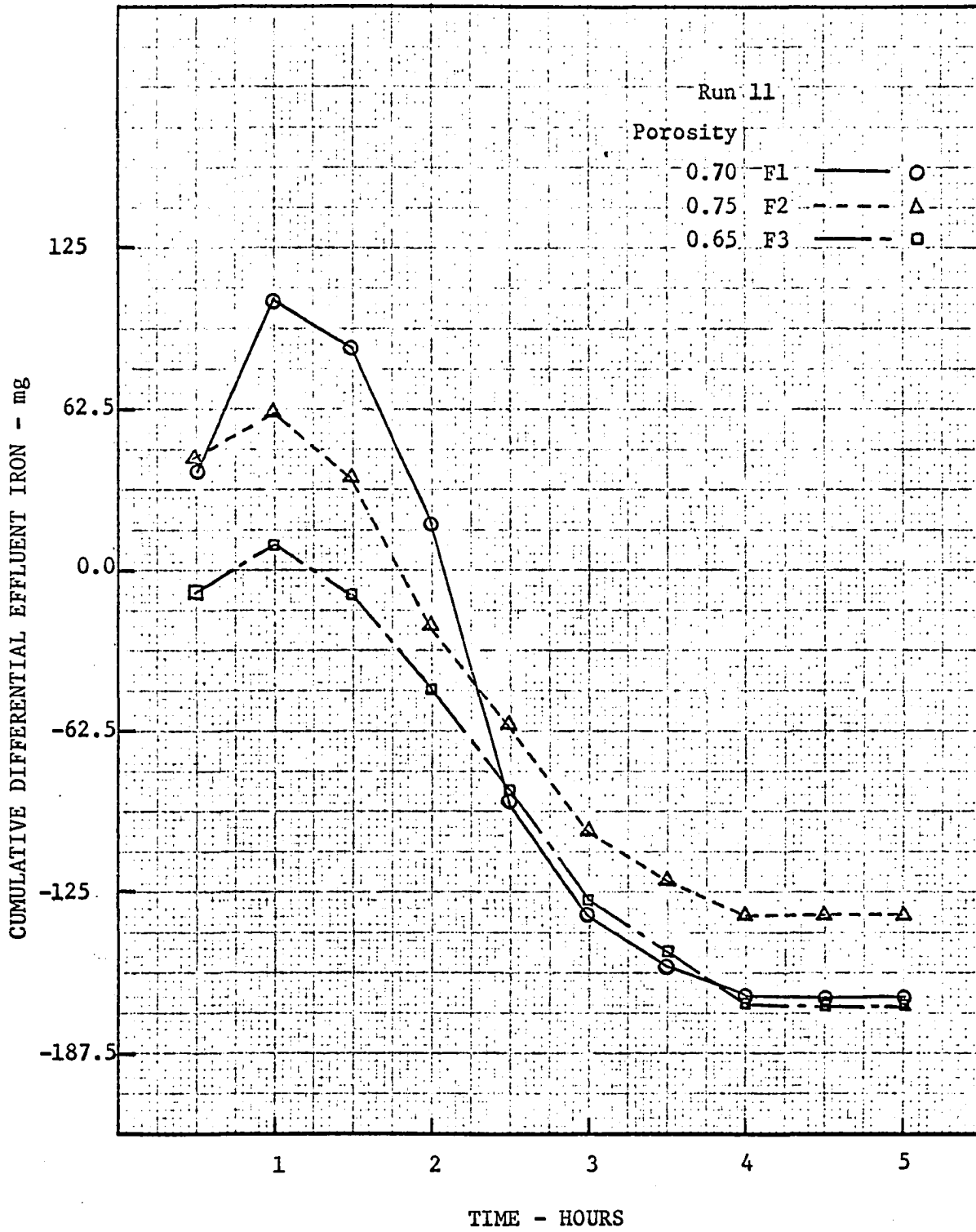


Fig. 13. Cumulative differential effluent iron vs. time, run 11

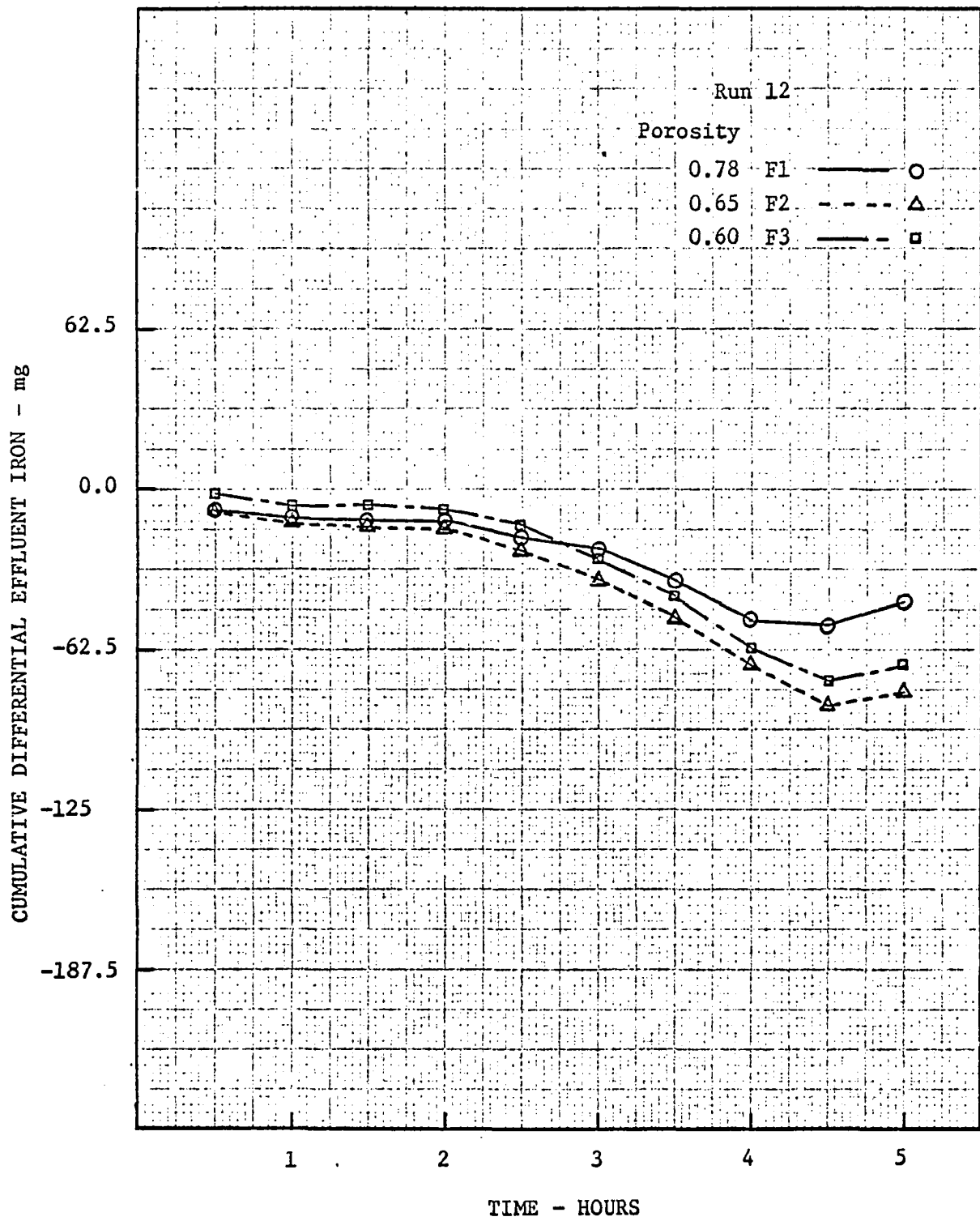


Fig. 14. Cumulative differential effluent iron vs. time, run 12

produced the filtrate of the best quality in the filtration run compared to the dirtying run.

An index called the effluent quality index was defined to comparatively grade the filters in each run. In each run the filter producing the best cumulative differential effluent quality was given an index value of 3, the next best quality was given an index value 2 and the worst quality was given an index 1. If two filters performed almost identically in a run then the two effluent quality index grades were divided between the two corresponding filters.

The values of the index for all the runs 7-12 and the corresponding porosities in each case are shown in Table 5.

Originally it was thought that the differential cumulative iron could be summed from run to run to give the basis for comparison. In practice it was found that even with the best possible experimental controls it was impossible to reproduce identical dirtying runs in the series, due to the inevitable fluctuations in flowrate and iron concentrations. This is well illustrated by seeing the shape of the curves in Figs. 9-14. It can be seen that in a particular run the three curves are similar in form, but from run to run considerable differences can be noted. However, within a single run the changes were made on all three filters simultaneously and comparisons within filters during a run were the best possible means of study. Since six expansions were studied, a bank of six filters would have provided a better apparatus than the three filters used in these experiments. Using the above artificial effluent quality index and repeating the runs so that each filter was subjected to all the expanded porosities

Table 5. Effluent quality index and porosity for series 2

Run number	Expanded porosity					
	0.55	0.60	0.65	0.70	0.75	0.78
Backwashing index						
7		2		3 ^a		1
8	1		2		3	
9	1			3		2
10	2	1			3	
11			3	2	1	
12		2	3			1
Cumulative effluent quality index	4	5	8	8	7	4

^aThe best performance in effluent quality was given an index 3 the next best 2 and the worst was given 1.

during backwash, differences due to variations in the sands of the filters were averaged and hence eliminated. Thus the index provides the best means of comparison of backwashing effectiveness between different expansions.

The variation of the cumulative effluent quality index (i.e. summing the index for all runs) with porosity for runs 7 to 12 shown in Table 5 is plotted graphically in Fig. 15. The results shown a maximum in the cumulative effluent quality index at a porosity of

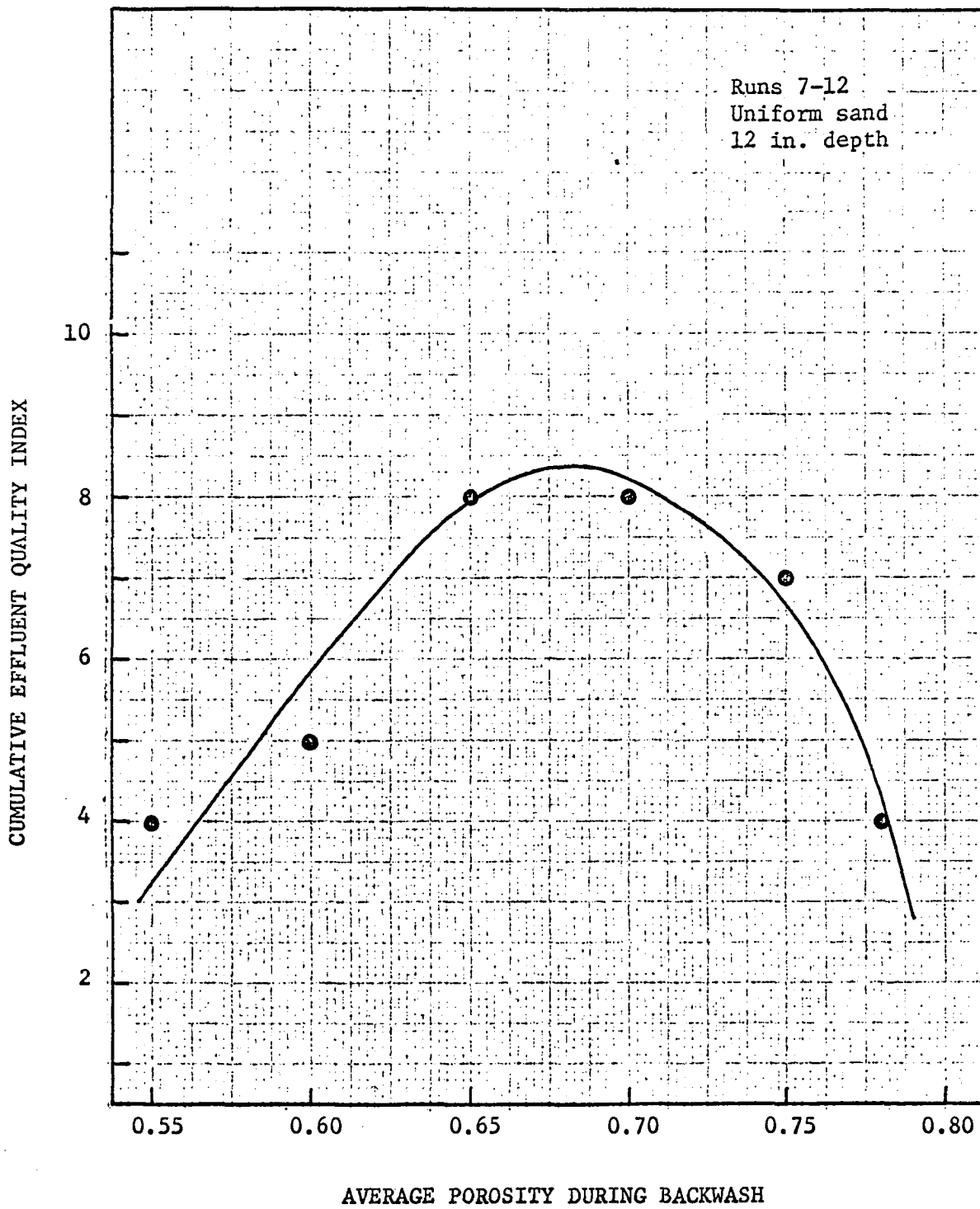


Fig. 15. Cumulative effluent quality index vs. porosity, series 2, 12 in. depth

0.65 to 0.70. The maximum indicates that the best effluent quality in the run following backwash is produced by backwashing the dirty filter at the expanded porosity of 0.65 to 0.70.

The same type of analysis was done for the effluent qualities measured at the depths of 3 in., 6 in. and 9 in. during series 2. The variations of the cumulative effluent quality index with porosity for all the depths of 3 in., 6 in., 9 in. and 12 in. are shown in Fig. 16.

The results for the runs 1-6 for the 12 in. depth are presented graphically in Fig. 17. The results at other depths were not analyzed due to the fact that the readings of effluent iron in run 1 were invalid due to storage of the samples for too long a period before analysis as already mentioned under experimental observations. Since a complete set of readings are required for an unbiased analysis at all porosities, the results for series 1 could not be analyzed.

The results of the variation of the cumulative effluent quality index with expansion for the graded sand for the full depth of 18 in. and for all depths of 3 in., 6 in., 12 in. and 18 in. are shown in Figs. 18 and 19. Also marked on figures are the experimentally determined porosities of the top 3 inches of the graded sand bed while in the fluidized state. The porosities corresponding to the expansions are also shown in the figures.

These porosities of the top 3 inches of the fluidized bed of graded sand were determined by several alternatives methods. The head loss readings in all three filters during backwashing of all the runs 20 to 25 gave 18 readings. The method of calculating the expanded porosity

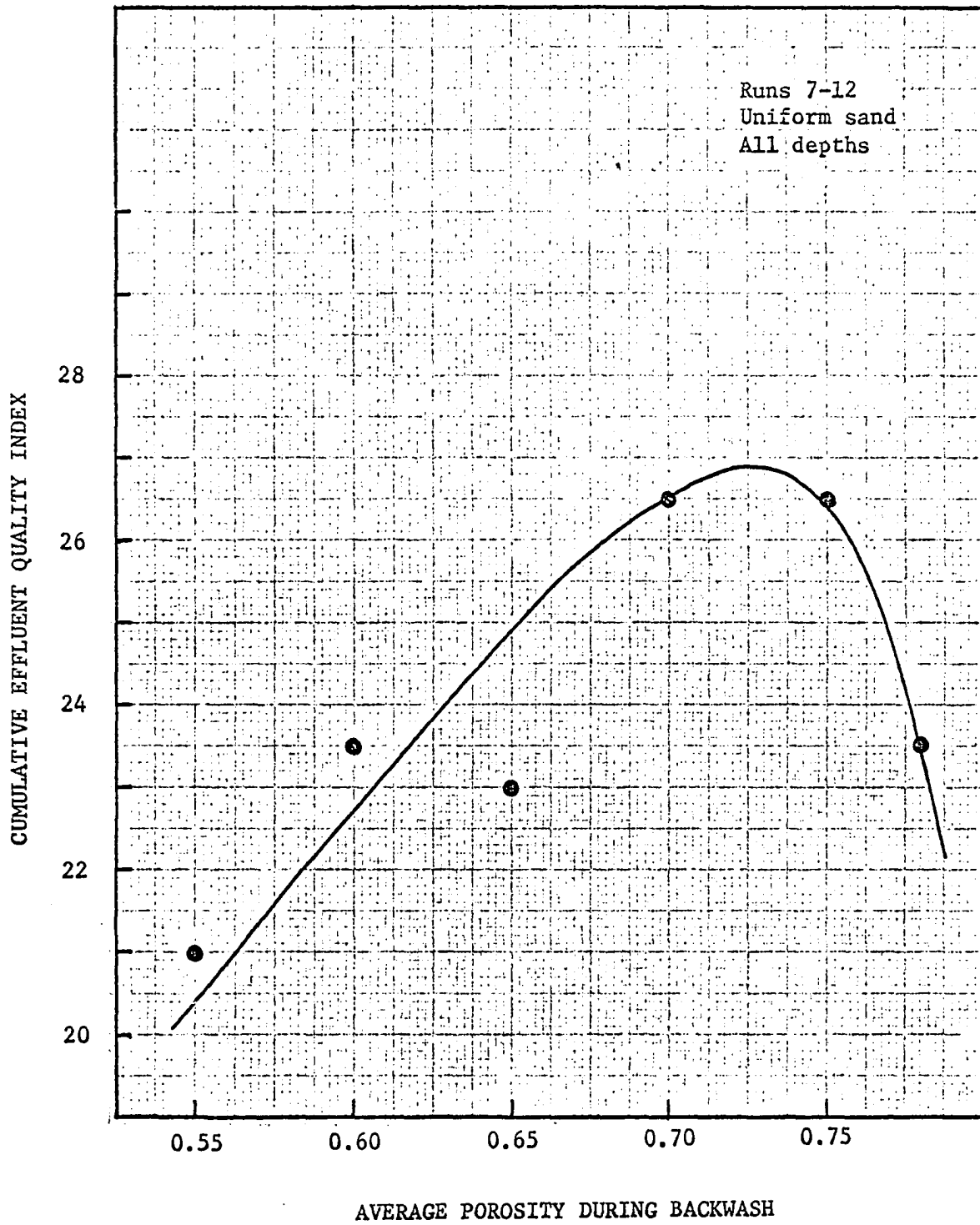


Fig. 16. Cumulative effluent quality index vs. porosity, series 2, all depths

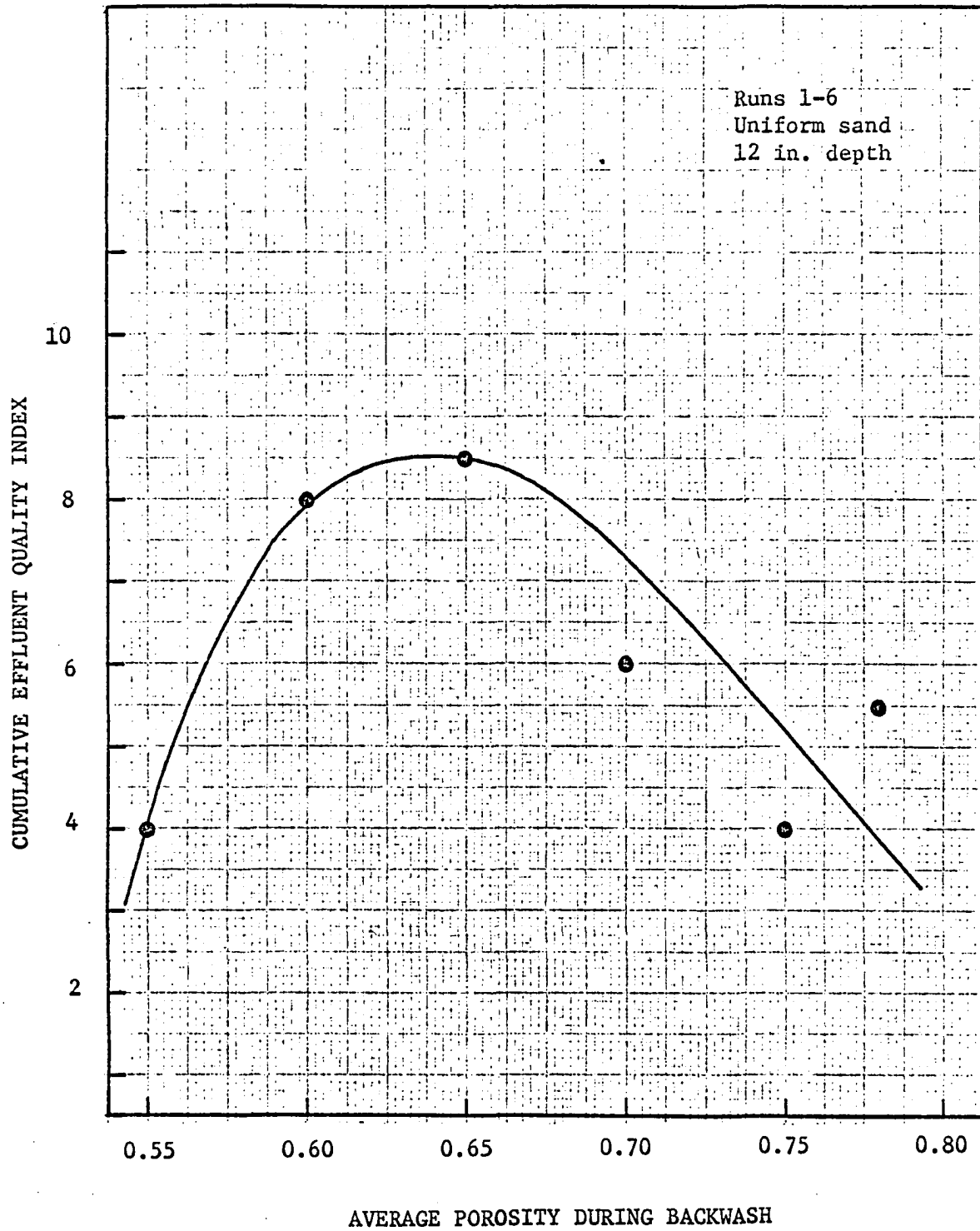


Fig. 17. Cumulative effluent quality index vs. porosity, series 1, 12 in. depth

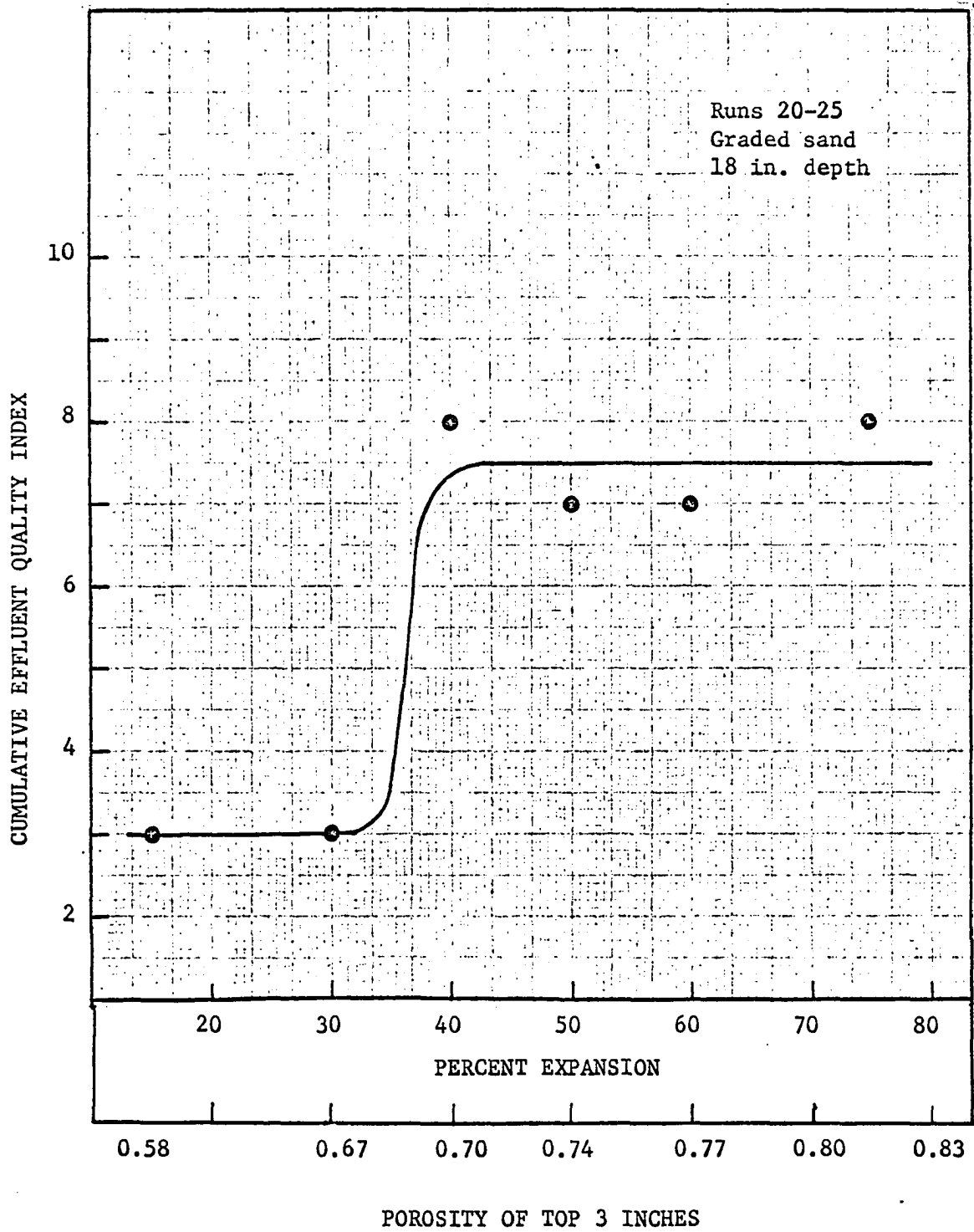


Fig. 18. Cumulative effluent quality index vs. expansion, series 3, 18 in. depth

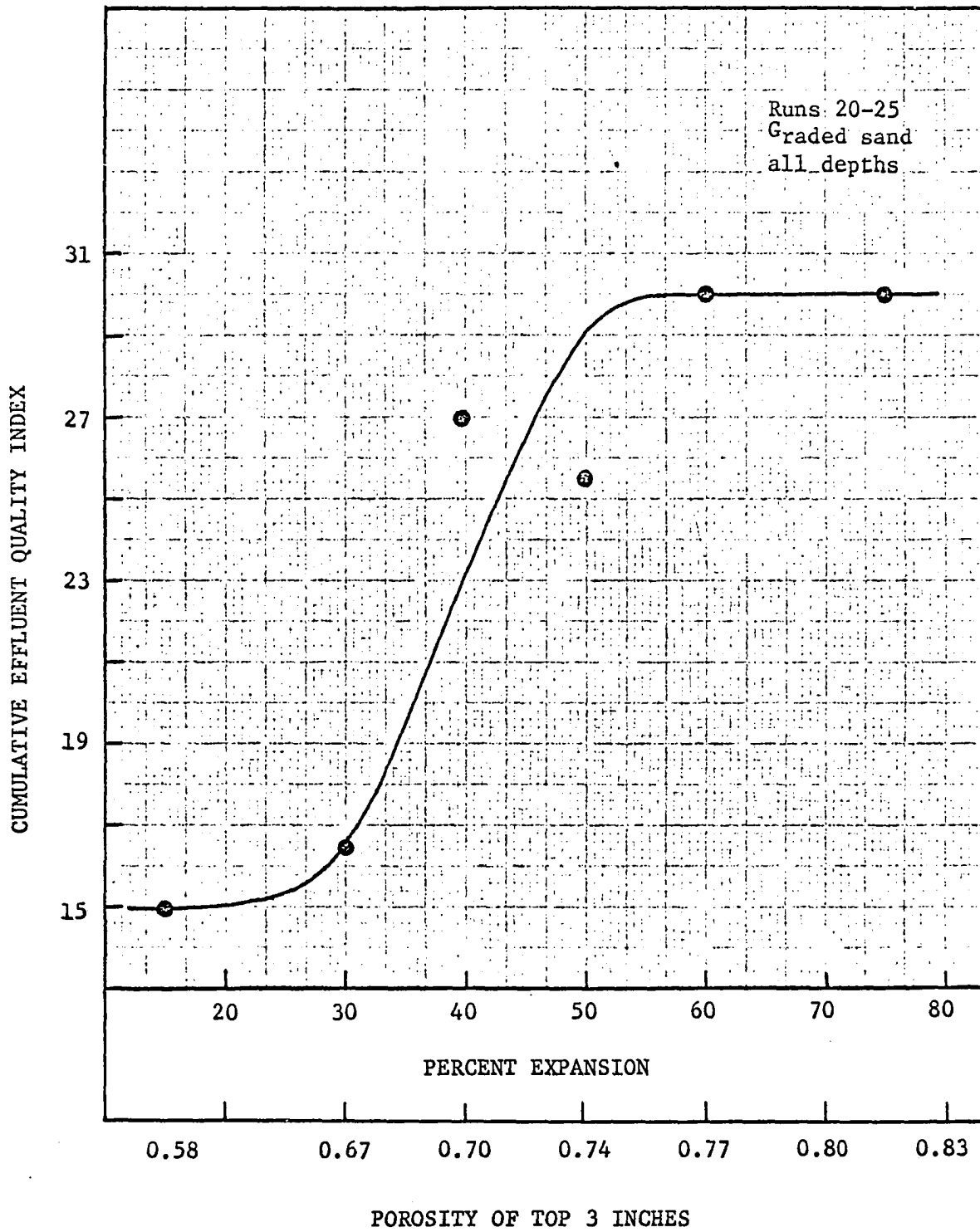


Fig. 19. Cumulative effluent quality index vs. expansion, series 3, all depths

from these head loss readings utilizing Eq. 52 is given in detail elsewhere (2). A special expansion study subsequent to series 3 was also made to determine the porosities of the top 3 in. section at the different expansions. This was made to provide more data (18 readings) under conditions which did not require fixed short time limits as the readings taken during the optimum backwash runs. Also utilized was a physical measurement of the porosity at 50 percent expansion by siphoning off the top 3 in. layer. The mean of 6 readings of porosity at each expansion, and the mean of 7 readings at the 50 percent expansion, are plotted as an expansion-porosity characteristic in Fig. 20. The values from the mean curve are those used for presenting the results and analysis for the graded sand.

All the results of series 1, 2 and 3 shown in Figs. 15 to 19 indicate quite clearly, that in every case the best effluent quality in the run following backwash is obtained by expanding the bed to porosities of 0.65 to 0.70 during backwashing.

2. Initial effluent quality and porosity

A similar technique as above was used to study the variation of initial effluent quality with porosity during the preceding backwash. The cumulative initial effluent index was given values of 3, 2 or 1 depending on the cumulative differential iron between runs B and A during the first 10 minutes of a run. The method was identical to that used to evaluate the effluent quality as already described. The results are shown graphically in Figs. 21 and 22, for the uniform sand and the graded sand respectively. The results are quite negative and

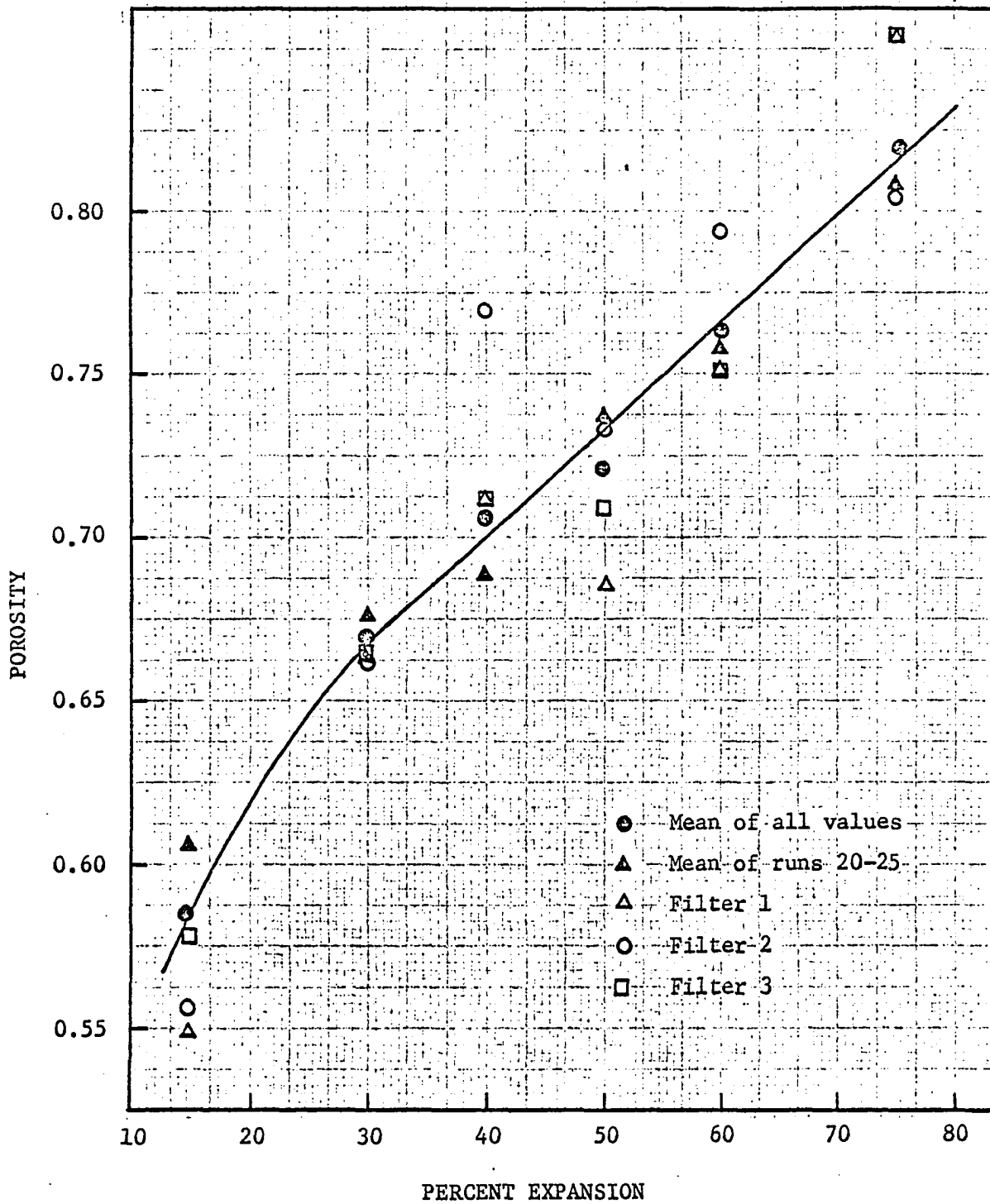


Fig. 20. Expansion-porosity characteristic for top 3 in. of graded sand

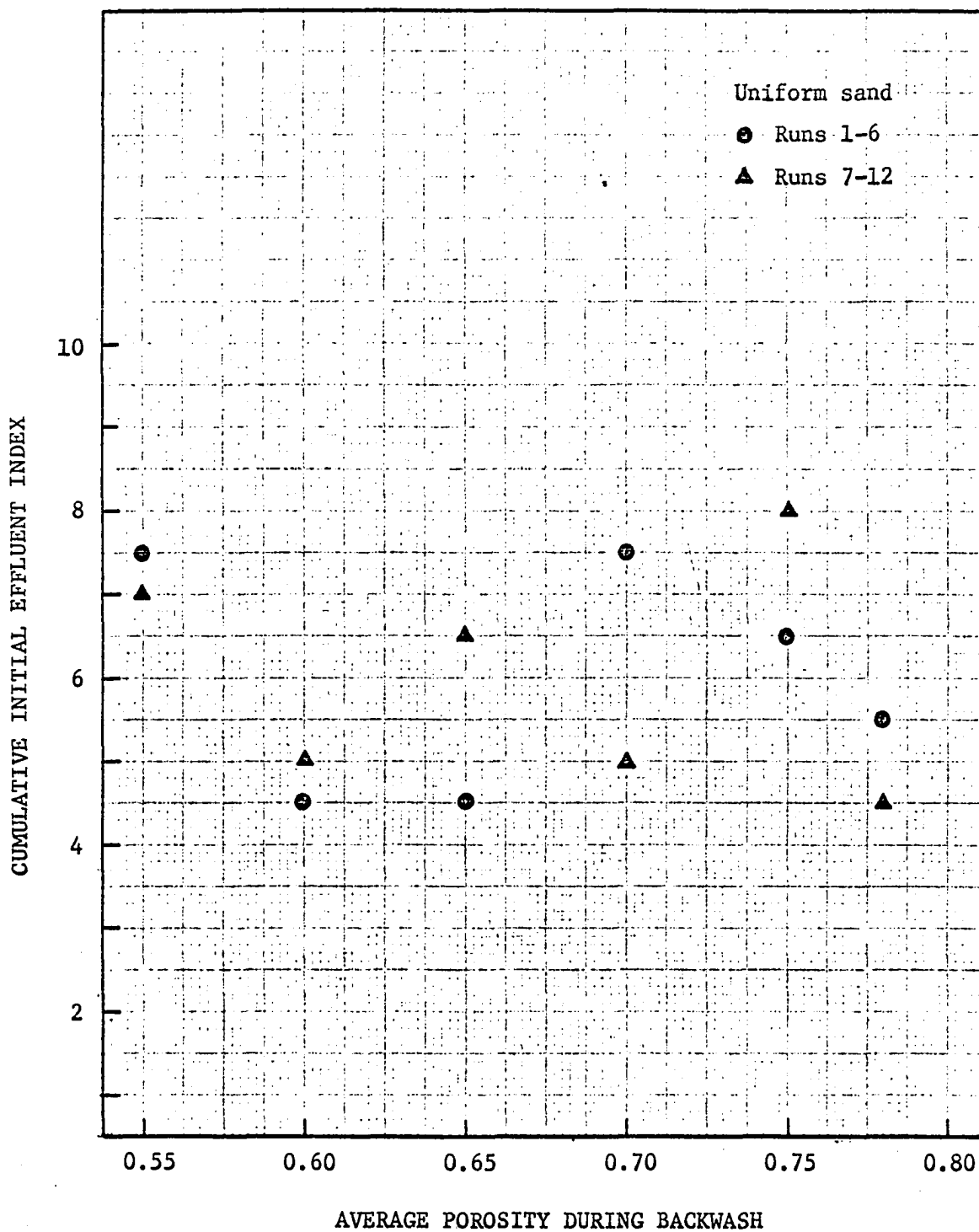


Fig. 21. Cumulative initial effluent index vs. porosity, series 1 and 2

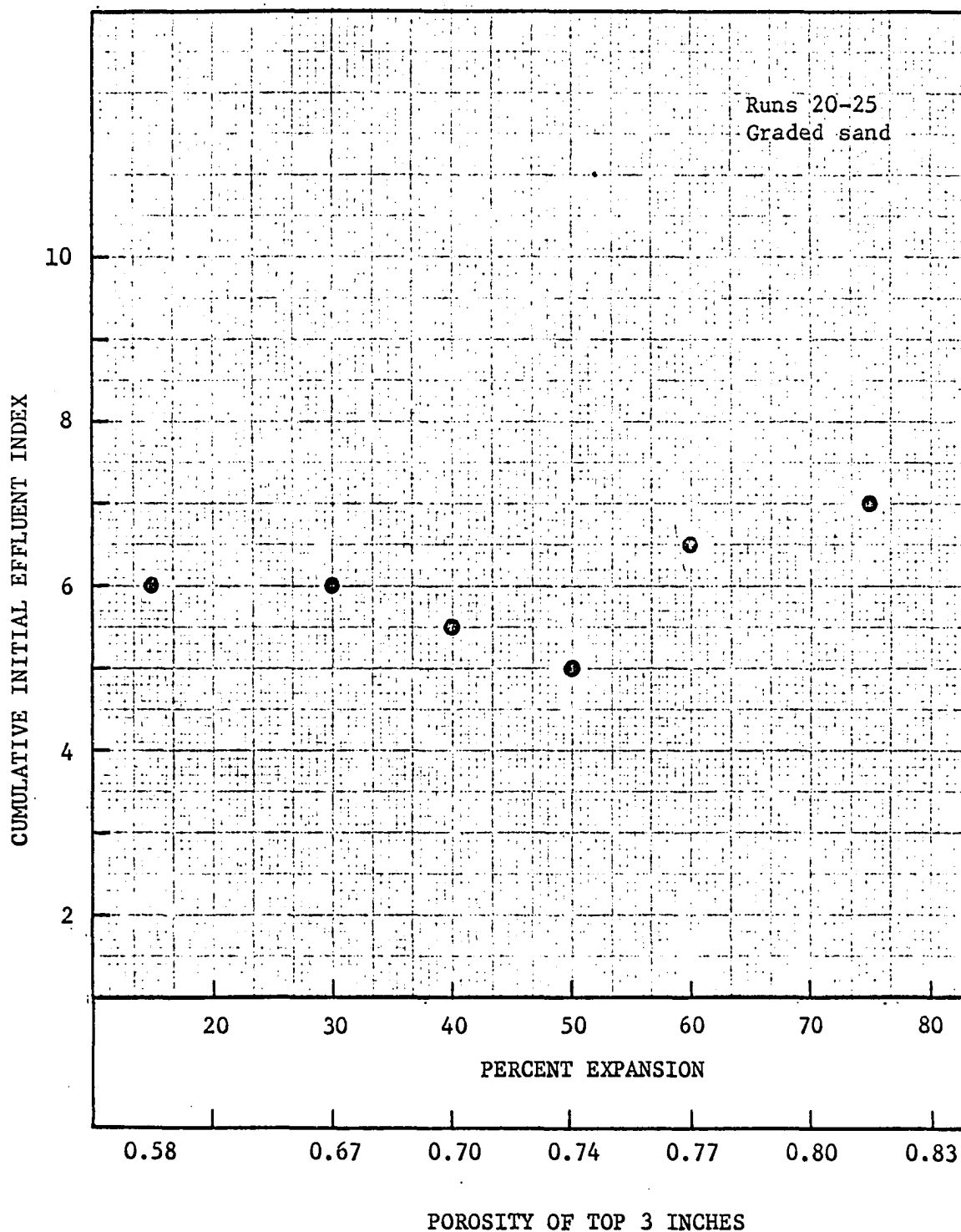


Fig. 22. Cumulative initial effluent index vs. expansion, series 3

indicate no relationship between the initial effluent quality in the run following backwash and the porosity of the expanded bed during backwashing.

It was felt that the initial effluent quality was not dependent on the backwash expansion but was a function of the rate of closure of the backwash valve. In order to test this hypothesis, the total iron in mg flushed out in the initial effluent during the first 15 min was plotted against the time of valve closure in Fig. 23. The graph shows that the total iron flushed out increases as the time of valve closure is reduced.

3. Head loss increases and porosity

A study was also made on the effect of backwash on the head losses in the run following backwash. Again comparison was made between filters based on the difference of head loss in run B over that of the dirtying run A. In order to consider the head loss increases at the time when the losses were at their greatest, the difference calculations were made on the head losses after 5 hours of filtration. The head loss increases from run A to B were measured at depths of 3 in., 6 in. and 9 in., for each of the three filters in runs 1-12. (A 12 in. reading could not be obtained because no piezometer tap was present at the bottom of the filter media.) For a given porosity, the cumulative head loss increase in the 3 in., 6 in. and 9 in. depths were found for each filter, and then the mean of this cumulative head loss increase for the three filters. The scheme of calculation is shown in Table 6 for series 2.

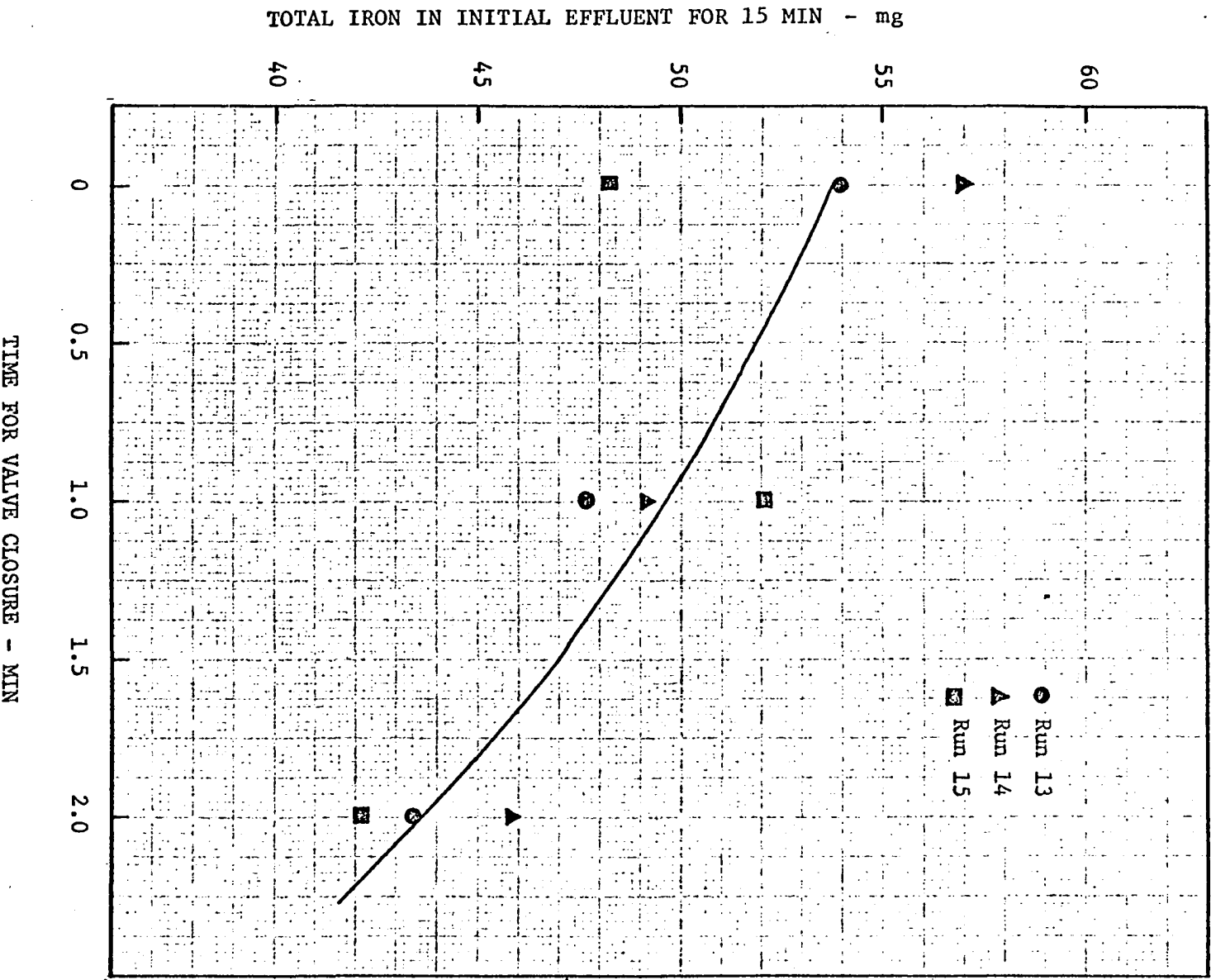


Fig. 23: Initial effluent quality vs. time of valve closure, runs 13-15

Table 6. Head loss increases from run A to B, uniform sand, series 2

Filter no.	Depth of filter - in.	Expanded porosity					
		0.55	0.60	0.65	0.70	0.75	0.78
Head loss increase - ft							
1	3	0.40	0.68	-0.09	0.36	0.16	0.29
	6	0.42	0.61	-0.11	0.37	0.08	0.32
	9	0.04	0.35	-0.10	0.35	-0.03	0.26
2	3	-0.27	-0.66	0.03	0.53	0.06	0.51
	6	-0.30	-0.71	0.01	0.48	0.08	0.60
	9	-0.00	-0.45	0.32	0.45	0.09	0.80
3	3	-0.06	0.36	-0.04	-0.03	-0.33	0.32
	6	-0.21	0.39	0.03	0.22	-0.27	0.38
	9	-0.34	0.38	-0.03	0.19	-0.30	0.24
Filter no.	Cumulative head loss increase at 3, 6 and 9 in. depths - ft						
1	0.86	1.64	-0.30	1.08	0.21	0.87	
2	-0.57	-1.82	0.36	1.46	0.23	1.91	
3	-0.61	1.13	-0.04	0.38	-0.90	0.94	
Mean cumulative head loss increase - ft	-0.11	0.32	0.01	0.97	-0.15	1.24	

The mean head loss increase from run A to run B as a function of the porosity during backwash is shown in Fig. 24 for series 1. The results indicate an extremely well defined curve with a striking minimum at a porosity of 0.70. This indicates that the minimum head loss increase in the run following backwash is produced by backwashing to the expected optimum porosity of 0.70. The result is even more remarkable when

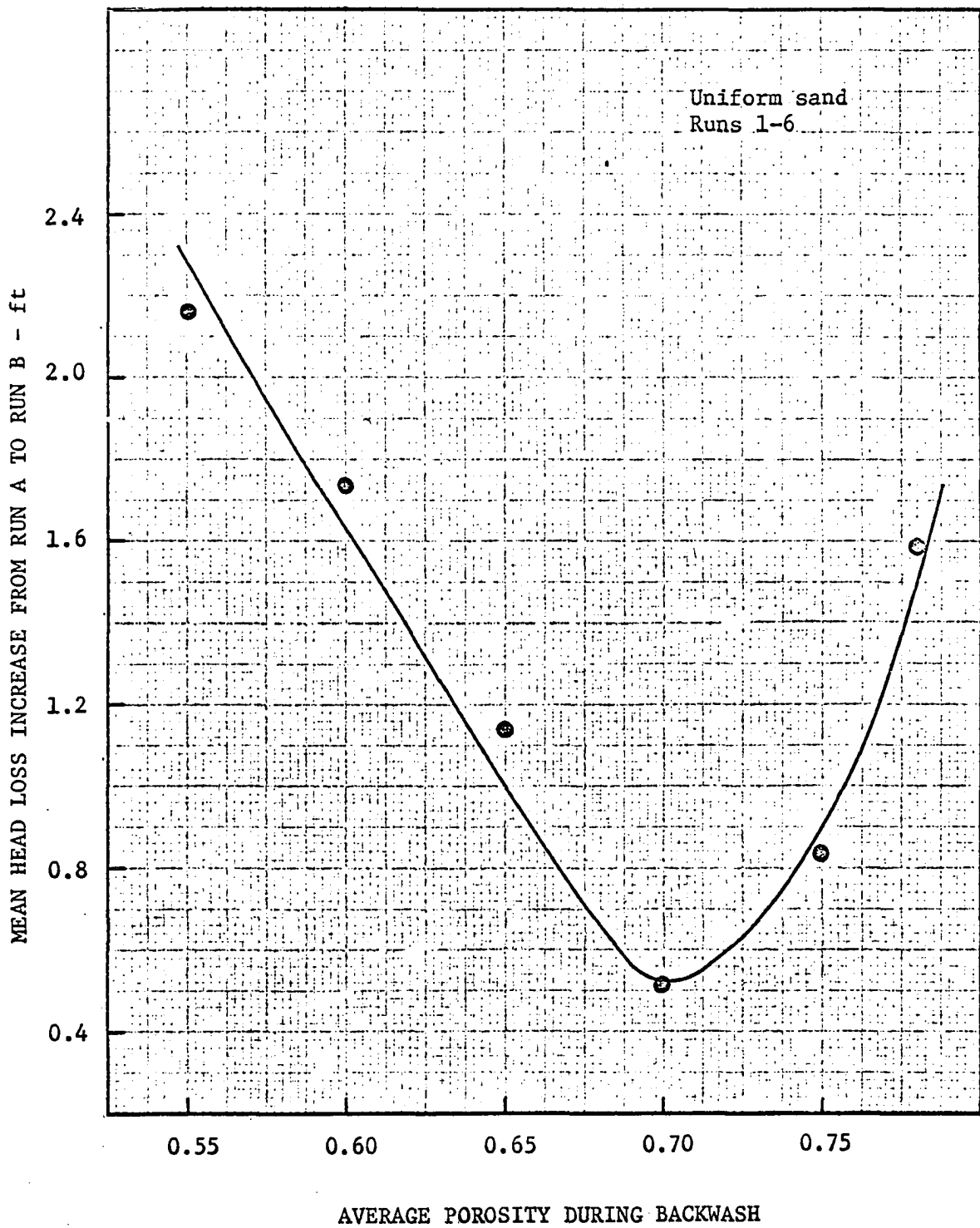


Fig. 24. Head loss increase vs. porosity, series 1

considered in conjunction with the results on the cumulative effluent quality index. They show unexpectedly that optimum backwashing not only produces a lower head loss in the run following backwash but also produces a better quality effluent. Thus, both parameters which limit a filtration run are enhanced and a larger volume of filtered water can be expected to be produced in filters washed optimally.

The results for series 2 do not show quite a consistent pattern as in Fig. 24 and are hence presented in tabular form in Table 6. If the four points corresponding to porosities of 0.60, 0.65, 0.75 and 0.78 are plotted they produce a curve very similar to that of Fig. 24.

The results for series 3 are also given in condensed form in Table 7. The head loss increases were calculated at five depths of 3 in., 6 in., 9 in., 12 in. and 15 in. The results are contradictory to those of series 1 and 2 and show an increasing asymptotic behavior of the head loss increases at expansions greater than 40 percent. The results of the head loss increases presented in this section are not very consistent in all three series.

4. Backwash water quality and porosity

The parameter which provided data which was the most consistent in all the runs was the backwash water quality. It enabled comparisons between different backwash porosities to be made on the basis of usage of equal quantities of washwater, even though the actual washwater used in the series 1 and 2 was dependent on the constant wash duration of 5 min. For series 3 the total volume of washwater used for the different

Table 7. Head loss increases from run A to B, graded sand, series 3

Expansion in percent					
15	30	40	50	60	75
Mean cumulative head loss increase at 3, 6, 9, 12, and 15 in. depths-ft					
-1.66	-0.35	-0.09	0.95	0.96	0.97

expansions was maintained the same for all the runs by varying the durations of wash.

The Figs. 25 and 26 illustrate the backwash water quality for series 1 in terms of the iron concentration in mg/l in samples of washwater as a function of the total volume of washwater used upto the time of sample collection. Using the time of collection of samples and the flowrate during that particular wash the total washwater used was calculated and plotted as the abscissae. The plotted points are from different filters and different runs but are grouped together to indicate the variation of backwash water quality with porosity. The apparent scatter in the points towards the end of the backwash is due to the graphs being plotted on logarithmic co-ordinates. The logarithmic co-ordinates were necessary in order to show the variations in backwash water quality which range from 1000 mg/l to 0.2 mg/l. However, for purposes of analysis the most relevant sections of these primary curves shown in Figs. 25 and 26, are the lower curved portions before the curves reach asymptotic values. Magnified curves of these sections for series 1 are shown in Fig. 27

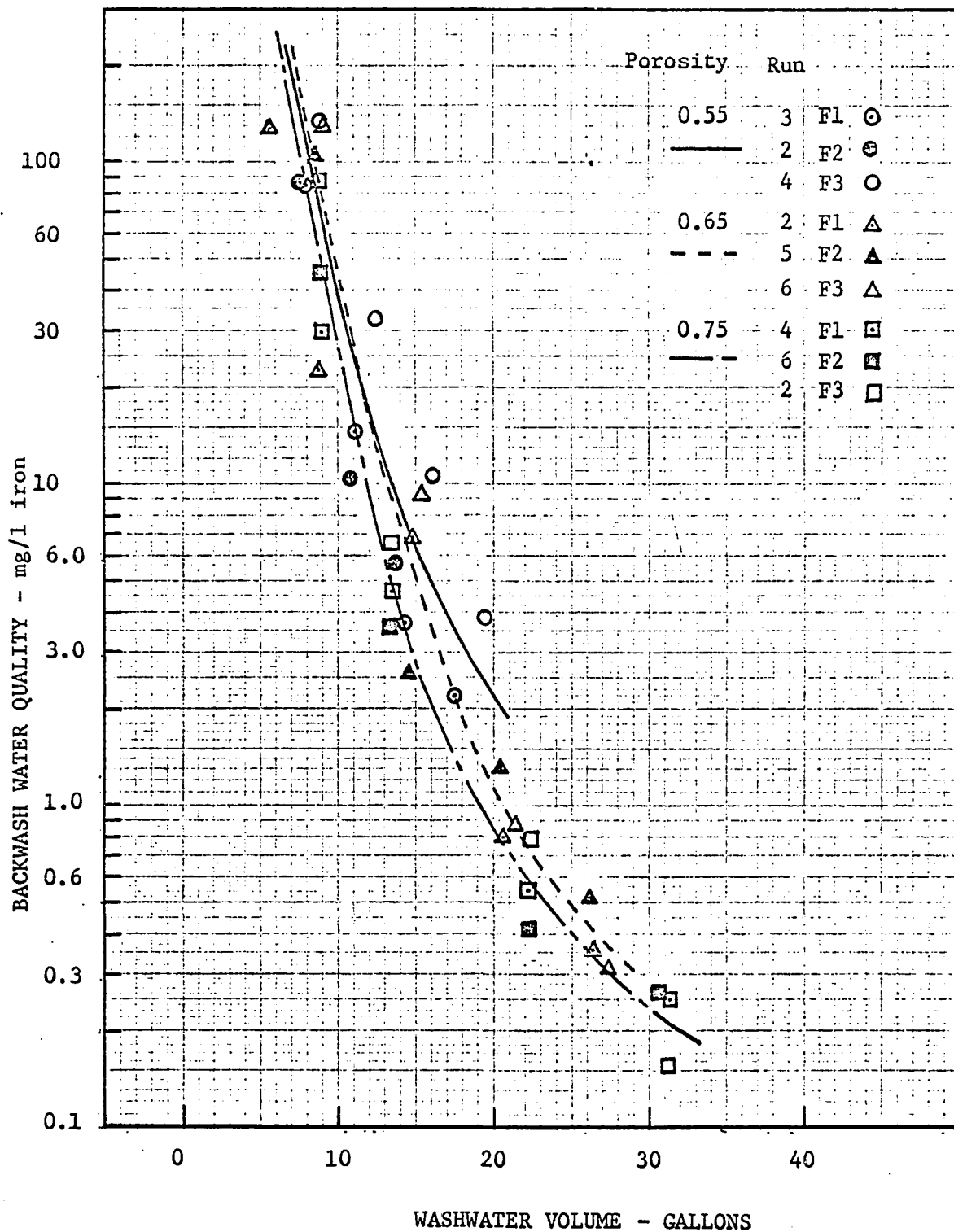


Fig. 25. Backwash water quality vs. washwater volume, series 1

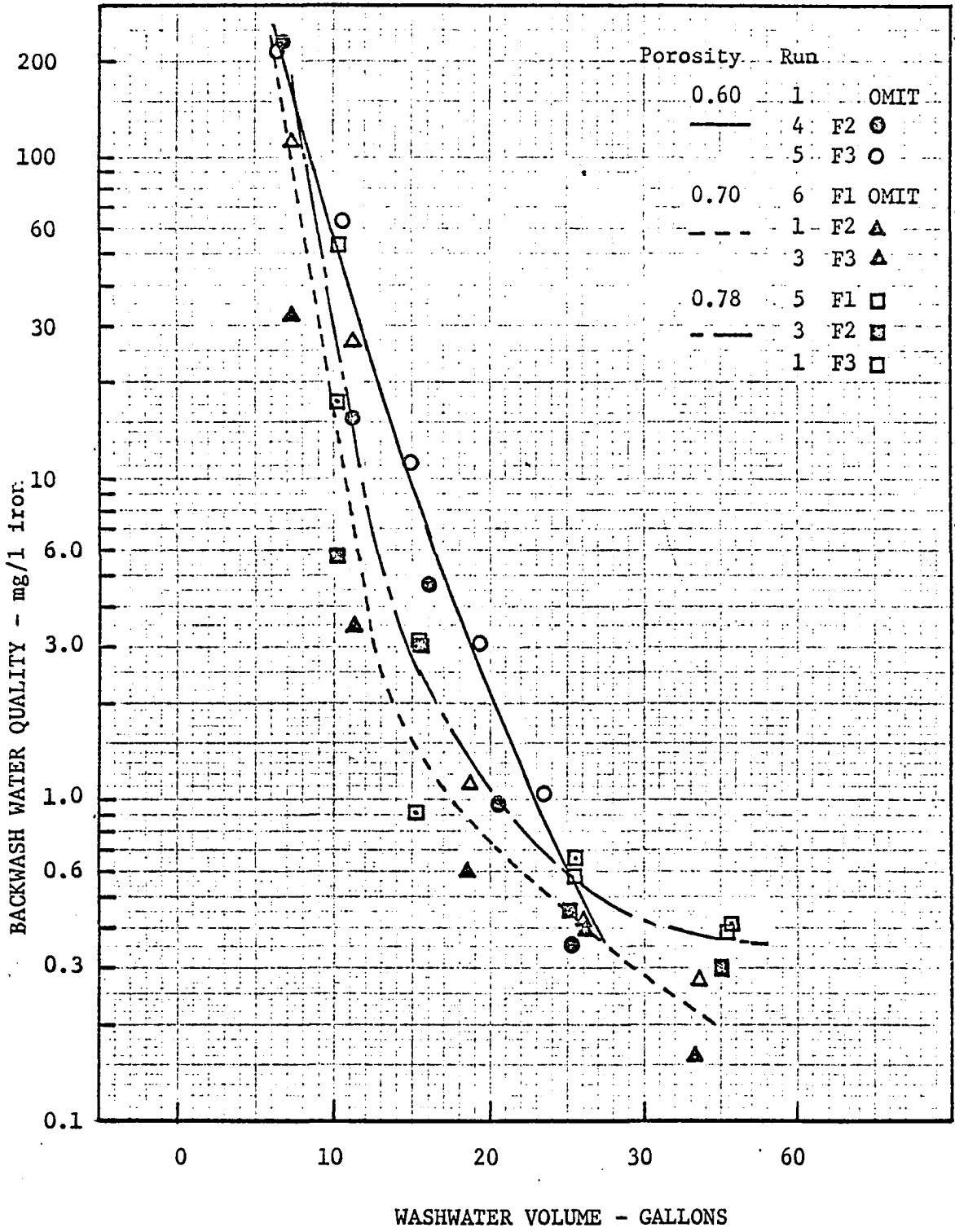


Fig. 26. Backwash water quality vs. washwater volume. series 1

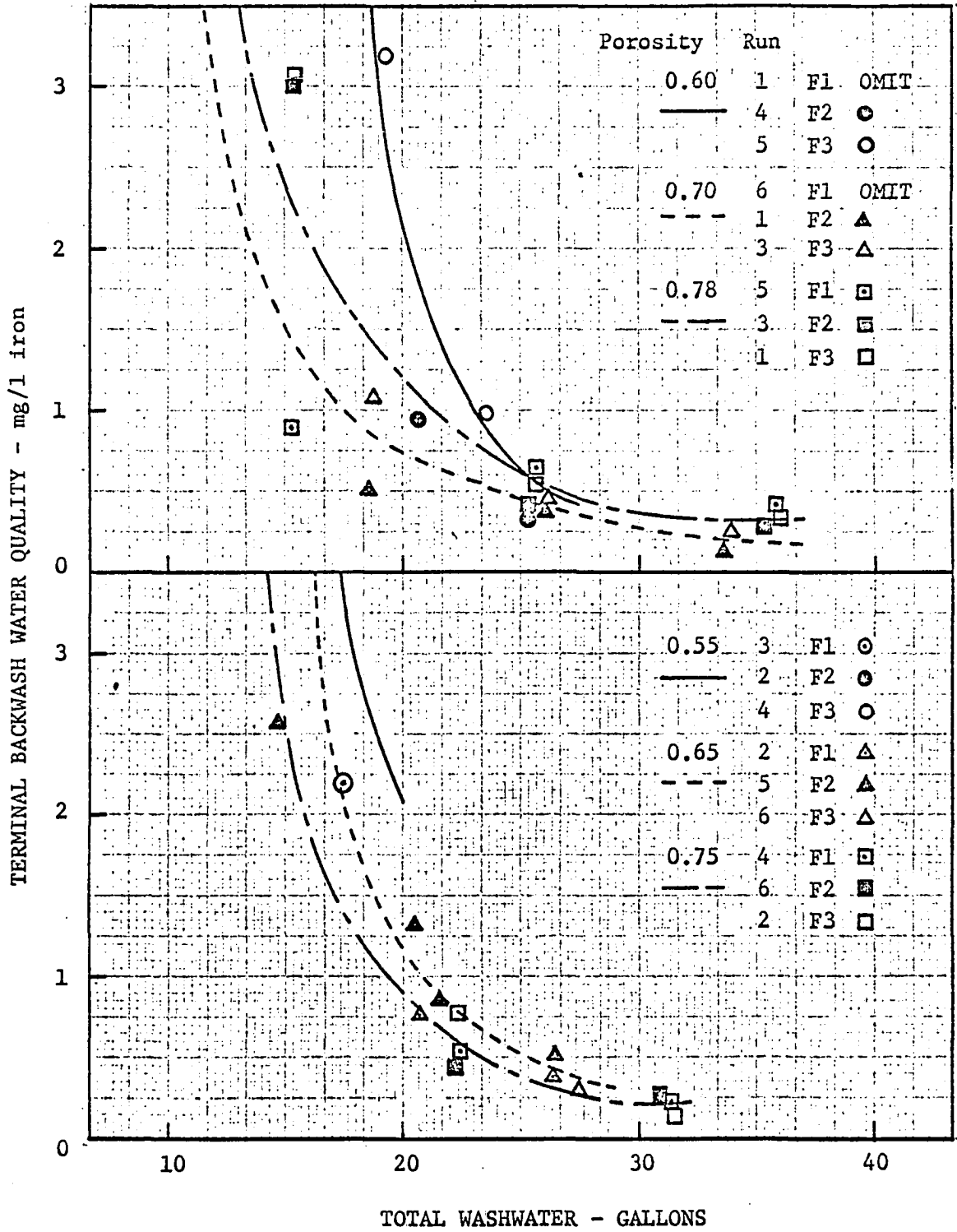


Fig. 27. Backwash water quality vs. washwater volume, series 1

in arithmetic co-ordinates. The lines drawn are smoothed curves through the means of the values from the three filters. The curves represent the mean variations of backwash water quality with volume of washwater at the different porosities.

The smoothed curves of Fig. 27, were used to prepare secondary curves showing the variations of final backwash water quality with porosity in Fig. 28 for constant volumes of total washwater. The points plotted are the intersections of ordinates at washwater volumes of 20 and 25 gallons respectively with the smoothed curves drawn in Fig. 27. The results show once again that the best terminal backwash water quality is achieved by backwash at the porosity of 0.70. This has resulted from analyses which consider backwashing to different expansions, but using a constant total volume of washwater. The results indicate that most effective backwash is achieved by expansion to porosities around 0.70.

An alternative graph also derived from Fig. 27 by considering the different volumes of washwater needed at the different expanded porosities to achieve a given terminal backwash water quality is shown in Fig. 29. A family of curves for terminal backwash water qualities of 0.75, 1.00 and 1.50 mg/l of iron is shown. These graphs show again that the minimum quantity of washwater necessary so as to obtain a given terminal backwash water quality occurs at the porosity of 0.70.

The above analyses should be restricted to the lower sections of the curves when the quality changes become small, since only in these sections are the results meaningful. A further discussion of this question is made in the section titled Analysis.

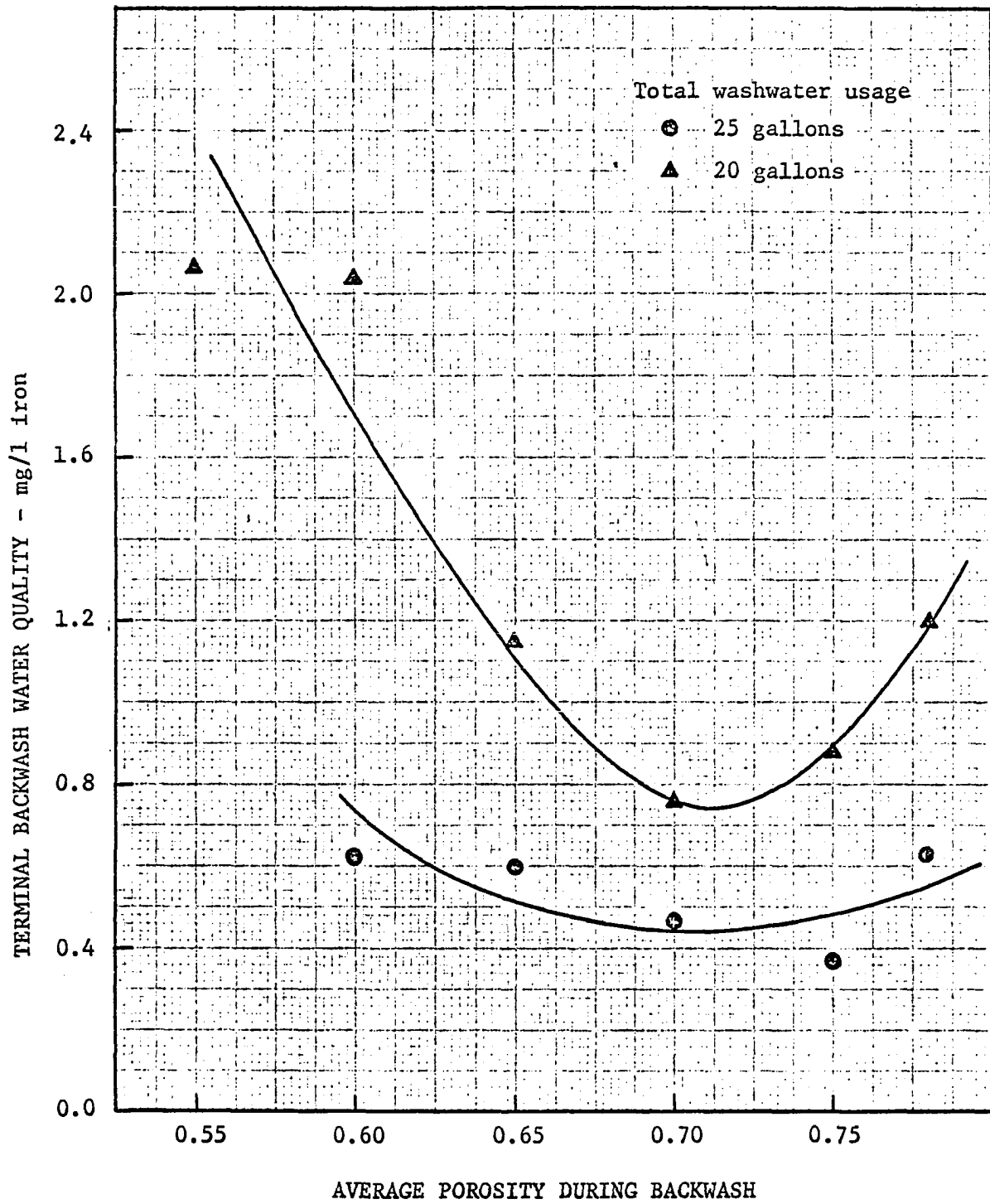


Fig. 28. Terminal backwash water quality vs. porosity, series 1

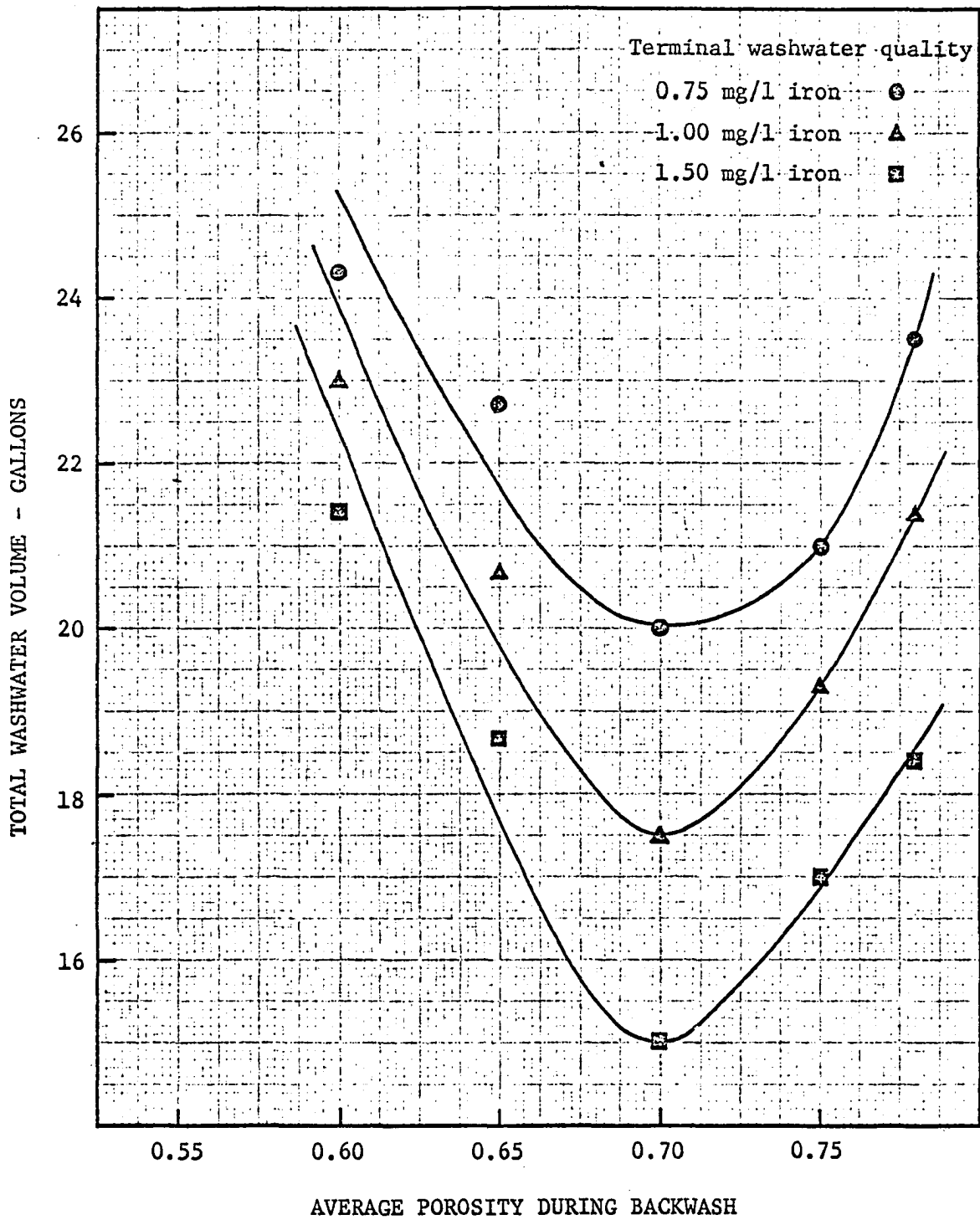


Fig. 29. Backwash water volume vs. porosity, series 1

Identically similar graphs resulted in all the experiments of series 2 for the uniform sand, and of series 3 for the graded sand. The sections of the primary graphs which are required for analysis are shown in Figs. 30 and 31. The secondary graphs developed from these figures are shown in Figs. 32, 33, 34 and 35. The results are remarkably consistent. In every graph a minimum in the total wash-water volume usage or the terminal washwater quality, occurred around the anticipated porosity range of 0.65 to 0.70. Thus, both of these parameters have provided still further evidence of the optimum theory developed in a previous chapter.

5. Physical sandwash and porosity

As already recorded an extra parameter to evaluate the effectiveness of backwash was proposed, based on the amount of iron removable from the sand by a physical wash. The washing procedure was simple abrasion using a magnetic stirrer under standard conditions. Considerable amounts of iron were removable from the sand by this method; thus providing final evidence for the fact that negligible collisions and abrasions between particles occurs in a fluidized bed. If there was considerable abrasion in the fluidized state it should not be possible to remove these large amounts of iron by a physical wash. The change in color of distilled water due to the magnetic stirrer wash in six samples of sand, is illustrated by the photographs in Fig. 6.

The iron removable from the graded sand in mg/g as a function of expansion is shown in Fig. 36. The points plotted are for the first two runs on the graded sand, namely runs 20 and 21. These runs were

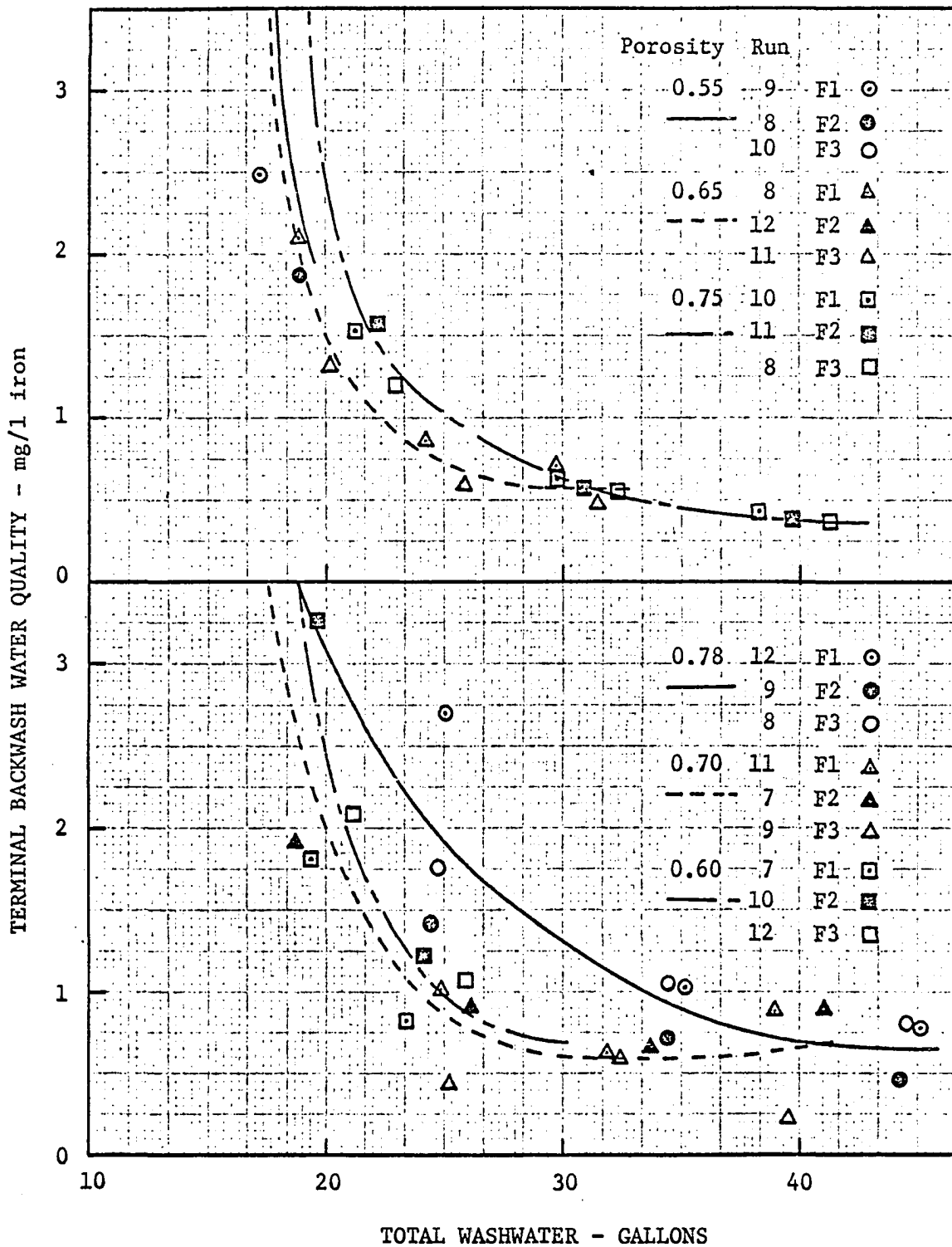


Fig. 30. Backwash water equality vs. washwater volume, series 2

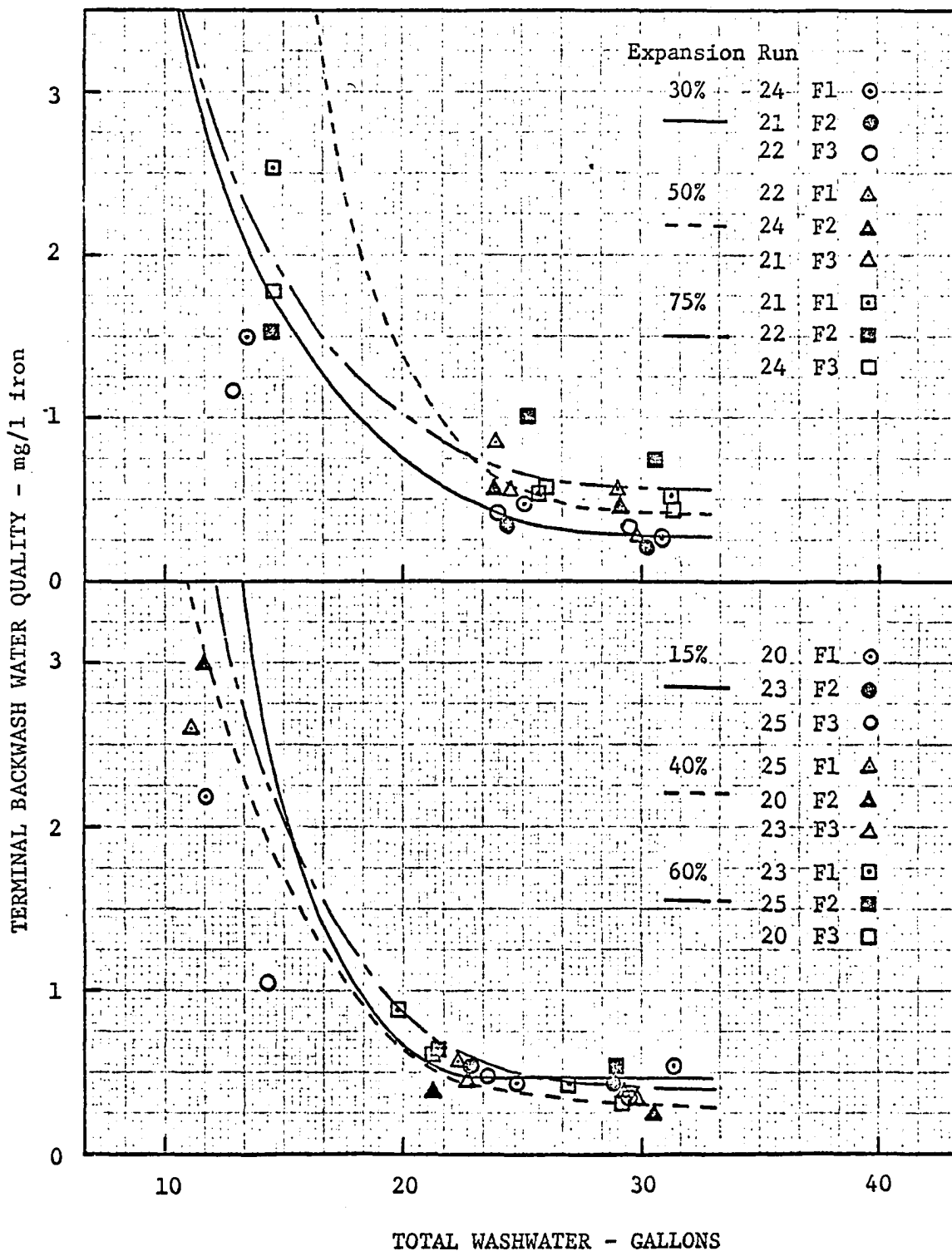


Fig. 31. Backwash water quality vs. washwater volume, series 3

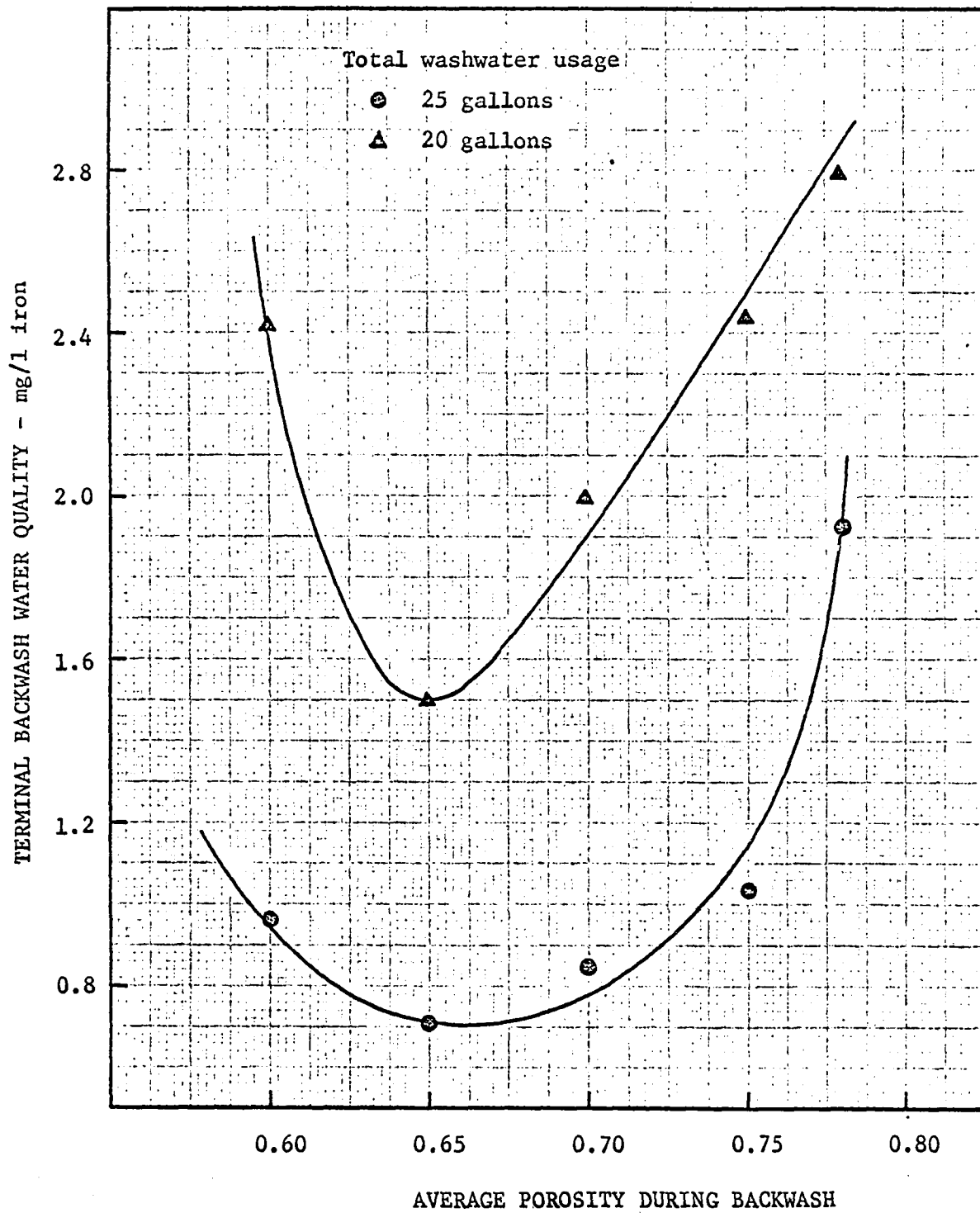


Fig. 32. Terminal backwash water quality vs. porosity, series 2

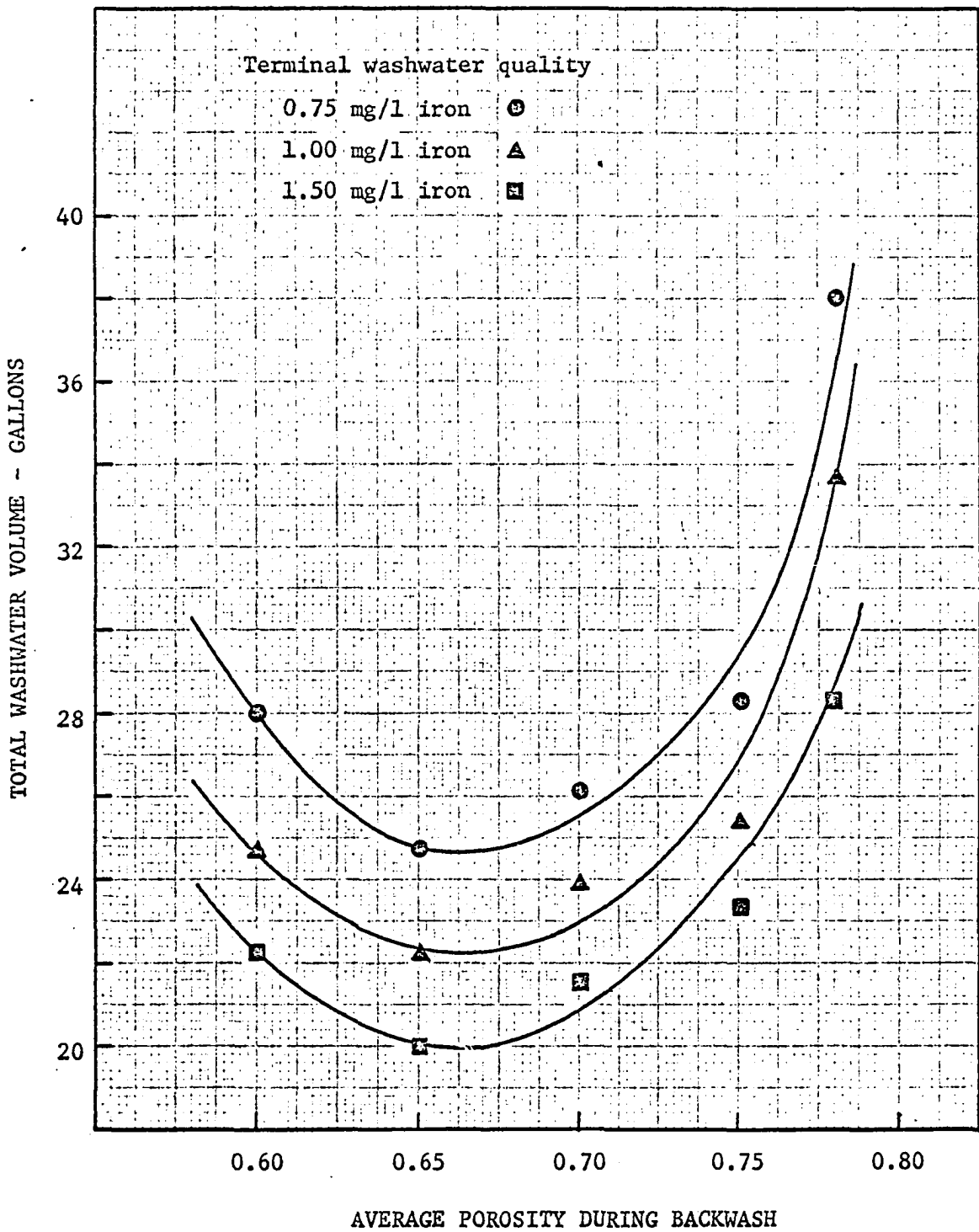


Fig. 33. Backwash water volume vs. porosity, series 2

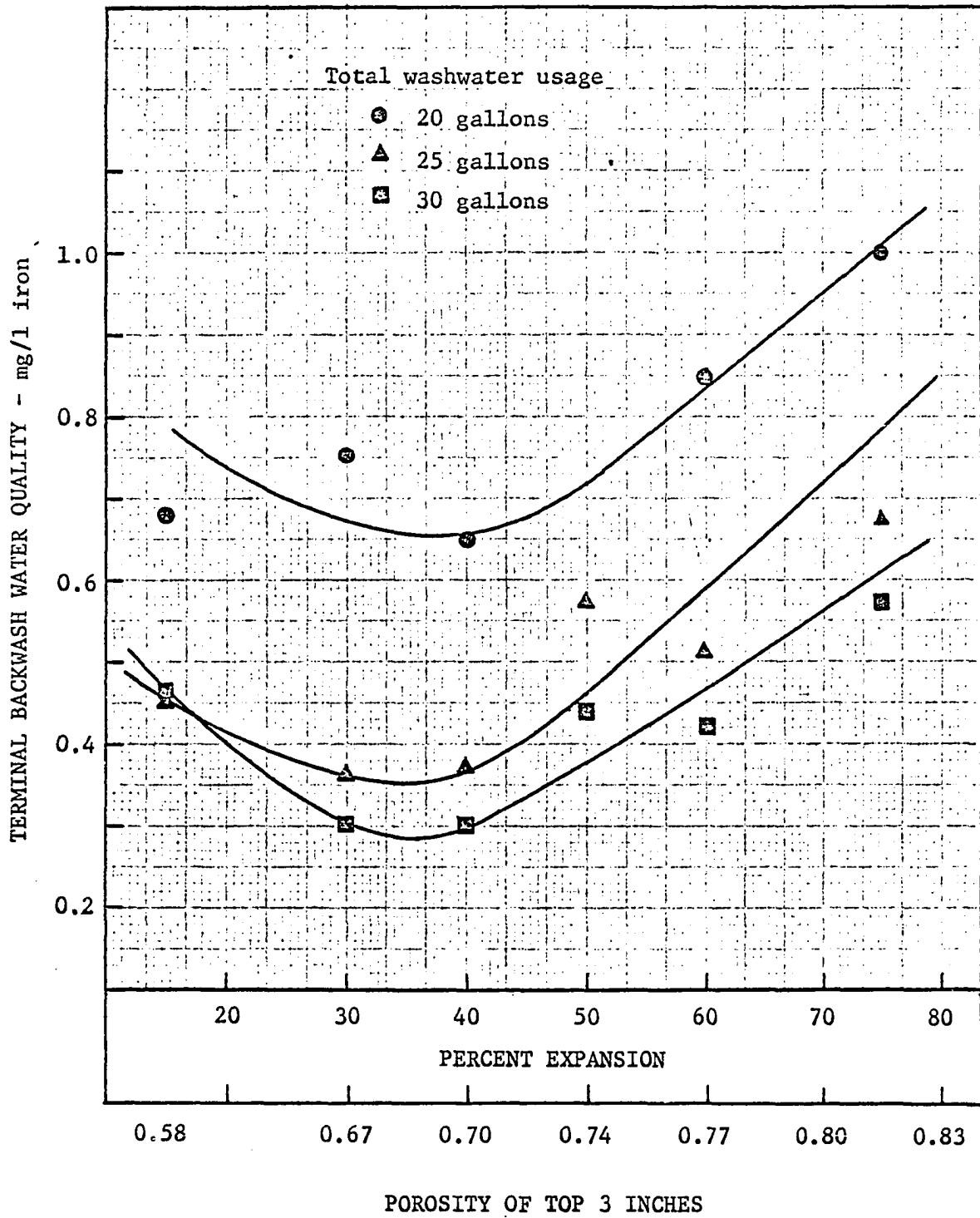


Fig. 34. Terminal backwash water quality vs. expansion, series 3

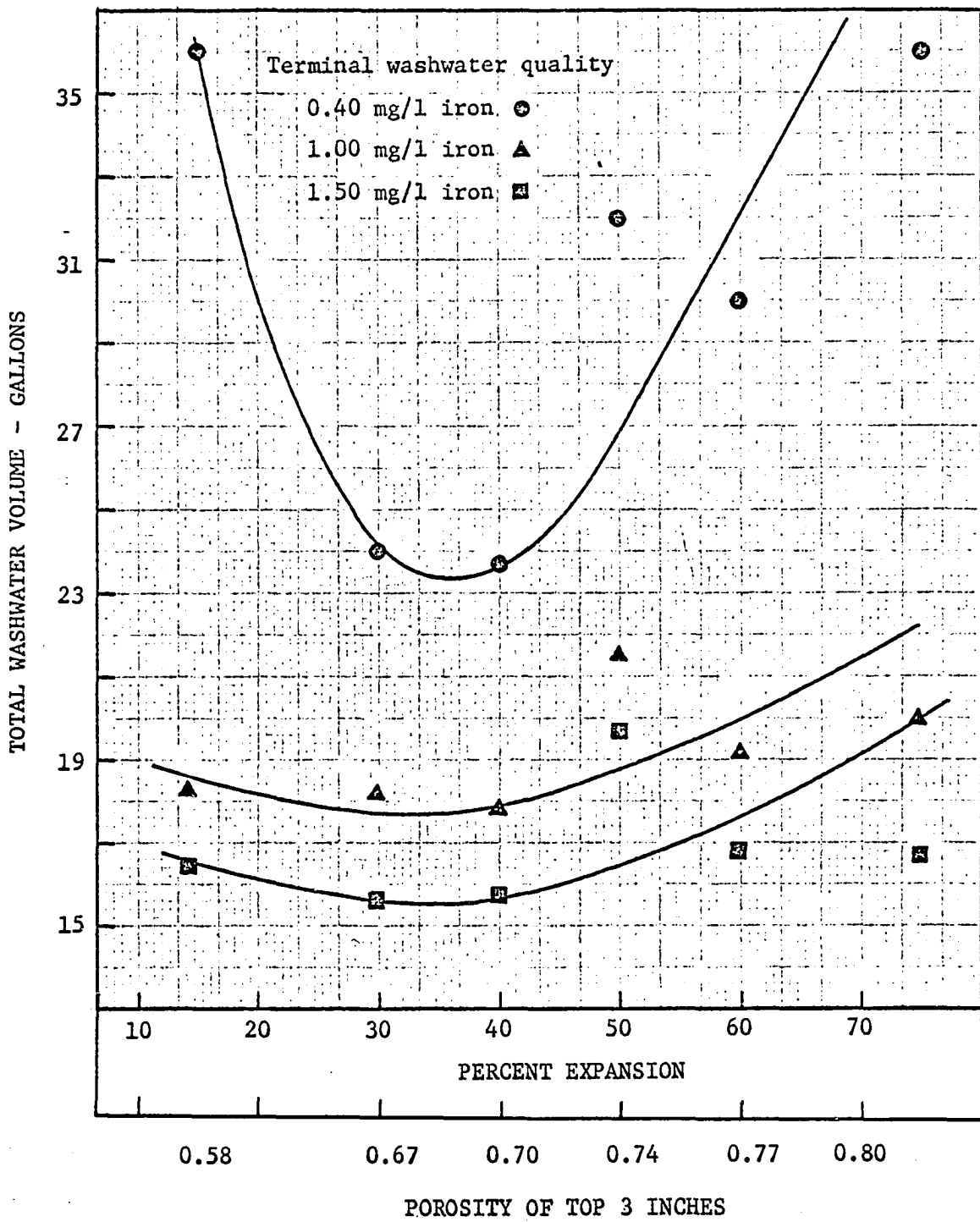


Fig. 35. Backwash water volume vs. expansion, series 3

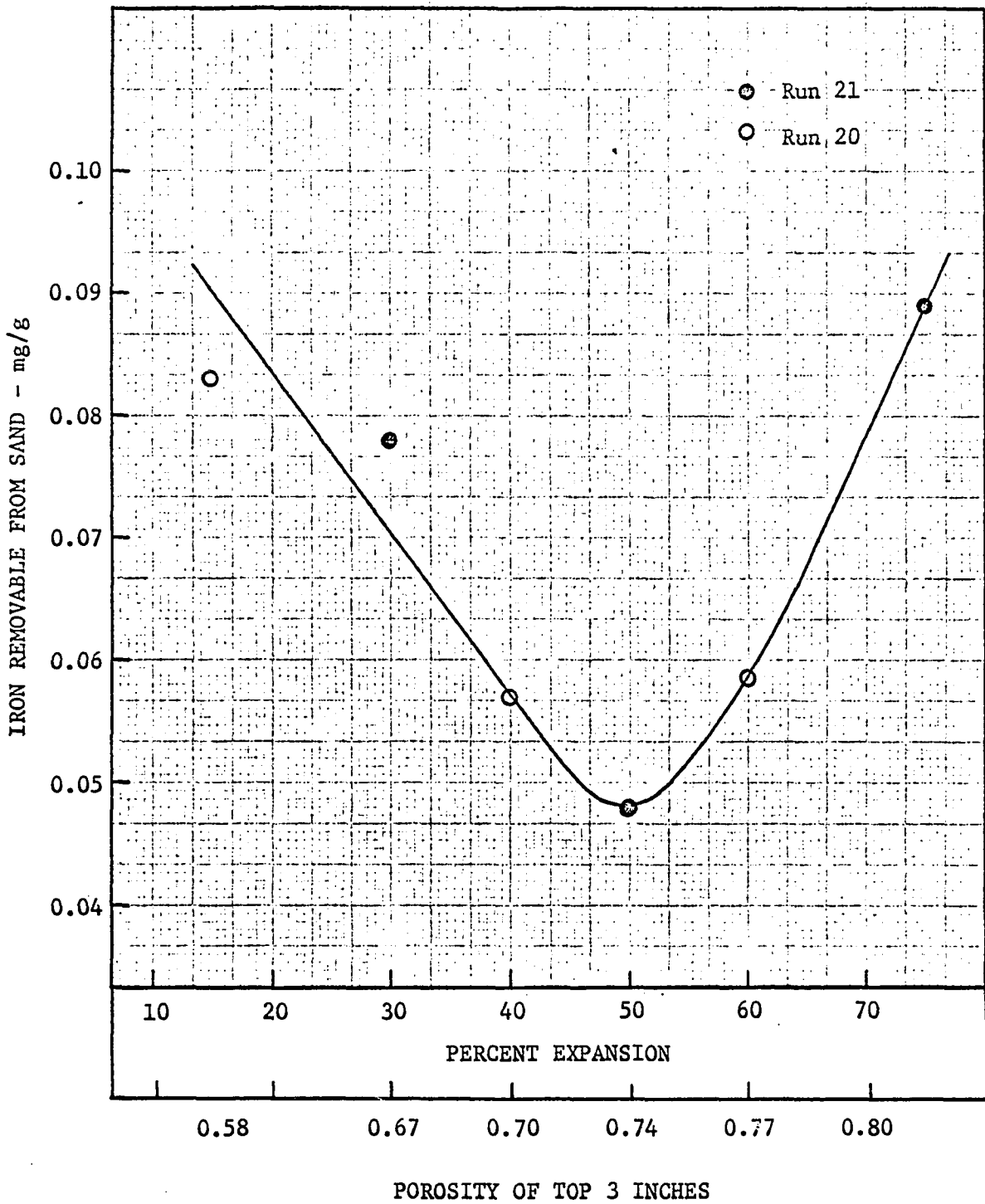


Fig. 36. Iron removable by physical abrasion test vs. expansion, runs 20 and 21

the initial runs made on the new graded sand after it had been subjected to one unnumbered run for purposes of coating the new sand with at least a small layer of the iron floc. Though similar measurements were made for all the runs of series 3 it was found that the results of runs 22 to 25 were subject to considerable error due to the following cause. In series 3, the influent suspension contained 7 mg/l iron and 0.10 mg/l of a non-ionic polyelectrolyte. As the series 3 progressed from run to run it was found that due to the added polyelectrolyte mudballs started building up. These were about 0.5-2.0 mm size and consisted entirely of globules of the precipitated iron without any sand within them. These were floating on top of the sand layer during fluidization and every time the sample of sand was drawn for analysis, considerable amounts of these mudballs or globules were drawn with the sand sample and caused the iron removable readings to be quite erratic from run to run. It was found that as the series of runs progressed the mudballs became bigger and bigger causing larger and larger errors. Even though a modified larger expansion wash, nearly 100 percent, was used for a few minutes during the standard cleaning at the start of each run, it was still not possible to remove substantial amounts of the mudballs.

Because of the above reason the physical abrasion test results of runs 22-25 were invalid and are not presented. However, in the runs 20 and 21 the mudballs were still very few in number and very small in size and did not substantially affect the readings.

The results shown in Fig. 36 reconfirm the fact indicated in the other sections that an expansion of about 40-50 percent produces the

cleanest sand in the graded filter. These expansions cause porosities of about 0.70-0.74 in the top 3 in. layer of the expanded bed of graded sand.

B. Analysis

1. An analytical summary of the results

The results presented in the preceding pages prove beyond little doubt the major thesis of this dissertation, that an optimum backwash occurs in a system, expanded to achieve a porosity of approximately 0.65 to 0.70 in the layers containing the most amounts of suspended matter. In the case of a uniform sand bed an expansion to a porosity of 0.70 is equivalent to nearly 100 percent expansion of its height. For a theoretical uniform sand consisting of identical particle sizes this expansion is an exact and fixed condition. However, in filtration practice uniform sand beds are never used, nor is it feasible to provide for 100 percent expansions because of unreasonably large backwash flows required. We are indeed fortunate that both these limitations are simultaneously removed by use of a graded sand. It can be shown that a 40 percent expansion of a typical graded filter sand causes the porosity of the top 3 in. layer to reach a value of 0.70; and it has been shown by use of four different parameters that the optimum backwash for the graded system occurs at expansions of about 40-45 percent. These values of expansion can be obtained in practice.

Table 8 summarizes the actual porosities at which the minima and maxima of all the curves occur. These points are the experimentally derived optima for the uniform and graded sands used in these studies.

Table 8. A summary of optimum backwash and porosity

Sand type	Fig. no.	Parameter used	Percent expansion	Optimum porosity
Uniform	15	effluent quality index		0.66
	16	effluent quality index		0.72
	17	effluent quality index		0.65
	24	head loss increase		0.70
	28	terminal backwash quality		0.71
		terminal backwash quality		0.71
	32	terminal backwash quality		0.65
		terminal backwash quality		0.67
	29	backwash water volume		0.70
		backwash water volume		0.70
		backwash water volume		0.70
	33	backwash water volume		0.67
		backwash water volume		0.67
		backwash water volume		0.67
	Graded	18	effluent quality index	45
19		effluent quality index	50	0.74
34		terminal backwash quality	38	0.69
		terminal backwash quality	36	0.68
		terminal backwash quality	38	0.69
35		backwash water volume	38	0.69
		backwash water volume	39	0.70
		backwash water volume	36	0.68
36		iron removable from sand	49	0.74

^aPorosity is that of the top 3 in. layer in expanded state.

The fourteen experimental values of the optimum backwash for the uniform sand should be compared with the theoretically derived optimum of 0.70 in page 87 of this dissertation. The results of theory and experiment are remarkably consistent. The nine values for the graded sand need to be compared with the theoretically calculated result of optimum shear stress shown to be at a porosity of 0.72 of the top 3 in. layer. Again the consistency between theory and experiment is amazing.

2. The evidence in the literature

A few points need to be made regarding this optimum of 40-45 percent for graded systems and the results reported in the sanitary engineering literature. The fact that effective backwash requires an expansion of about 50 percent for graded systems has been a well known rule of thumb in filtration design and practice. This rule developed originally from the work of Hulbert and Herring (46) in 1929. Their results have already been quoted in some detail in a previous chapter.

Several workers have suggested during the last decade that expansions of 20-25 percent maybe sufficient for effective backwash (9, 20, 49, 71). None of these papers however, provide fundamental considerations or experimental results which are valid to draw this conclusion. Baylis (9) suggested the figure without any experimental work. Camp et al. (20) reported this expansion as suitable for all filters, on the basis that serious problems did not occur in the operation of the Billerica water treatment plant. But it needs to be pointed out that the Billerica plant had multi media filters, and expansions of 20-25 percent easily give porosities of about 0.70 in the top coal layer.

This can be seen in the results reported by these workers themselves. This, in fact, is additional evidence for the hypothesis of this dissertation.

Johnson and Cleasby (49) reported an optimum of 16-18 percent for the Ames treatment plant. However, they did not backwash the filters at expansions greater than this figure of 16-18 percent after the dirtying run, even though the backwash system was capable of obtaining expansions of 21 and 22 percent. They based their conclusion on the fact that the water quality in the filtration run after backwash at 16-18 percent was better than that of the dirtying run. The dirtying run was preceded by a backwash of 21-22 percent expansion for long durations, hence they deduced that 16-18 percent expansion was the optimum. Most of the experimental results of this dissertation also give a similar result, namely that the effluent quality in the dirtying run was often better than that of the filtration run. Still the optimum effluent quality clearly occurred at porosities of 0.70, since a definite maximum occurred at this porosity. Ulug's work (71) and the reasons which caused him to draw an invalid conclusion have already been dealt with in some detail.

Thus, it is seen that careful analysis indicates that the results reported in the literature (46, 20) are consistent with the theory and experimental work of this dissertation. It also needs to be remembered that effective backwashing does not necessarily mean optimum backwashing and due to the rather flat nature of the shear stress maximum it is possible to backwash filters effectively even though the optimum condition is not obtained. In case one may be tempted to run away with

the idea that a lower expansion may result in a saving of washwater, Figs. 29, 33 and 35 need to be remembered. They clearly show that backwashing at lower expansions than the optimum necessarily results in the usage of larger amounts of washwater to achieve a given bed cleanliness.

On the basis of the results reported by Camp et al. (20) it is probable that expansions of 20-25 percent will probably yield optimum cleaning of the coal layers in multi media filters. However, a further expansion maybe needed to remove the solids trapped in the sand-coal interface and the sand layer by further optimum cleaning. This requires a step-wise expansion of multimedia filters for optimum cleaning. This has already been shown by Rimer (60) to be the most effective backwash procedure, thus providing further evidence in the literature for the theory advanced in this dissertation. Experiments using similar procedures as those in this thesis, to verify more conclusively the ranges of optimum backwash for coal beds and multi-media filters are probably the most important experiments needed to extend this study.

3. Rationalization of parameters and results

It is necessary for the sake of completeness to dwell on whether the optima indicated by the various parameters are consistent with one another and whether they can in combination be rationalized in terms of the best cleaning of the filter. It needs to be noted that these rationalizations are purely for the purpose of detailed analysis of the consistency of all the results, and are not in any way needed for proving the central thesis of optimum backwash. The experimental

results themselves have independently sufficed to prove that optimum backwash occurs at a porosity of 0.65-0.70.

a. Cumulative effluent quality The effluent quality in the run following backwash is probably the most difficult to explain on the basis of the best cleaning of the sand. The chief difficulty lies in the fact that all the variables controlling filtration affect both halves of the dual runs, and the differences in which we are interested are extremely small. However, (i) by repeating the experiments so that each filter is subjected to all the expansions and hence reducing the variations from filter to filter, (ii) by considering cumulative differences in the effluent in runs A and B, thus magnifying the differences due to the different backwash rates, and (iii) by only considering comparative differences between the different filters during a single run, thus eliminating the differences that occur from run to run, it has been shown that the results of the variation of cumulative effluent quality index with porosity can be reproduced quite well in the two series of runs on uniform sand (series 1 and 2).

The question arises, why does best cleaning of the sand produce the best cumulative effluent quality index in the next run. In filtration, the removal of suspended solids passes progressively to the deeper layers of the filter. Assuming the optimum backwash produces the cleanest filter throughout its entire depth, we could expect that as filtration proceeds the cleaner new layers of the bed brought into effect in filtration, causing the quality to continuously indicate improved performance over that of a less clean filter. Thus even though the differences in cleanliness between the filters backwashed

to different expansions are small, these cumulative effects in the filtrate quality should be detectable. This is a possible hypothesis for the improved effluent quality.

b. Initial effluent quality The next question that would probably be asked is, why does not the improved cleaning also cause the initial effluent to indicate an optimum. The writer of this dissertation proposes a hypothesis that not only answers this question, but also answers another question in filtration theory and practice which has been noted by almost all researchers, but has still not been satisfactorily explained. This is the initial degradation of quality. It is hypothesized that the initial effluent quality is chiefly due to solids that have been shaken loose from the sand particles as the fluidized bed becomes a fixed bed. It has been found by all researchers that an initial degradation of the effluent occurs in most filter runs. Cleasby (24) using his own data as well as that in the literature showed that the maximum turbidity or iron content occurred at approximately the theoretical time required to displace the water from the filter and the following turbidimeter. If we accept the hypothesis that no collisions occur in the fluidized state, then when the bed is made a fixed bed the material shaken loose will occupy the filter bed and will be flushed out during the initial minutes of the filter run causing the degradation in quality. If this is the cause of the degradation in initial effluent, we should expect that an instantaneous closure of the valve will shake loose more material than a slow closure of the valve. Some experimental evidence for this hypothesis is presented in Fig. 23. However, more detailed work is necessary for a more definitive conclusion. An

experiment using radioactive iron was proposed to provide this extra evidence, but it had to be omitted due to several unresolved problems. It is suggested that this is a possible avenue for further research.

The above hypothesis, has some a posteriori justification, on the results of Figs. 21 and 22. These graphs show that there exists no direct correlation between the backwash expansion and the initial effluent quality. This is to be expected in these runs because the valve closure rate was kept identical in all the runs. Thus, the primary variable controlling the initial degradation seems to be the valve closure rate and the consequent jarring of the coated material from the sand grains, when they come in contact with one another on the fluidized bed being made a fixed bed.

c. Backwash water quality and the sand wash experiments These studies provide the best and most direct evidence for optimum backwash effectiveness. From the Figs. 29, 33 and 35 it can be seen that usage of backwash water to obtain a given terminal backwash water quality is minimized by expanding the bed to the optimum porosities. The percentage savings in washwater from washing at the optimum porosity compared with an expansion of say 50 percent (porosity = 0.60) are of the order of 40 to 50 percent for series 1 and about 15 percent for series 2. Similarly, backwashing at 40 percent expansion saves approximately 30 percent washwater compared with washing at 20 percent expansion to obtain a terminal quality of 0.4 mg/l for the graded sand in series 3. However, for backwashing to terminal qualities of 1.0 or 1.5 mg/l results in savings of washwater of only 6-8 percent. It should be recognized that these results of washwater savings are somewhat

variable due to the fact that they are obtained from projections of curves such as in Fig. 31. Thus, it is seen that even though theory predicts only small changes in the shear force intensities around the maximum, savings in washwater volume can be made by operation at optimum conditions.

The iron washing experiment in Fig. 36 indicates that the thickness of the coatings on the sand are minimized by optimum backwash. Comparing the optimum expansion at 48 percent with expansions of 20 percent, it is seen that the amount of iron removable decreases by approximately 85 percent. Thus substantially heavier coatings will be left on the sand by backwash to expansions of 20 percent which are commonly used. These fundamental properties provide some long term means of controlling filtration in treatment plants. For example, by backwashing at optimum conditions the sand growth can be minimized, at plants where increased sizes may result in progressively poorer quality. These effects should be measurable over perhaps a period of about a year and full scale treatment plant operations should be studied for periods of about this length of time to provide additional evidence for the above conclusions.

Theoretical considerations already discussed in detail, indicate (1) a maximum dispersion in the turbulent backwashed solids-fluid regime, and (ii) also indicate a maximum in the shear stress, around the porosity of 0.70. The above results should be analyzed with these two facts clearly borne in mind. The reason why the minimum backwash volume occurs is because of the maximum in the turbulent dispersion. This causes the suspended solids to be dispersed from the backwashed

bed in the quickest way when backwashed at optimum conditions. This results in minimum use of washwater volume to obtain given terminal washwater quality. This general characteristic can be noted in all the Figs. 27, 30 and 31.

In addition, the theory developed indicates a maximum shear stress at the porosities near 0.70. Thus, maximum removal of the coatings occurs at optimum backwash. Hence we should expect that the asymptotic terminal washwater quality reached, to have, the least concentrations of iron when backwashed under optimum conditions. Only the runs of series 3 were made with equal total volumes of washwater. This tendency for the optimum backwash water quality to reach the lowest concentrations of iron can be clearly seen in the graphs shown in Fig. 31 for the series 3. The expansions of the graded sand corresponding to these asymptotic minima are 30 and 40 percent.

The above two effects in combination cause the minima in the curves of backwash water quality (Figs. 28, 32 and 34) and backwash water volume (Figs. 29, 33 and 35) with porosity. In addition, the cause for the coatings on the sand to reach a minimum thickness under optimum backwash conditions is also explained by the maximum shear stress.

Thus it is seen that the experimental results and the optimum backwashing theory are entirely consonant with one another.

4. A concluding summary

The results summarized and the analyses presented in this section give a complete picture of optimum backwashing. The experimental

results are entirely consistent with the theory of optimum backwash developed in a previous chapter and provide excellent confirmation of the theoretical results. It has been shown that optimum backwash simultaneously provides these advantages, (i) a better effluent in the following run, (ii) a lower head loss in the following run depending on the properties of the filtered solids, (iii) a minimum usage of wash water and (iv) a minimum growth of the coatings on the sand. This plurality of advantages should considerably improve the performance of most filtration plants, if optimum backwashing is put into operation.

VIII. DESIGNING FOR OPTIMUM BACKWASH

A. The Effective Size as Controlling Parameter

The following is a tentative model proposed for the design of optimum backwash systems for graded sand. It utilizes the mathematical model for expansion developed by the writer in a previous work (2) and combines it with the central result of this dissertation.

Fig. 37 shows the sieve analyses of the graded sand and the top 3 in. layer of the sand when it was fluidized to an expansion of 50 percent. From the graphs it is seen that the 60 percent size of the top 3 in. layer is identical with the 10 percent size of the graded sand.

Based on the above result it is postulated that the optimum condition for graded sand can be determined as the expansion of the 10 percent size or the effective size, treated as the average size of the top layer. This has some qualitative validity, as Hazen originally defined the 10 percent size as the size controlling the filtration characteristics of the sand and we can expect most removals of suspended matter to be achieved by this sand size.

B. An Illustrative Design Calculation

Design Problem:

Calculate the flowrate for optimum backwashing of a graded sand filter of effective size 0.45 mm and uniformity coefficient 1.47 which has a specific gravity of 2.648 and a fixed bed porosity of 0.412. The

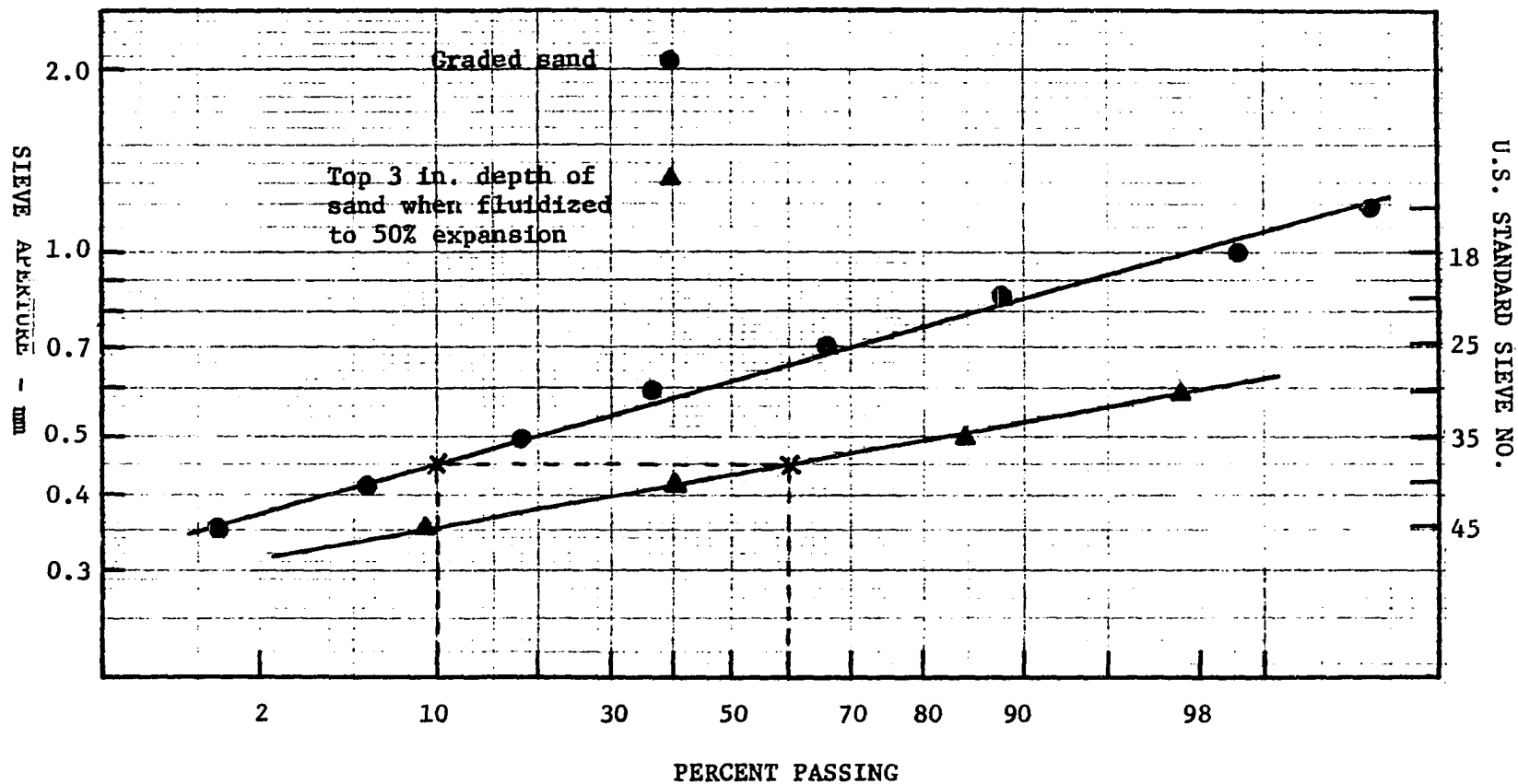


Fig. 37. Sieve analyses of graded sand and the top 3 in. layer

backwash water is at a temperature of 25°C and the sand is fluidized in a 6 inch diameter filter.

Solution:

Assume that the effective size of 0.45 mm is the 60 percent size of the top 3 in. layer for use in the Amirtharajah and Cleasby model for expansion (3).

$$\text{The minimum fluidization velocity } V_{mf} = \frac{0.00381(d_{60\%})^{1.82}[\gamma_f(\gamma_s - \gamma_f)]^{0.94}}{\mu^{0.88}} \quad (60)$$

where,

V_{mf} = minimum fluidization velocity based on open tube in
gpm/sq ft

$d_{60\%}$ = 60 percent finer size of particles in mm

γ_f = specific weight of fluid in lb/cu ft

γ_s = specific weight of solid in lb/cu ft

μ = fluid viscosity in centipoise

Hence,

$$\begin{aligned} V_{mf} &= \frac{0.00381 \times 0.45^{1.82} [62.4(2.648 \times 62.4 - 62.4)]^{0.94}}{0.8954^{0.88}} \\ &= 3.76 \text{ gpm/sq ft} \\ V_s &= 8.45 V_{mf} \quad (61) \\ &= 8.45 \times 3.76 \\ &= 31.8 \text{ gpm/sq ft} \end{aligned}$$

Therefore,

$$\begin{aligned}
 (\text{Re})_{\text{mf}} &= \frac{\rho_f (d_{60\%}) V_{\text{mf}}}{\mu} \\
 &= \frac{1.0(\text{g/cc}) \times 0.045(\text{cm}) \times 30.48(\text{cm/ft}) \times 3.76(\text{gpm/sq ft})}{0.8954 \times 10^{-2}(\text{poise})(\text{g/cm sec/poise}) \times 448.8(\text{gpm/cfs})} \\
 &= 1.29 \\
 \text{Re}_o &= 8.45 (\text{Re})_{\text{mf}} \\
 &= 8.45 \times 1.29 \\
 &= 10.9
 \end{aligned}$$

The following two equations have already been presented as Eqs. 53 and 54.

$$\begin{aligned}
 n &= \left(4.45 + \frac{18d_{60\%}}{D_t}\right) \text{Re}_o^{-0.1} \\
 &= \left(4.45 + \frac{18 \times 0.45}{6 \times 25.4(\text{cm/ft})}\right) 10.9^{-0.1} \\
 &= 3.54
 \end{aligned}$$

$$V = K\epsilon^n$$

therefore,

$$V_{\text{mf}} = K(\epsilon_{\text{mf}})^n$$

$$3.76 = K(0.412)^{3.54}$$

hence,

$$K = 86.9 \text{ gpm/sq ft}$$

It is assumed in the above calculation that the porosity of the top layer is the same as that of the entire bed. This is not exactly true in reality. A higher degree of accuracy can be obtained by using the actual porosity of the top layers. From the writer's optimum backwash theory the optimum porosity is given by,

$$\begin{aligned}\epsilon_{\text{optimum}} &= \frac{(n - 1)}{n} \\ &= \frac{(3.54 - 1)}{3.54} \\ &= 0.72\end{aligned}$$

This calculated optimum porosity for the graded sand should be compared with the average of the optimum porosities measured by the various parameters and previously summarized in Table 8. This average of the experimental values for optimum porosity was 0.71 for the top 3 in. layer.

The superficial velocity to obtain this porosity is,

$$\begin{aligned}V &= K\epsilon^n \\ &= 86.9 \times 0.72^{3.54} \\ &= 27.1 \text{ gpm/sq ft}\end{aligned}$$

Optimum backwash velocity = 27.1 gpm/sq ft

To determine the actual expansion of the graded sand it is necessary to recalculate the expansion of the graded bed for the superficial velocity of 27.1 gpm/sq ft. It should be noted that the optimum porosity of 0.72

calculated above refers to the top 3 in. layer only, and cannot be used to calculate the percentage expansion of the total bed. The method of calculating the expansion of a graded bed for a given superficial velocity has already been dealt with in detail elsewhere (2, 3) and will not be repeated here. For the graded sand the expansion corresponding to the flow rate of 27.1 gpm/sq ft is 49 percent.

A further fact regarding the optimum backwash for graded sands needs to be noted. The larger sand sizes at the lower sections of the bed have larger values of the Reynolds No. for settling Re_o . Thus the value of n from Richardson and Zaki's Eq. 53 is also reduced. However, the effect of the reduction is small since the power of Re_o involved in the equation for n is -0.1 . In any case, the decreased value of n results in a reduced value for the optimum porosity given by $\frac{(n-1)}{n}$. For example, the 60 percent size of the graded sand is 0.66 mm. It has an n value of 3.2 and hence an optimum porosity of 0.69. Thus, it is seen that the reduction in porosity from that of the top 3 in. layer is rather small. However, this reduction in optimum backwash for coarser material predicts the correct trend. This conclusion was also drawn on the basis of shear force calculations by Johnson and Cleasby (49). This fact also aids in the optimum backwash of graded systems. It means that, when the topmost layers reach their optimum porosity, the larger particles lower down are also simultaneously closer to their optimum backwash, since the optimum for the larger particles is less than that for the smaller particles. This reduction in the value of the optimum porosity for the larger particles produces a better cleaning of a graded bed, in comparison with a system which has no such effect.

The above model, especially the use of the effective size as controlling the optimum backwash characteristics is based on very limited data. The equality of the 60 percent size of the top layer and the 10 percent size of the whole graded bed shown in Fig. 37, occurred by chance on analyzing the top 3 in. of the bed when fluidized to an expansion of 50 percent. The top 3 in. analyzed corresponded to the top 2 in. of the fixed bed. An analysis of the top layer of the fixed bed of any other thickness other than 2 in. will not produce this relation between the 60 percent size of the top 3 in. fluidized layer and the 10 percent size of the whole fixed bed. The 3 in. fluidized layer at 50 percent expansion was chosen for analysis, as the porosity of this layer matched the theoretical results of optimum porosity. Thus, the relation between the 60 percent size in the top layer and the 10 percent size of the whole graded sand which was obtained from a 50 percent expansion holds only for this value of expansion. However, the above method should give reasonable predictions of the expansions needed for optimum backwashing of graded systems.

For a more sophisticated model it is necessary to optimally balance the variations of suspended solid removal from top to bottom in the filter, with the gradations in media size and hence obtain an integrated result for a graded system. This is probably the next significant theoretical improvement that can be made to the writer's mathematical theory of optimum backwash.

IX. SUMMARY AND CONCLUSIONS

The goal towards which this dissertation was directed was to provide a study of the optimum backwash of sand filters in a closed cycle of theory and experiment. The work was founded on the solid base of turbulence theory and the fluidization literature, and the major threads of development leading to the central conclusions can be traced as follows.

The review of the literature in sanitary engineering indicates that upto the present time, filter backwashing is dominated by rules of thumb and design-d by rules from experience. Since a backwashed filter is a particulate fluidized bed, the studies in fluidization are directly applicable to it. During the last two decades, studies in fluidization have uncovered significant properties of a fluidized bed which are directly useful in studies of filter backwashing. They are as follows:

(i) Particle collisions in a fluidized bed do not occur to any significant extent. Hence abrasion as a mechanism of cleaning a backwashed filter is of negligible importance. Theoretical reasons, experimental results and a posteriori justifications, have been used by several researchers to prove this point. This fact of negligible collisional interactions is also permeating the sanitary engineering literature.

(ii) The interaction of the suspended solids and the fluidizing fluid within a fluidized bed creates random fluctuating velocities having statistical means over sufficiently long periods. This causes a fluidized bed to have fundamental similarities to a turbulent fluid

field, and Taylor's theory of statistical turbulence can be applied to it.

(iii) Application of Taylor's theory of diffusion to determine the dispersion characteristics of a particulate fluidized bed leads to the important result that most turbulence parameters such as eddy diffusivity, Peclet No. and the scale of turbulence maximized at expanded porosities of 0.65-0.70. Thus, optimum dispersion in the fluid field occurred at these porosities.

The basics of turbulence needed to understand the development of Taylor's theory, and the major results obtained by applying the statistical theory of turbulence to fluidization, such as the optima at the porosity of 0.70, are presented in detail in the initial chapters of this dissertation.

The fact of negligible particle collisions and the consequent limited cleaning by abrasion shows that the fluidized bed is an inherently unsatisfactory process for cleaning a dirty filter. Since the main mechanism of cleaning is due to hydrodynamic effects, it was hypothesized by the writer of this dissertation, that within the constraint that fluidization is not an excellent process for cleaning, the best cleaning that can be achieved is to expand the bed to the porosities of 0.65 to 0.70; this being the range of porosities wherein most turbulence parameters had a maximum.

Using the above hypothesis as a basis, a theoretical investigation was made to determine if it could be shown that a maximum did occur in the hydrodynamic shear at the expanded porosity of 0.65-0.70.

A new mathematical theory for optimum backwash was hence developed by the writer in Chapter V by combining the following three well known equations.

Camp's equation for shear stress,

$$S = \sqrt{[\mu g \rho_f \frac{V}{\epsilon} (\frac{dh}{dz})]} \quad (51)$$

The constant head loss equation for fluidized beds,

$$(\frac{dh}{dz}) = \frac{(\rho_s - \rho_f) \cdot (1 - \epsilon)}{\rho_f} \quad (52)$$

Richardson and Zaki's equation for the superficial velocity as modified by Amirtharajah and Cleasby (3),

$$V = K\epsilon^n \quad (53)$$

Elimination of $(\frac{dh}{dz})$ and V from the equations gives the important equation of the new theory which relates the shear stress to the porosity,

$$S = \alpha \sqrt{(\epsilon^{n-1} - \epsilon^n)} \quad (55)$$

Using classical optimization theory and differentiating S with respect to ϵ gives the result for maximum shear stress,

$$\text{Porosity for maximum shear stress, } \epsilon_{\text{optimum}} = \frac{(n - 1)}{n}$$

The value of n for the sands normally used in filtration are 3.1-3.4. Substituting these values of n in the above equation gives the result that the maximum shear stress occurs at porosities of 0.68-0.71.

Thus, the new theory gives a result which is deducible mathematically, that a maximum in the hydrodynamic shear also occurs in the same range of expanded porosities (0.65-0.71) as that indicated by the maxima in the turbulence parameters.

The entire experimental investigation was designed to verify the above theoretical result. Two series of 6 dual runs each, were made on a bank of three filters containing 12 in. deep uniform sands. All three filters were dirtied under identical conditions and then backwashed at different expansions. A run following the backwash was used to comparatively evaluate the effectiveness of backwash on the effluent quality and the head loss increase in the run following backwash. A precision calibration technique was used to measure the effluent quality accurately and the experiment was designed to nullify the effects of the variation from run to run and from filter to filter. Five different parameters, (a) effluent quality index, (b) initial effluent quality, (c) head loss increase, (d) terminal backwash water quality and (e) backwash water volume were used to evaluate the effectiveness of backwash at different porosities ranging from 0.55 to 0.78. The results are summarized in Table 8 and indicate that every one of these parameters excluding the initial effluent quality had an optimum in the range of 0.65-0.72. The calculated theoretical result for optimum backwash for this sand was, at an expanded porosity of 0.70. The calculation procedure for determining n uses the expansion model of Amirtharajah and Cleasby (3) and

is shown for the graded sand in the previous chapter. A hypothesis that the initial effluent quality is a function of the valve closure rate, with some limited experimental results has also been presented to show why this parameter did not indicate the optimum. The parameters indicate that optimum backwashing aids several characteristics of filtration. In particular suspensions, a simultaneous improvement of head loss and effluent quality can be obtained. The backwash water volume parameter indicates that optimum backwash can result in savings of washwater of the order of 20-25 percent from the backwash rates being used presently.

The optimum porosities of 0.65-0.70 for uniform sands require expansions of the order of 75 to 100 percent. If these are the expansions required then the above studies are of purely theoretical interest. However, it was hypothesized that for graded systems the filtered solids were removed in the upper layers of the filter which were composed of the smaller particles of sand. Thus expansions of far smaller degree for graded systems should provide the necessary porosities for optimum backwash. The next stage of the experimental investigation studied optimum backwash for a typical graded sand.

The third series of 6 dual runs was made on the graded sand for backwash expansions of 15 percent to 75 percent. These expansions had porosities of 0.58-0.82 in the top 3 in. layer of the expanded bed. Similar criteria as those used for the uniform sand were used to evaluate the effectiveness of the different backwash expansions. In addition, an extra criterion based on a physical wash with a magnetic stirrer which caused cleaning by abrasion on samples of sand after

backwash was also used. The results for the graded system are also summarized in Table 8 and showed that all these parameters indicated an optimum backwash at expansions in the range of 38-49 percent. These expansions corresponded to measured porosities of 0.69-0.74 in the top 3 in. layer of the fluidized beds. The calculated theoretical result for optimum backwash of this graded sand is presented in Chapter VIII. It indicates that the optimum porosity is 0.72 in the top 3 in. layer.

Thus it is seen that excellent confirmation of the theoretical deductions is given by the experimental results. They also prove that optimum backwash of graded systems can be utilized in practice and enlightened operational practices should result in savings of washwater volume of the order of 20-25 percent.

A mathematical model for designing optimum backwash systems is also presented in the previous chapter. It combines the expansion model developed by the writer in a previous study (2, 3) with the present optimum backwash theory. Using the model the actual flowrate and the corresponding expansion for optimum backwash of a graded system can be calculated for purposes of design.

The following are possible studies which need to be made to extend and amplify the results of this dissertation.

(i) Optimum backwash studies of graded coal systems, similar to the experimental studies presented here. It is predicted that optimum expansions will probably result in the range of bed depth expansion of 20-25 percent, since coal beds have fixed bed porosities of the order of 0.50.

(ii) Optimum backwash studies of multi-media systems. Based on the writer's theory it is expected that step-wise increases of wash will probably give the optimum backwash. Rimer (60) has already presented some evidence confirming this result.

(iii) The most immediate theoretical development required is the development of a more sophisticated model for optimum backwash of graded systems. The model should attempt to optimally balance the variation of suspended solids removal with depth, with the gradations in media size.

An attempt has been made in the above dissertation to provide a fundamental study of backwashing sand filters, complete in theory and experiment, for determining optimum systems. It is hoped that the primary philosophy of the scientific method - argument and experience as enunciated by da Vinci and stated in the opening paragraph would have been achieved in this work, at least in some small extent.

X. LITERATURE CITED

1. Adler, I. L. and Happel, J. The fluidization of uniform smooth spheres in liquid media. Chemical Engineering Progress Symposium Series 58, No. 38: 98-105. 1962.
2. Amirtharajah, A. Expansion of graded sand filters during backwashing. Unpublished M.S. thesis. Ames, Iowa, Library, Iowa State University of Science and Technology. 1970.
3. Amirtharajah, A. and Cleasby, J. L. Predicting expansion of filters during backwashing. Submitted for publication in the Journal of the American Water Works Association. 1971.
4. Anderson, T. B. and Jackson, R. The nature of aggregative and particulate fluidization. Chemical Engineering Science 19: 509-511. 1964.
5. Babbitt, H. E., Doland, J. J. and Cleasby, J. L. Water supply engineering. 6th ed. New York, N.Y., McGraw-Hill Book Co., Inc. 1967.
6. Backwashing sand filters--round table discussions. Water Works and Wastes Engineering 1: No. 1, 74-75; No. 2, 80-82; No. 3, 76-78; No. 4, 70-71. 1964.
7. Baumann, E. R. and Oulman, C. Sand and diatomite filtration processes. In Gloyna, E. F. and Eckenfelder, W. W., Jr., editors. Water quality improvement by physical and chemical processes. pp. 104-131. Austin, Texas, University of Texas Press. 1970.
8. Baylis, J. R. Experiences in filtration. Journal of the American Water Works Association 29: 1010-1048. 1937.
9. Baylis, J. R. Nature and effects of filter backwashing. Journal of the American Water Works Association 51: 126-156. 1959.
10. Baylis, J. R. Review of filter design and methods of washing. Journal of the American Water Works Association 51: 1433-1454. 1959.
11. Baylis, J. R. Washing and maintenance of filters. Journal of the American Water Works Association 46: 176-186. 1954.
12. Beek, W. J. [Discussion of] The longitudinal dispersion of liquid in a fluidized bed. Symposium on the interaction between fluids and particles. Proc. London, Institution of Chemical Engineers 1962: 163-165. 1962.

13. Bird, R. B., Stewart, W. E. and Lightfoot, E. N. Transport phenomena. New York, N.Y., John Wiley and Sons, Inc. 1960.
14. Brodkey, R. A. The phenomena of fluid motions. Reading, Mass., Addison-Wesley Publishing Co. 1967.
15. Buevich, Yu. A. and Markov, V. G. Pseudo-turbulent diffusion of particles in homogeneous suspensions. International Chemical Engineering 10: 570-575. 1970.
16. Cairns, E. J. and Prausnitz, J. M. Longitudinal mixing in fluidization. American Institute of Chemical Engineers Journal 6: 400-405. 1960.
17. Cairns, E. J. and Prausnitz, J. M. Macroscopic mixing in fluidization. American Institute of Chemical Engineers Journal 6: 554-560. 1960.
18. Camp, T. R. [Discussion of] Theory of water filtration. Journal of the Sanitary Engineering Division, American Society of Civil Engineers 91: 55-69. October, 1965.
19. Camp, T. R. Theory of water filtration. Journal of the Sanitary Engineering Division, American Society of Civil Engineers 90: 1-30. 1964.
20. Camp, T. R., Graber, S. D. and Conklin, G. F. Backwashing of granular water filters. Submitted for publication in the Journal of the Sanitary Engineering Division, American Society of Civil Engineers. 1971.
21. Camp, T. R. and Stein, P. C. Velocity gradients and internal work in fluid motion. Journal of the Boston Society of Civil Engineers 30: 219-237. 1943.
22. Cleasby, J. L. Filter rate control without rate controllers. Journal of the American Water Works Association 61: 181-184. 1969.
23. Cleasby, J. L. Filtration. In Weber, W. J., Jr., editor. Physicochemical processes in water and wastewater treatment. In print. New York, N.Y., John Wiley and Sons, Inc. 1971.
24. Cleasby, J. L. Selection of optimum filtration rates for sand filters. Unpublished Ph.D. thesis. Ames, Iowa, Library, Iowa State University of Science and Technology. 1960.
25. Cleasby, J. L. and Baumann, E. R. Selection of sand filtration rates. Journal of the American Water Works Association 54: 579-602. 1962.

26. Cleasby, J. L., Williamson, M. M. and Baumann, E. R. Effect of filtration rate changes on quality. *Journal of the American Water Works Association* 55: 869-877. 1963.
27. Corrsin, S. Theories of turbulent dispersion. In Favre, A., editor. *The Mechanics of Turbulence*. Pp. 27-52. New York, N.Y., Gordon and Breach Science Publishers, Inc. 1964.
28. Curle, N. and Davies, H. J. *Modern fluid dynamics*. Princeton, New Jersey, D. Van Nostrand Co., Inc. 1968.
29. Davidson, J. F. and Harrison, D. *Fluidised particles*. New York, N.Y., the Syndics of the Cambridge University Press. 1963.
30. Edeline, F., Tesarik, I. and Vostrcil J. Fluidization of flocs produced in chemical or biological treatment plants. *International Association on Water Pollution Research Conference Proceedings 1969*: 523-531. 1969.
31. Elms, J. W. *Water purification*. New York, N.Y., McGraw-Hill Book Co., Inc. 1917.
32. Ewing, G. W. *Instrumental methods of chemical analysis*. 3rd ed. New York, N.Y., McGraw-Hill Book Co., Inc. 1969.
33. Fair, G. M. and Geyer, J. C. *Water supply and waste water disposal*. 8th ed. New York, N.Y., John Wiley and Sons, Inc. 1958.
34. Fair, G. M., Geyer, J. C. and Okun, D. A. *Water and wastewater engineering*. Vol. 2. New York, N.Y., John Wiley and Sons, Inc. 1968.
35. Fair, G. M. and Hatch, L. P. Fundamental factors governing the streamline flow of water through sand. *Journal of the American Water Works Association* 25: 1551-1565. 1933.
36. Friedlander, S. K. and Topper, L. *Turbulence—Classic Papers on Statistical Theory*. New York, N.Y., Interscience Publishers Inc. 1961.
37. Galloway, T. R. and Sage, B. H. A model of the mechanism of transport in packed, distended and fluidized beds. *Chemical Engineering Science* 25: 495-516. 1970.
38. Ghosh, M. M., O'Connor, J. T. and Engelbrecht, R. S. Precipitation of iron in aerated ground waters. *Journal of the Sanitary Engineering Division, American Society of Civil Engineers* 90: SA1, 199-213. 1966.

39. Handley, D., Doraiswamy, A., Butcher, K. L. and Franklin, N. L. A study of the fluid and particle mechanics in liquid-fluidized beds. Transactions of the Institution of Chemical Engineers 44: T260-T273. 1966.
40. Hanratty, T. J., Latinen, G. and Wilhelm, R. H. Turbulent diffusion in particulate fluidized beds of particles. American Institute of Chemical Engineers Journal 2: 372-380. 1956.
41. Hebert, R. E. Development of a new type of rapid sand filter. Journal of the Sanitary Engineering Division, American Society of Civil Engineers 92: 31-39. 1966.
42. Hinze, J. O. Turbulence. New York, N.Y., McGraw-Hill Book Co., Inc. 1959.
43. Hirsch, A. A. Filter backwashing tests and upflow equalization. Journal of the Sanitary Engineering Division, American Society of Civil Engineers 94: 129-146. 1968.
44. Hudson, H. E. Filter washing experiments at the Chicago experimental plant. Journal of the American Water Works Association 27: 1547-1564. 1935.
45. Hudson, H. E. Operating characteristics of rapid sand filters. Journal of the American Water Works Association 51: 114-125. 1959.
46. Hulbert, R. and Herring, F. W. Studies on the washing of rapid filters. Journal of the American Water Works Association 21: 1445-1513. 1929.
47. Ives, K. J. Theory of filtration. International Water Supply Congress and Exhibition, Vienna, 1969, Special Subject No. 7: K3-K28. 1969.
48. Jackson, R. The mechanics of fluidized beds: Part I: The stability of the state of uniform fluidization. Transactions of the Institution of Chemical Engineers 41: 13-21. 1963.
49. Johnson, R. L. and Cleasby, J. L. Effect of backwash on filter effluent quality. Journal of the Sanitary Engineering Division, American Society of Civil Engineers 92: 215-228. 1966.
50. Kada, H. and Hanratty, T. J. Effects of solids on turbulence in a fluid. American Institute of Chemical Engineers 6: 624-630. 1960.
51. Kramers, I. H., Westermann, M. D., de Groot, J. H. and Dupont, F. A. A. The longitudinal dispersion of liquid in a fluidized bed. Symposium on the interaction between fluids and particles.

- Proc. London, Institution of Chemical Engineers 1962: 114-119. 1962.
52. Lemlich, R. and Caldas, I. Heat transfer to a liquid fluidized bed. American Institute of Chemical Engineers Journal 4: 376-380. 1958.
 53. Leva, Max. Fluidization. New York, N.Y., McGraw-Hill Book Co., Inc. 1959.
 54. McCune, L. K. and Wilhelm, R. H. Mass and momentum transfer in solid-liquid system. Industrial and Engineering Chemistry 41: 1124-1134. 1949.
 55. Murray, J. D. Mathematical aspects of bubble motion in fluidized beds. Chemical Engineering Progress Symposium Series 62, No. 62: 71-82. 1966.
 56. Murray, J. D. On the mathematics of fluidization: Part 1: Fundamental equations and wave propagation. Journal of Fluid Mechanics 21: 465-493. 1965.
 57. O'Melia, C. R. and Crapps, D. K. Some chemical aspects of rapid sand filtration. Journal of the American Water Works Association 56: 1326-1344. 1964.
 58. Reynolds, O. On the dynamical theory of incompressible viscous fluids and the determination of the criterion. Transactions of the Royal Society (London) 186A: 123-164. 1895.
 59. Richardson, J. F. and Zaki, W. N. Sedimentation and fluidisation: Part I. Transactions of the Institution of Chemical Engineers 32: 35-53. 1954.
 60. Rimer, A. E. Filtration through a trimedia filter. Journal of the Sanitary Engineering Division, American Society of Civil Engineers 94: 521-540. 1968.
 61. Rowe, P. N. Drag forces in a hydraulic model of a fluidized bed. Part II. Transactions of the Institution of Chemical Engineers 39: 175-180. 1961.
 62. Rowe, P. N. and Henwood, G. A. Drag forces in a hydraulic model of a fluidized bed. Part I. Transactions of the Institution of Chemical Engineers 39: 43-54. 1961.
 63. Ruckenstein, E. Homogeneous fluidization. Industrial and Engineering Chemistry Fundamentals 3: 260-268. 1964.

64. Singer, P. C. and Stumm, W. The solubility of ferrous iron in carbonate - bearing waters. *Journal of the American Water Works Association* 62: 198-202. 1970.
65. Slis, P. L., Willemse, T. W. and Kramers, H. The response of the level of a liquid fluidized bed to a sudden change in the fluidizing velocity. *Applied Science Research* 8: 209-218. 1959.
66. Standard methods for the examination of water and wastewater. 12th ed. New York, N.Y., American Public Health Association. 1965.
67. Stookey, L. L. Ferrozine - A new spectrophotometric reagent for iron. *Analytical Chemistry* 42: 779-781. 1970.
68. Taylor, G. I. Statistical theory of turbulence. Parts I-IV. *Proceedings of the Royal Society A151*: 421-478. 1935.
69. Taylor, G. I. The spectrum of turbulence. *Proceedings of the Royal Society A164*: 476-490. 1938.
70. Tesarik, I. [Discussion of] Theory of water filtration. *Journal of the Sanitary Engineering Division, American Society of Civil Engineers* 91: SA2, 74-80. April, 1965.
71. Ulug, S. E. The backwashing of rapid sand filters. Unpublished thesis for the Diploma of membership of Imperial College of Science and Technology. London, United Kingdom, Library, Imperial College of Science and Technology, University of London. 1967.
72. Volpicelli, G., Massimilla, L. and Zenz, F. A. Non homogeneities in solid-liquid fluidization. *Chemical Engineering Progress Symposium Series* 62, No. 67: 42-50. 1966.
73. Zenz, F. A. and Othmer, D. F. Fluidization and fluid particle systems. New York, N.Y., Reinhold Publishing Corporation. 1960.

XI. ACKNOWLEDGMENTS

The author wishes to express his sincere appreciation to his major professor, Dr. J. L. Cleasby for his guidance, encouragement and helpful suggestions during the entire course of this study.

Acknowledgment is also expressed to Professor E. R. Baumann and the Engineering Research Institute of Iowa State University, who in combination always found the necessary funds to support the author and his studies, whenever the need arose.

The author would like to express appreciation of the award of a Fellowship for the year '70-'71 by the Iowa State University Research Foundation; this Fellowship supported him during a considerable period of the studies reported herein.

Mention needs also to be made of the discussions with Dr. C. Oulman, which helped in the evaluation of the chemical analytical procedures and also helped to crystallize some of the theoretical ideas developed by the author.

Acknowledgment is also expressed to Professor W. H. Abraham of the Department of Chemical Engineering, who reviewed the contents of the chapter on the theories of turbulence.

Many thanks are due to Mr. Timothy Dunlay, whose unstinting help in the experimental phase of the study contributed in no small way to the successful completion of the experimental runs.

The author would also like to thank his wife, who has helped in many ways during his entire academic program.